

# Impact of neutrino interaction uncertainties on oscillation fits using VALOR

Costas Andreopoulos<sup>1,2</sup>

IPPP/NuSTEC topical meeting on neutrino-nucleus scattering,  
Durham, 18-20 April 2017

<sup>1</sup>University of Liverpool, <sup>2</sup>STFC Rutherford Appleton Laboratory

April 19, 2017



UNIVERSITY OF  
**LIVERPOOL**



Science & Technology Facilities Council  
**Rutherford Appleton Laboratory**

# Outline

- LBL oscillation analysis and neutrino interaction effects
- Current T2K oscillation results and systematics
- Physics systematics for future LBL
  - A study for DUNE

---

Was asked to focus on VALOR (<https://valor.pp.rl.ac.uk>) results.

# What are we hoping to learn?

Study of neutrino masses and mixings the only known **window to new physics**.

Several key questions:

- **What is the neutrino mass generation mechanism?**
  - Could the neutrino be a Majorana particle?
  - Why are the masses so small?
- **What do neutrinos tell us about flavour?**
  - Nearly (exactly?) maximal mixing observed: ‘ $\mu$ ’ and ‘ $\tau$ ’ flavour interchangeable!
- **What is the connection between quarks and leptons?**
  - Why the corresponding mixing matrices are so different?
- **What are the implications for the universe we live in?**
  - Baryon asymmetry of the universe: Leptogenesis requires CPV + Majorana mass
  - Dark matter: Sterile neutrino is a candidate.

# Leptonic CP violation

The CP-violating phase in PMNS is largely unconstrained.

The magnitude of the CP effect is given by the **Jarlskog Invariant**:

$$J_{CP}^{PMNS} = \frac{1}{8} \sin 2\theta_{12} \sin 2\theta_{13} \sin 2\theta_{23} \cos \theta_{13} \sin \delta_{CP}$$

Given the current best fit values, and assuming the normal hierarchy:

$$J_{CP}^{PMNS} = 0.035 \sin \delta_{CP}$$

In contrast, in the quark sector, despite the large value of the CP phase:

$$J_{CP}^{CKM} \approx (3 \pm 1) \times 10^{-5}$$

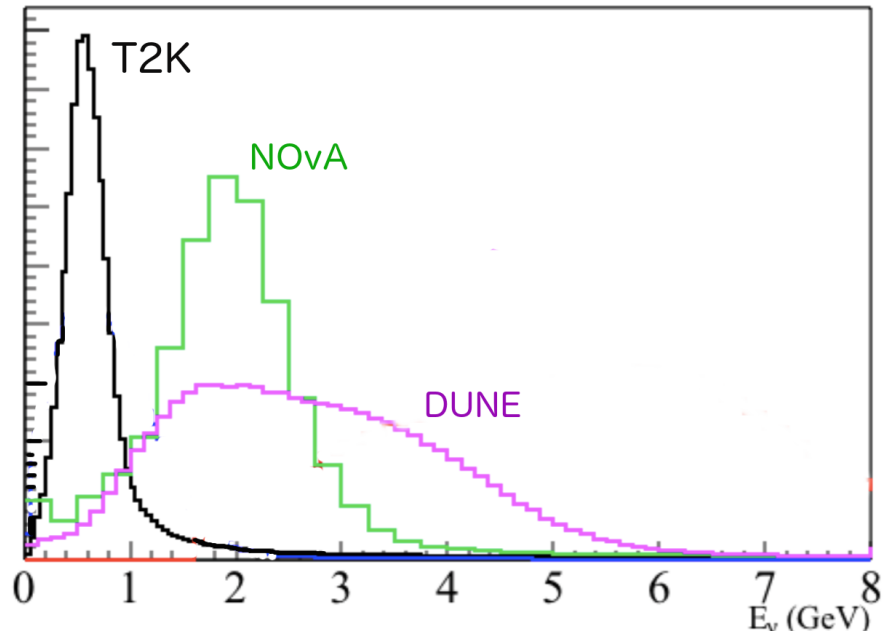
$J_{CP}^{PMNS}$  is **potentially large!**

Measurement of leptonic CPV could have a tremendous impact on our understanding of the origin of the **Baryon Asymmetry of the Universe**.

# Why few-GeV neutrino beams?

Maximize oscillation probability at "atmospheric" squared mass splitting:

$$1.267 \frac{|\Delta m_{32}^2|(\text{eV}^2/c^4) \cdot L(\text{km})}{E_\nu(\text{GeV})} = \frac{\pi}{2} \xrightarrow{|\Delta m_{32}^2| \approx 2.4 \times 10^{-3} \text{ eV}^2/c^4} E_\nu(\text{GeV}) = 0.002 \cdot L(\text{km})$$

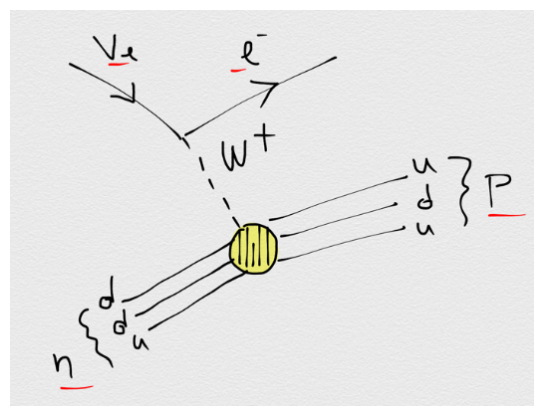
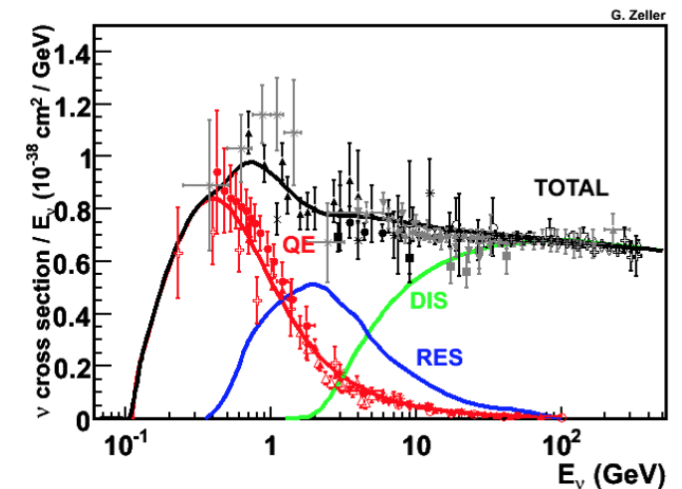
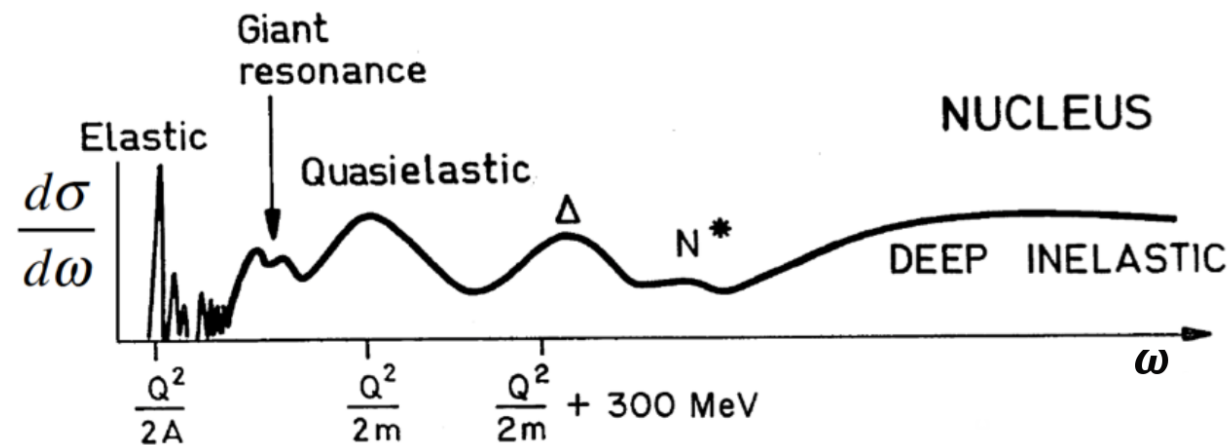


	L (km)	E (GeV)
T2K	292	0.6
NOvA	810	1.6
DUNE	1300	2.6

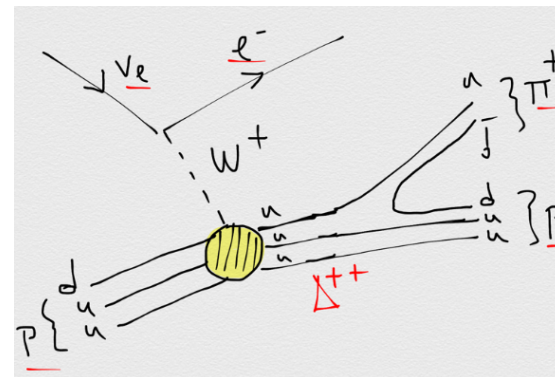
- Boundary between perturbative and non-perturbative regimes
- Using nuclear targets but in a kinematical regime where
  - a) the impulse approximation is poor, and
  - b) intranuclear hadron rescattering effects are substantial.

# Scattering mechanisms at the few-GeV energy range

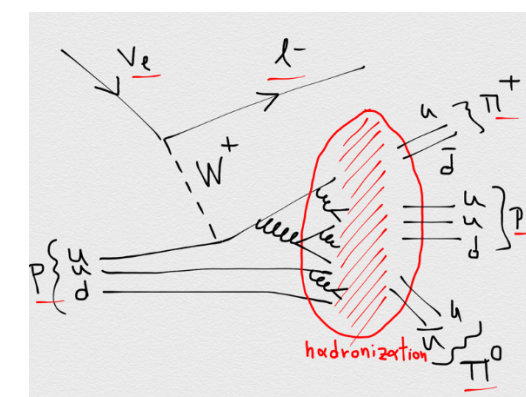
Broad energy range: Several scattering mechanisms are important.



QE



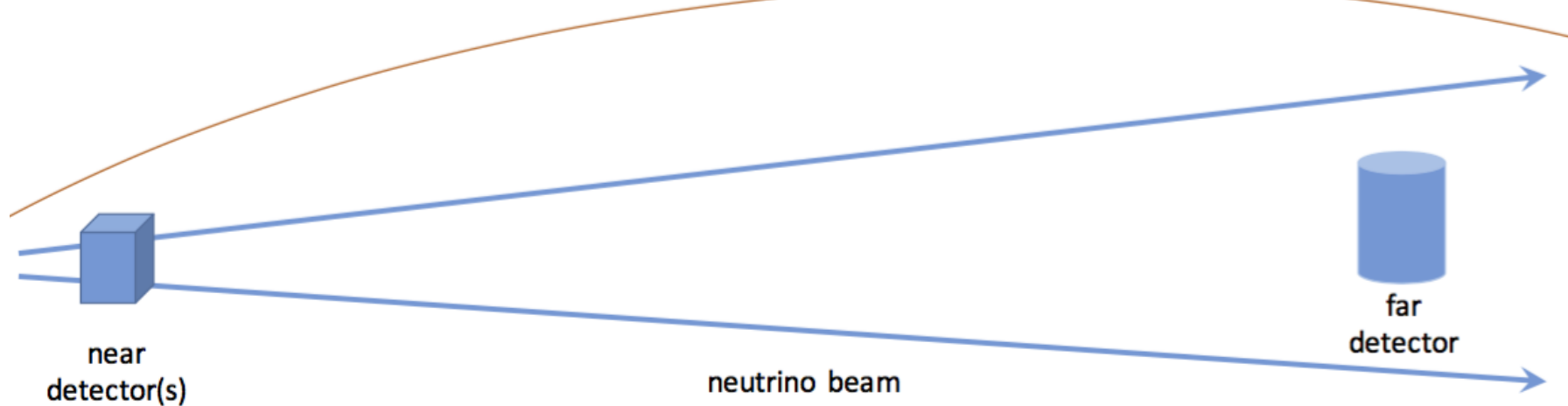
Δ



DIS

# Two-Detector Oscillation Experiments

To mitigate the effect of (flux and interaction) uncertainties with detectors at multiple baselines



Near to Far extrapolation:

- Provides data-driven estimate of unoscillated event rate at the Far detector.
- Influenced by uncertainties in the knowledge of flux and cross-sections.

# Extrapolation from Near to Far Detector

The mantra of an LBL experiment is that reliance on models is limited by using 2 "functionally identical" detectors (Near and Far).

Very schematically, the event rate at the Far and Near detector is given by:

$$N_{\nu_\mu; \text{Far}}(E_\nu) \propto \epsilon_{\nu_\mu; \text{Far}}(E_\nu) \times \Phi_{\nu_\mu; \text{Far}}(E_\nu) \times \sigma_{\nu_\mu}(E_\nu, A) \times P_{\nu_\mu \rightarrow \nu_\mu}(E_\nu)$$

$$N_{\nu_\mu; \text{Near}}(E_\nu) \propto \epsilon_{\nu_\mu; \text{Near}}(E_\nu) \times \Phi_{\nu_\mu; \text{Near}}(E_\nu) \times \sigma_{\nu_\mu}(E_\nu, A)$$

Therefore, for functionally identical detectors ( $\epsilon_{\nu_\mu; \text{Far}}(E_\nu) \approx \epsilon_{\nu_\mu; \text{Near}}(E_\nu)$ ) with a nuclear target of the same atomic mass A:

$$N_{\nu_\mu; \text{Far}}(E_\nu) \propto N_{\nu_\mu; \text{Near}}(E_\nu) \times \frac{\Phi_{\text{Far}}(E_\nu)}{\Phi_{\text{Near}}(E_\nu)} \times P_{\nu_\mu \rightarrow \nu_\mu}(E_\nu)$$

Cancelled detector efficiency and cross-section errors. Flux information enters in a ratio, so only the uncorrelated Far/Near uncertainty plays a role.

# Reliance on models

In practise, the situation is **substantially more complicated**:

- There is no such thing as "functionally identical" detectors
  - Near detector closer to source and at shallower depth
    - Different beam-related backgrounds
    - Different flux (line source vs point source, oscillations!)
  - High rate in the Near hall can necessitate different technology
    - Uncorrelated detector systematics between Near and Far detectors
    - Different acceptance from the (usually  $4\pi$ ) Far detector
    - Different nuclear targets
- The true neutrino energy is not known on an event-by-event basis
  - The true neutrino energy comes from a broad distribution
  - The mapping between the true and reconstructed energy is driven by detailed event characteristics (ID and momentum of all f/s particles)
  - Complex detector response/acceptance for each f/s.

It is **impossible to avoid reliance on models**.

- But models not predictive enough (**Nice summary by Steve yesterday**)

# Reliance on models: $\nu_e$ and $\bar{\nu}_e$ cross-sections

- Large observed value of  $\theta_{13}$  a **mixed blessing**
- Large  $\nu_e$  and  $\bar{\nu}_e$  appearance rate

$$P(\nu_\mu \rightarrow \nu_e) \simeq \boxed{\sin^2 2\theta_{13} \times \sin^2 \theta_{23} \times \frac{\sin^2[(1-x)\Delta]}{(1-x)^2}} \quad \text{Phys. Rev. D64 (2001) 053003}$$

Leading term

CP violating  $-\alpha \sin \delta_{CP} \times \sin^2 2\theta_{12} \sin 2\theta_{13} \sin 2\theta_{23} \times \sin \Delta \frac{\sin[x\Delta]}{x} \frac{\sin[(1-x)\Delta]}{(1-x)}$   
“+” for antineutrino

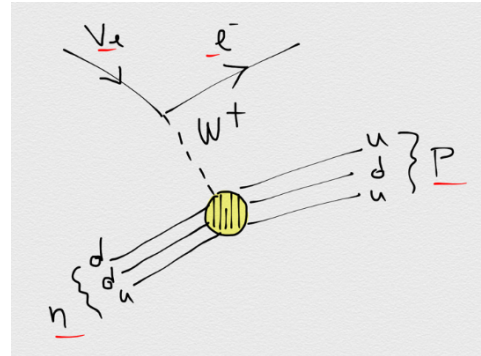
CP conserving  $\alpha \cos \delta_{CP} \times \sin 2\theta_{12} \sin 2\theta_{13} \sin 2\theta_{23} \times \cos \Delta \frac{\sin[x\Delta]}{x} \frac{\sin[(1-x)\Delta]}{(1-x)}$   
 $+ O(\alpha^2)$   $x = \frac{2\sqrt{(2)G_F N_e E}}{\Delta m_{31}^2} \quad \alpha = \left| \frac{\Delta m_{21}^2}{\Delta m_{31}^2} \right| \sim \frac{1}{30} \quad \Delta = \frac{\Delta m_{31}^2 L}{4E}$

- But small CP asymmetry!

$$A_{CP} \propto \frac{\sin 2\theta_{12}}{\sin \theta_{13}} \sin \delta_{CP}$$

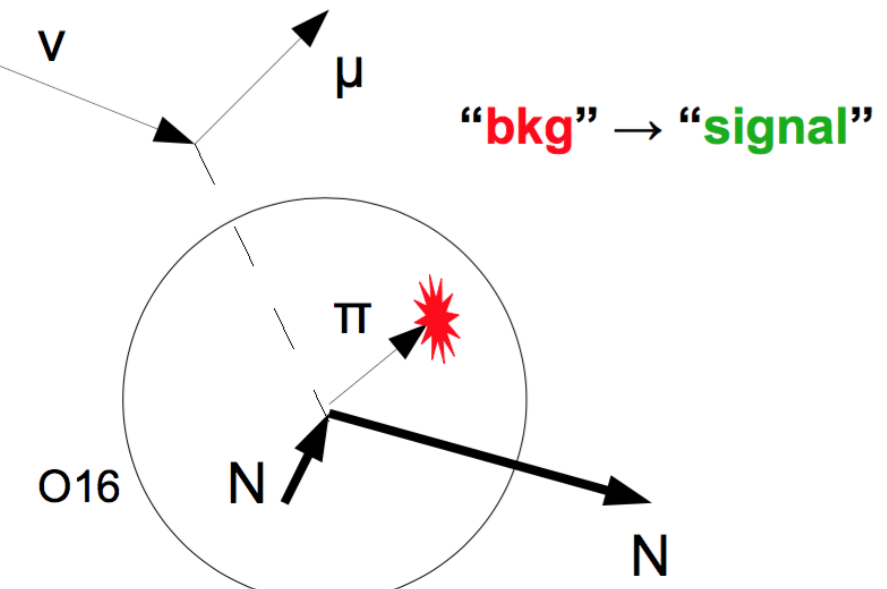
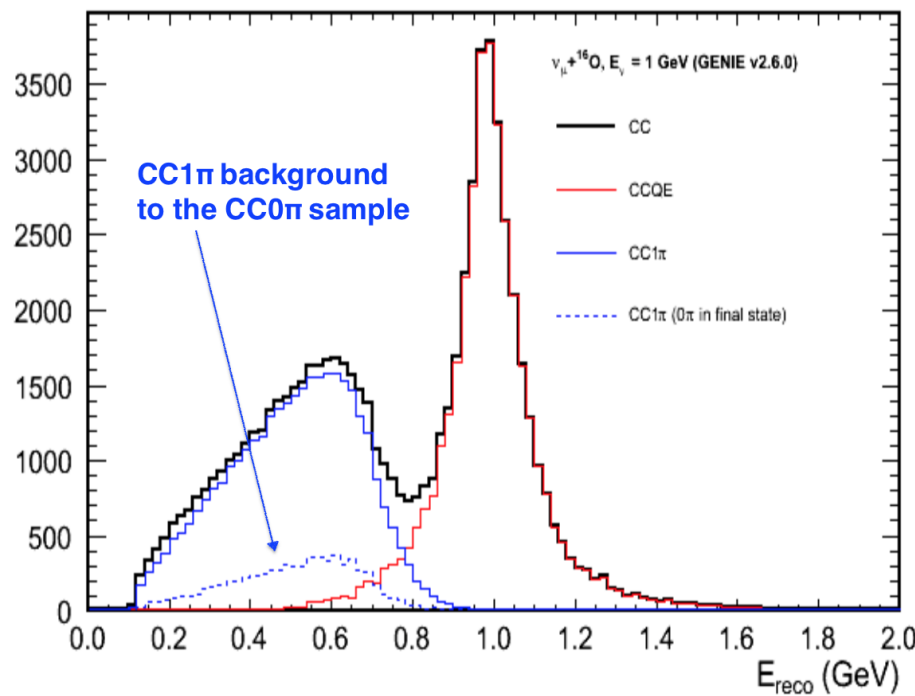
- “Signal” systematics important
  - Oscillation “signal” absent from NDs
  - Intrinsic  $\nu_e$  contamination low and at different energy range

# Reliance on models: Neutrino energy reconstruction

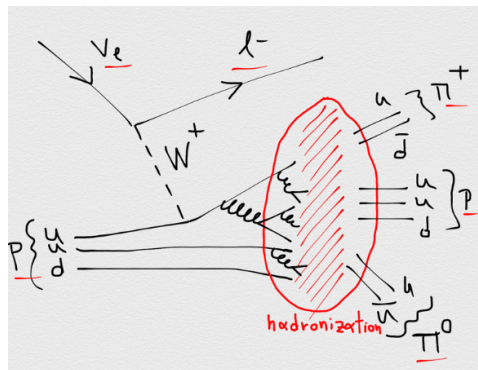


Reconstruction based on **2-body kinematics** for QE-enhanced samples

$$E_\nu = \frac{m_p^2 - (m_n - E_b)^2 - m_\ell^2 + 2(m_n - E_b)E_\ell}{2(m_n - E_b - E_\ell + p_\ell \cos\theta_\ell)}$$

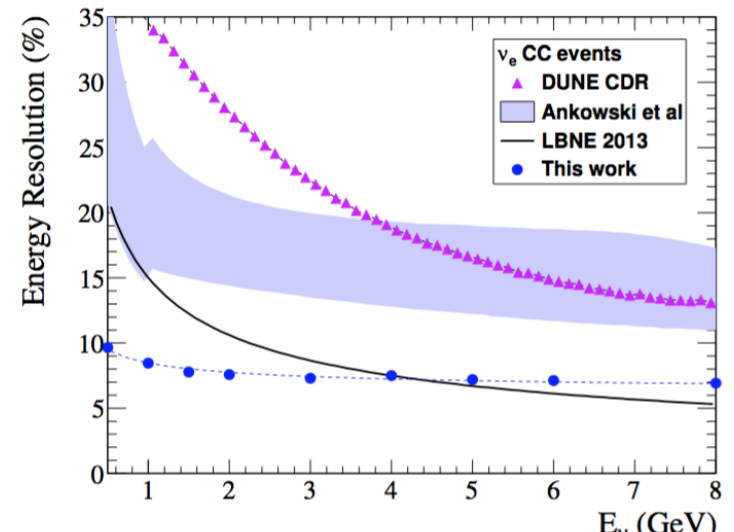
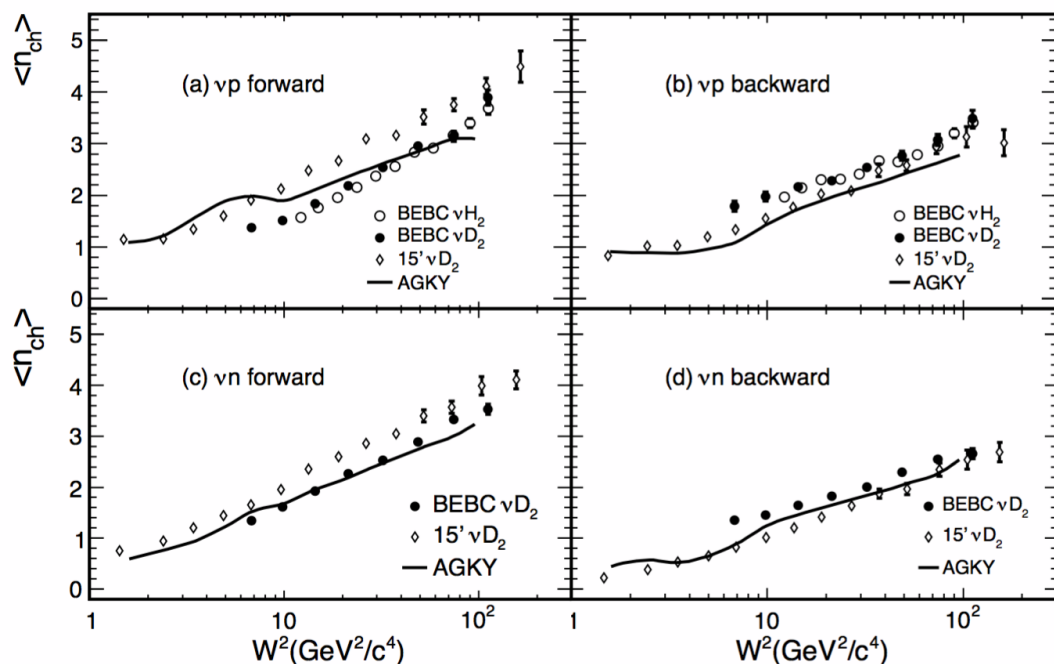


## Reliance on models: Neutrino energy reconstruction



## **Calorimetric approach to energy reconstruction:**

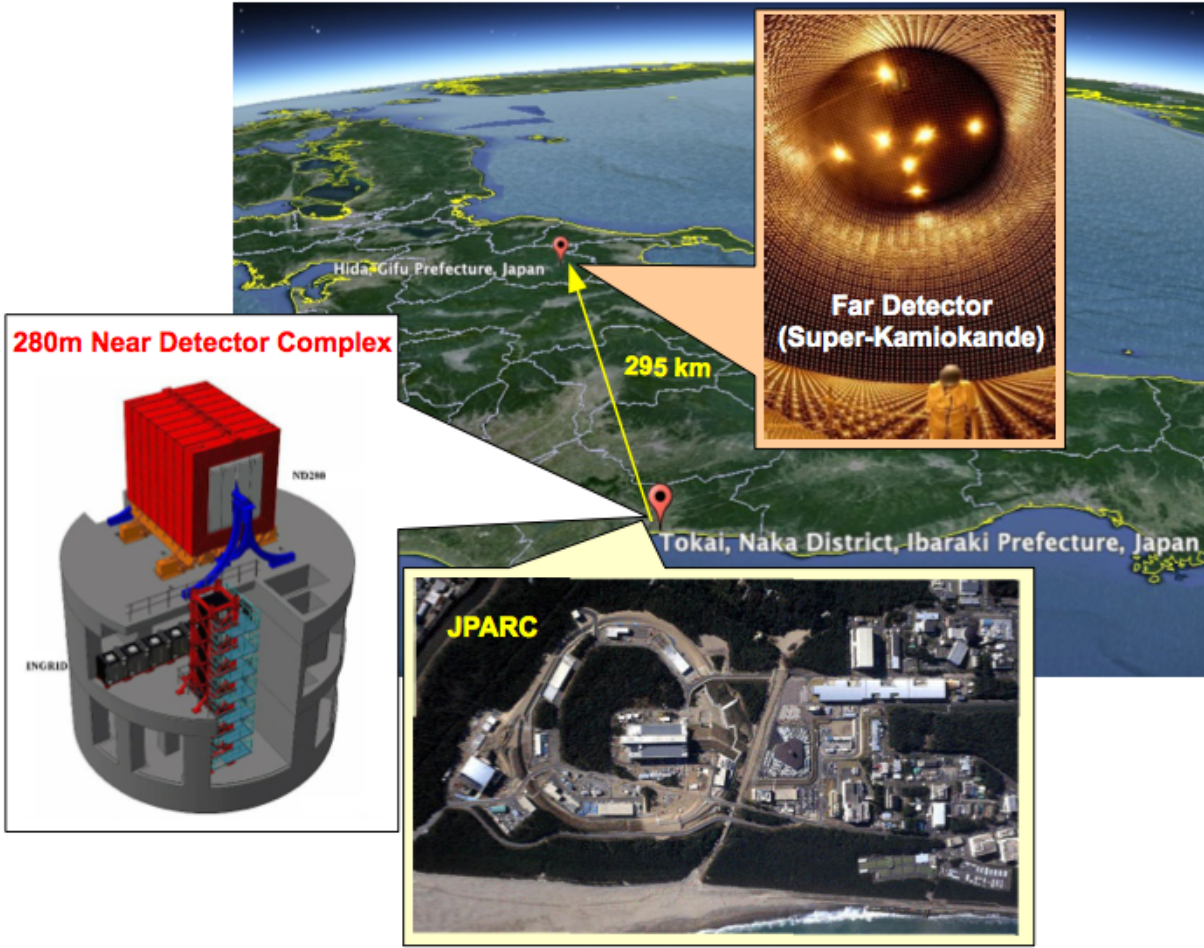
$$E_\nu = E_{leptonic} + E_{hadronic}$$



[arXiv:1607.00293]

[Eur.Phys.J.C63:1-10,2009]

# T2K Experiment



- Pure  $\nu_\mu$  beam.
- Produced using the 30-GeV proton beam at J-PARC
- Design Power of 750 kW (420 kW achieved to date)
- Far detector: SuperK 50-kton (22.5 kton fiducial) water Cherenkov detector, 2.5 degrees off-axis, 295 km away.
- Neutrino flux at SuperK peaked at  $\sim 0.6$  GeV.
- L/E tuned to the ‘atmospheric’  $\Delta m^2$  scale ( $\sim 2.4 \times 10^{-3}$  eV $^2/c^4$ ).

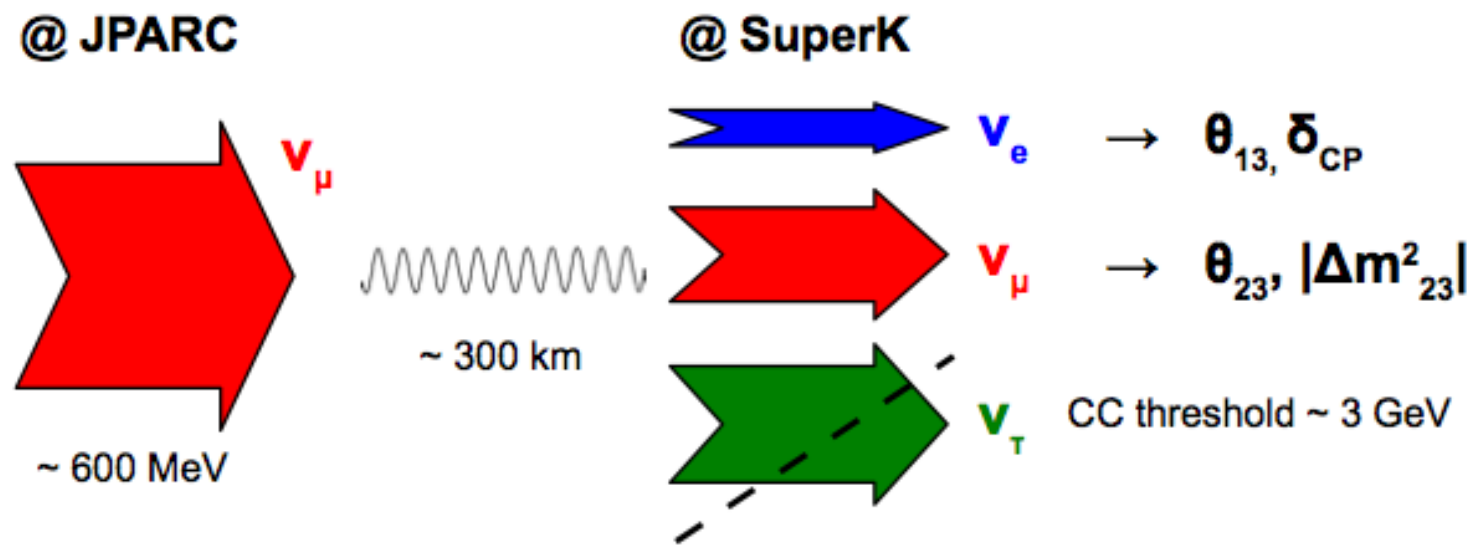
# Measuring neutrino oscillations at T2K

# Muon-neutrino disappearance ( $\nu_\mu \rightarrow \nu_\mu$ )

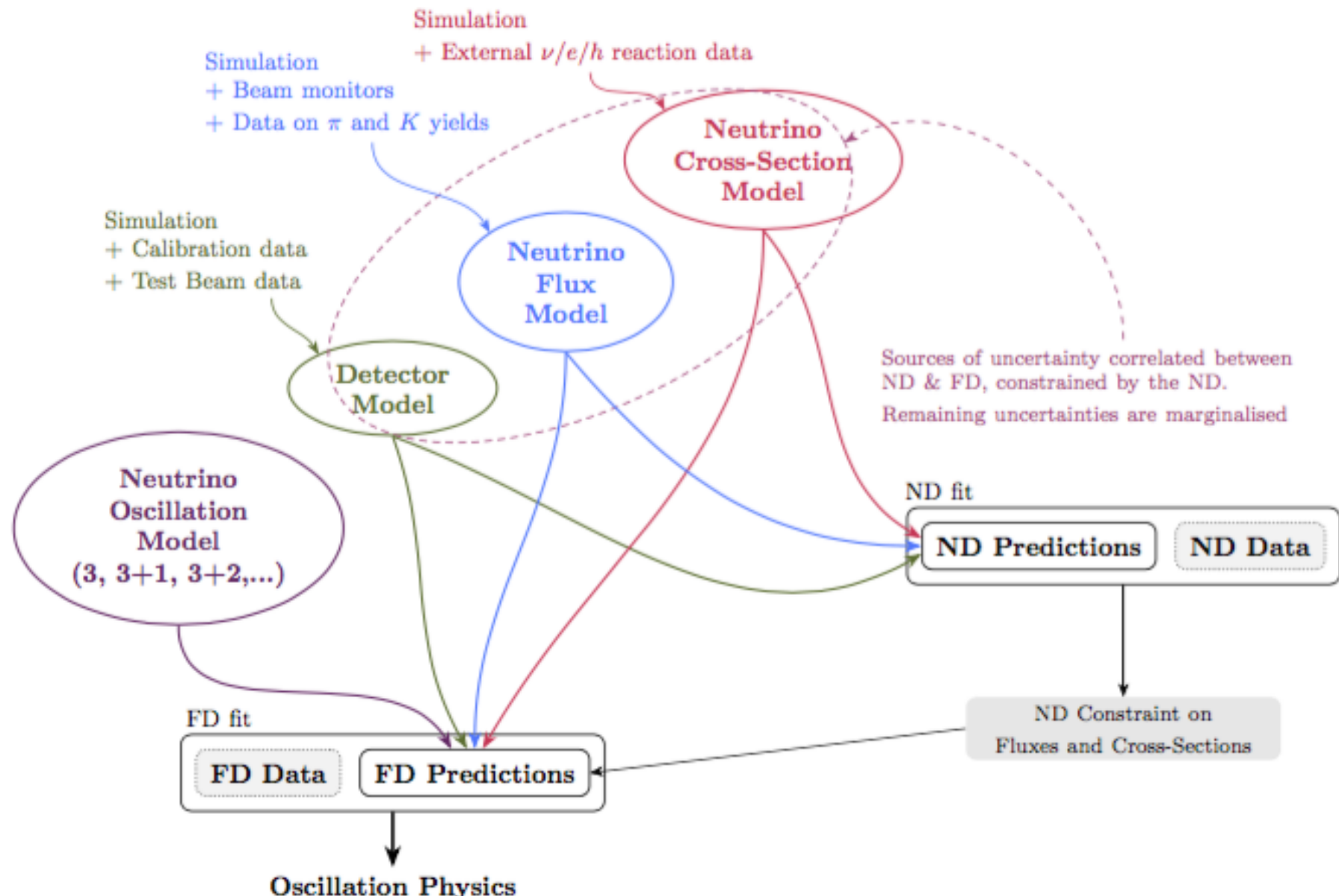
$$P(\nu_\mu \rightarrow \nu_\mu) = 1 - \cos^4\theta_{13} \cdot \sin^2 2\theta_{23} \cdot \sin^2\left(\frac{\Delta m_{31}^2 L}{4F}\right) + \text{sub-leading terms}$$

# Electron-neutrino appearance ( $\nu_\mu \rightarrow \nu_e$ )

$$P(\nu_\mu \rightarrow \nu_e) = 4 \cdot \cos^2 \theta_{13} \cdot \sin^2 \theta_{13} \cdot \sin^2 \theta_{23} \cdot \sin^2 \left( \frac{\Delta m_{31}^2 L}{4F} \right) + \text{sub-leading terms}$$



# Oscillation analysis method



# Systematics constraint from the Near Detector

**Substantial flux and cross-section uncertainties** remain from the tuning of MC simulations using external data.

Further reduction of systematic errors possible using Near Detector data:

- Fit of flux and cross-section systematic parameters using several exclusive / semi-inclusive Near Detector samples.
- Each observed event sample populates a different area of the kinematic phase space ( $E_\nu$ ,  $W$ ,  $Q^2$ ) and is a different mixture of true interaction modes.

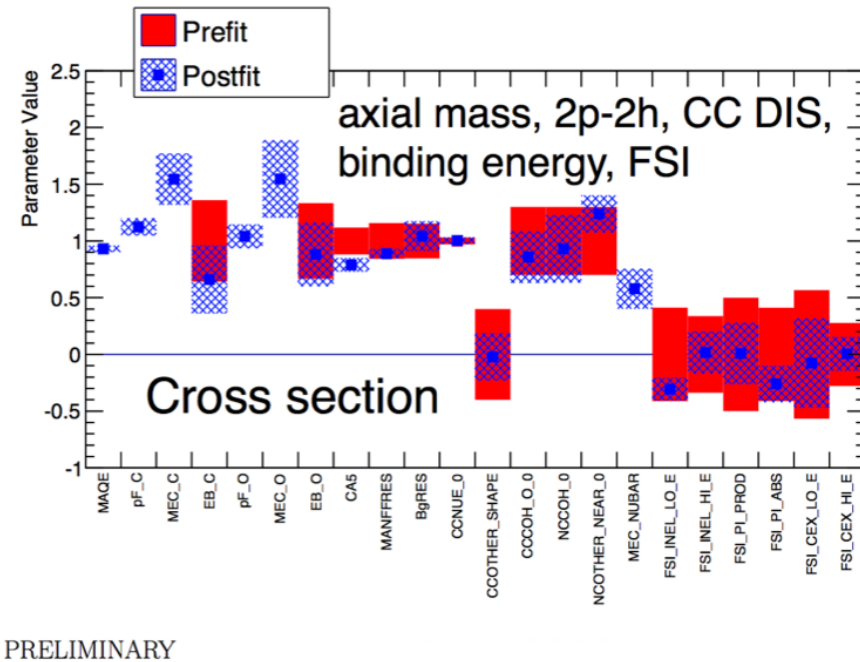
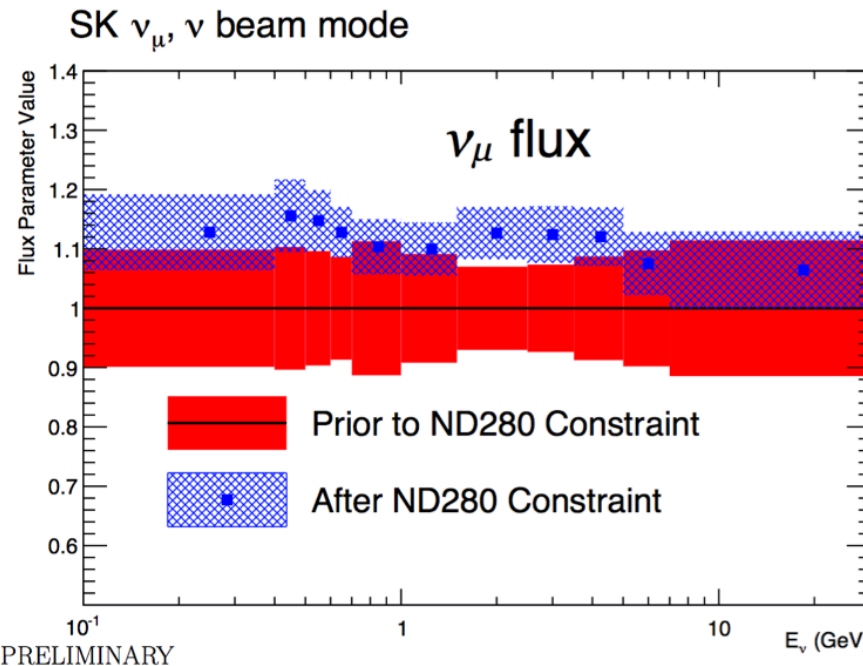
Possible to **cut the correlations between systematic parameters** and place **stringent constraints**.

Best-fit values of systematic parameters also provide an ‘indirect extrapolation’ from the Near to the Far detector.

More details on the T2K interaction model and ND fits in Asher’s talk next!

# Systematics constraint from the Near Detector

Simultaneous fit to Near Detector neutrino and anti-neutrino event samples  
**constraints flux and cross-section systematics.**



- Flux parameters increase by  $\sim 15\%$ .
- Cross-section parameters consistent with nominal values.
- Flux and cross-section parameter highly anti-correlated after the Near Detector data fit.
- Systematic uncertainties in neutrino oscillation analyses from 12-14% to 5-6%.

# Composition of analysis samples

## $\nu$ -mode, 1-ring $\mu$ -like candidates

	$\nu_\mu$	$\nu_e$	$\bar{\nu}_\mu$	$\bar{\nu}_e$	Osc. $\nu_e$	Osc. $\bar{\nu}_e$	Total
CCQE	71.194	0.037	4.620	0.002	0.190	0.002	76.045
CC1pi	18.214	0.019	1.686	0.001	0.061	0.001	19.981
CCcoherent	0.351	0.000	0.086	0.000	0.001	0.000	0.438
MEC	20.442	0.011	0.910	0.000	0.045	0.000	21.408
CCother	8.340	0.009	0.533	0.001	0.002	0.000	8.885
NC1pi0	0.580	0.018	0.019	0.001	N/A	N/A	0.617
NC1piPM	4.253	0.096	0.153	0.009	N/A	N/A	4.511
NCcoherent	0.017	0.000	0.002	0.000	N/A	N/A	0.019
NCother	3.229	0.130	0.178	0.013	N/A	N/A	3.550
NC1gamma	0.004	0.000	0.000	0.000	N/A	N/A	0.004
Total	126.624	0.321	8.185	0.027	0.299	0.003	135.459

- 56% CC QE
- 16% CC 2p-2h
- 15% CC 1 $\pi$

## $\nu$ -mode, 1-ring e-like candidates

	$\nu_\mu$	$\nu_e$	$\bar{\nu}_\mu$	$\bar{\nu}_e$	Osc. $\nu_e$	Osc. $\bar{\nu}_e$	Total
CCQE	0.056	2.129	0.001	0.088	15.875	0.099	18.249
CC1pi	0.016	0.348	0.000	0.027	1.688	0.017	2.096
CCcoherent	0.000	0.002	0.000	0.002	0.015	0.002	0.021
2p-2h	0.008	0.710	0.000	0.022	3.901	0.019	4.659
CCother	0.001	0.045	0.000	0.003	0.029	0.001	0.080
NC1pi0	0.524	0.012	0.017	0.001	N/A	N/A	0.553
NC1piPM	0.099	0.002	0.003	0.000	N/A	N/A	0.105
NCcoherent	0.174	0.004	0.018	0.001	N/A	N/A	0.197
NCother	0.126	0.005	0.008	0.001	N/A	N/A	0.139
NC1gamma	0.464	0.007	0.021	0.001	N/A	N/A	0.494
Total	1.469	3.264	0.069	0.145	21.508	0.138	26.594

# Effect of systematics on SuperK predictions

$\nu$ -mode, 1-ring  $\mu$ -like candidates

Source of uncertainty	$\delta N_{SK}/N_{SK}$
SKDet+FSI+SI	4.13%
SKDet only	3.86%
FSI+SI only	1.48%
Flux	3.60%
Flux (pre-fit)	7.63%
2p-2h (corr)	3.46%
2p-2h-bar (corr)	0.20%
NC other (uncorr)	0.78%
NC 1gamma (uncorr)	0.00%
XSec nue/numu (uncorr)	0.01%
XSec Tot (corr)	4.00%
XSec Tot	4.08%
XSec Tot (pre-fit)	7.73%
Flux+XSec (ND280 constrained)	2.79%
Flux+XSec (All)	2.90%
Flux+XSec+SKDet+FSI+SI	5.03%
Flux+XSec+SKDet+FSI+SI (pre-fit)	12.0%

$\nu$ -mode, 1-ring e-like candidates

Source of uncertainty	$\delta N_{SK}/N_{SK}$
SKDet+FSI+SI	3.46%
SKDet only	2.39%
FSI+SI only	2.50%
Flux	3.64%
Flux (pre-fit)	8.94%
2p-2h (corr)	3.87%
2p-2h bar (corr)	0.05%
NC other (uncorr)	0.16%
NC 1gamma (uncorr)	1.44%
XSec nue/numu (uncorr)	2.65%
XSec Tot (corr)	4.13%
XSec Tot	5.12%
XSec Tot (pre-fit)	7.17%
Flux+XSec (ND280 constrained)	2.88%
Flux+XSec (All)	4.17%
Flux+XSec+SKDet+FSI+SI	5.41%
Flux+XSec+SKDet+FSI+SI (pre-fit)	11.9%

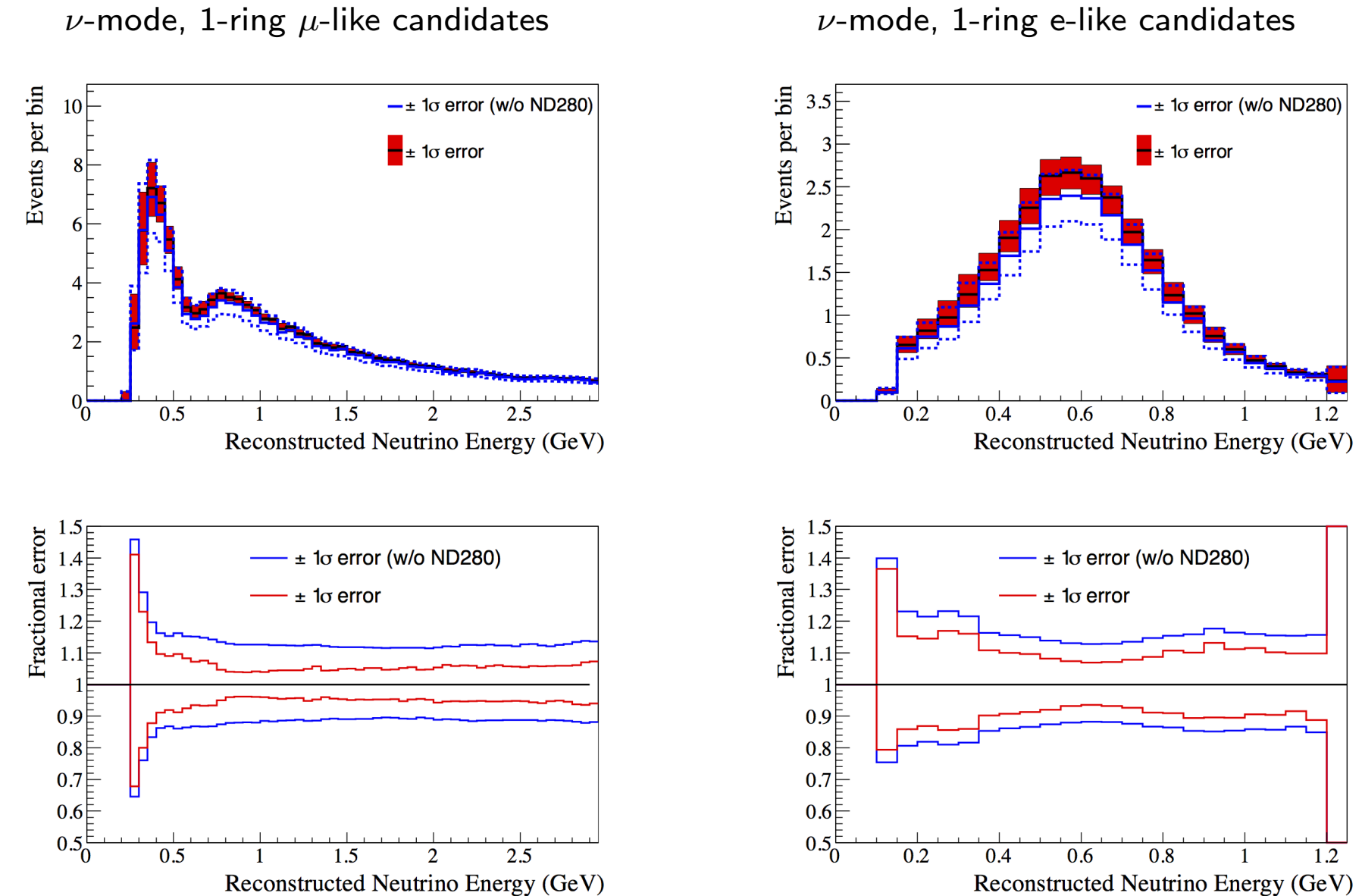
Effect of  $1\sigma$  variations on the total number of events 1-ring  $\mu$ -like and e-like events for neutrino mode given by all the systematic uncertainties, obtained by performing 10k toys MC.

The RMS of the distribution is assumed to be the  $1\sigma$  uncertainty.

Using:  $\delta_{CP} = -1.601$ ,  $\theta_{23} = 0.528$  and  $\Delta m_{32}^2$  ( $\Delta m_{13}^2$ ) =  $2.509 \times 10^{-3} \text{ eV}^2/c^4$ .

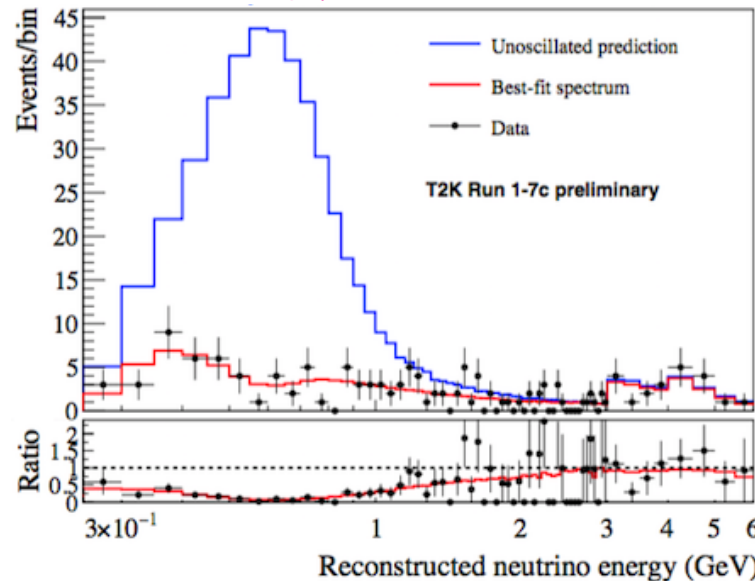
The global values from PDG 2016 are used as uncertainties on  $\sin^2 \theta_{13}$ ,  $\sin^2 \theta_{12}$  and  $\Delta m_{21}^2$ .

# Effect of systematics on SuperK predictions

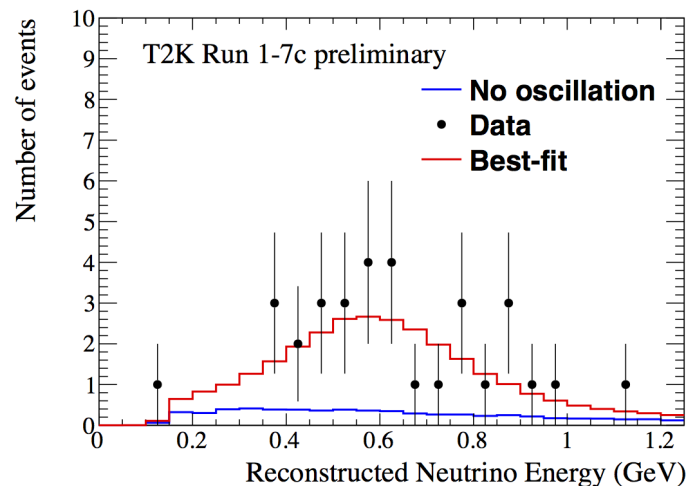


# T2K 1-ring $\mu$ -like and e-like candidates

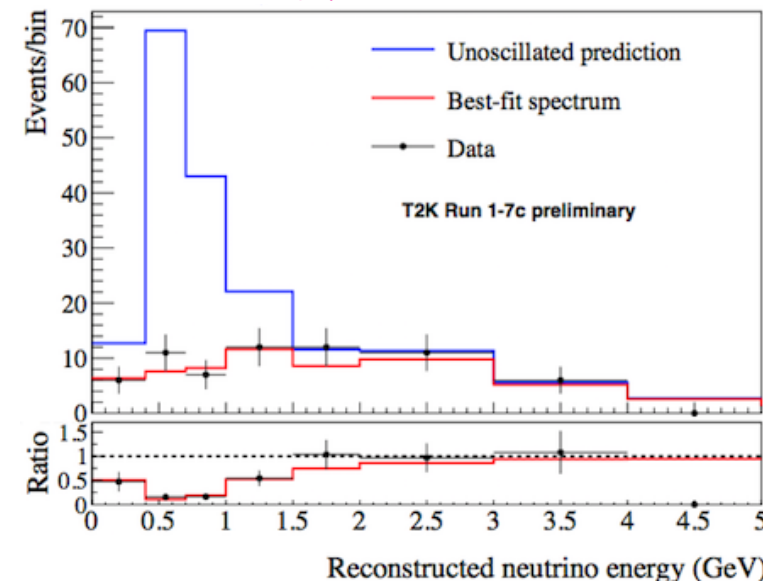
$\nu$ -mode, 1-ring  $\mu$ -like candidates:



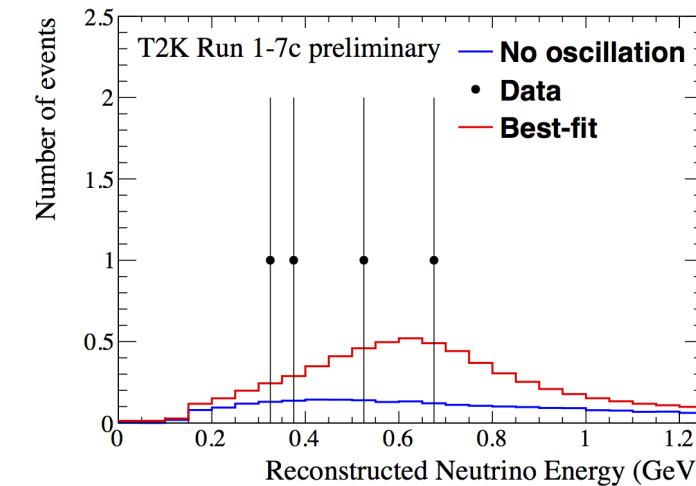
$\nu$ -mode, 1-ring e-like candidates:



$\bar{\nu}$ -mode, 1-ring  $\mu$ -like candidates:



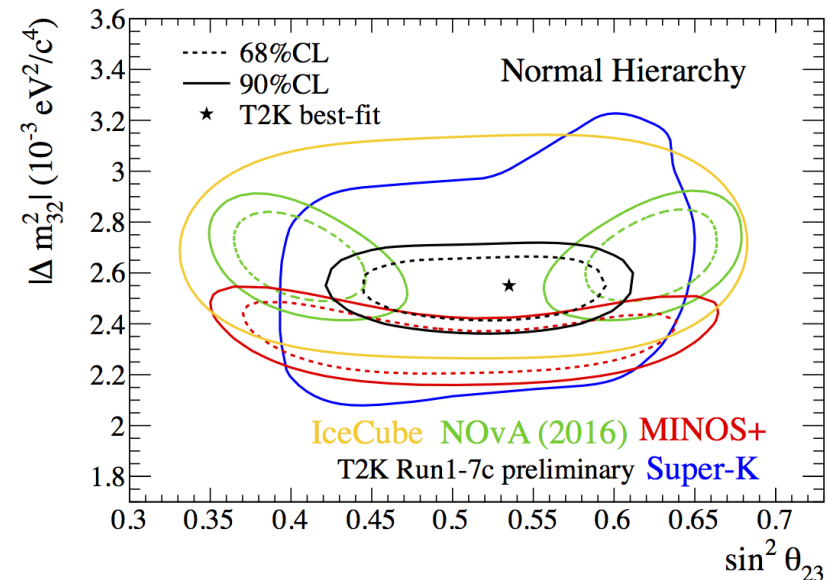
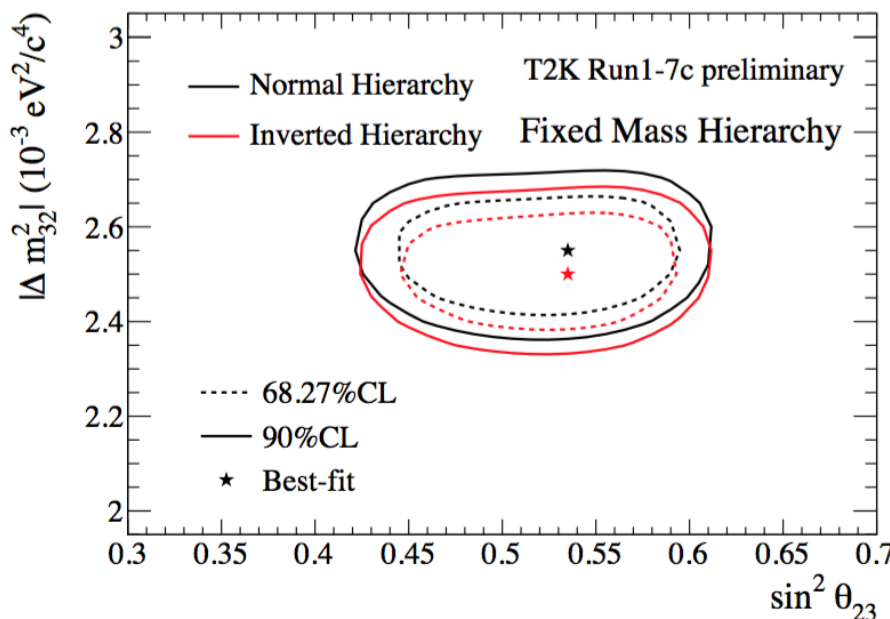
$\bar{\nu}$ -mode, 1-ring e-like candidates:



# T2K joint 3-flavour analysis: $\sin^2\theta_{23}$ and $|\Delta m_{32}^2|$

Joint measurement of  $\sin^2\theta_{23}$  and  $|\Delta m_{32}^2|$

- The  $\nu_\mu, \bar{\nu}_\mu$  disappearance constrain  $\sin^2 2\theta_{23}$  and  $|\Delta m_{32}^2|$ .
- The  $\nu_e, \bar{\nu}_e$  appearance samples help lift the  $\theta_{23}$  octant degeneracy.

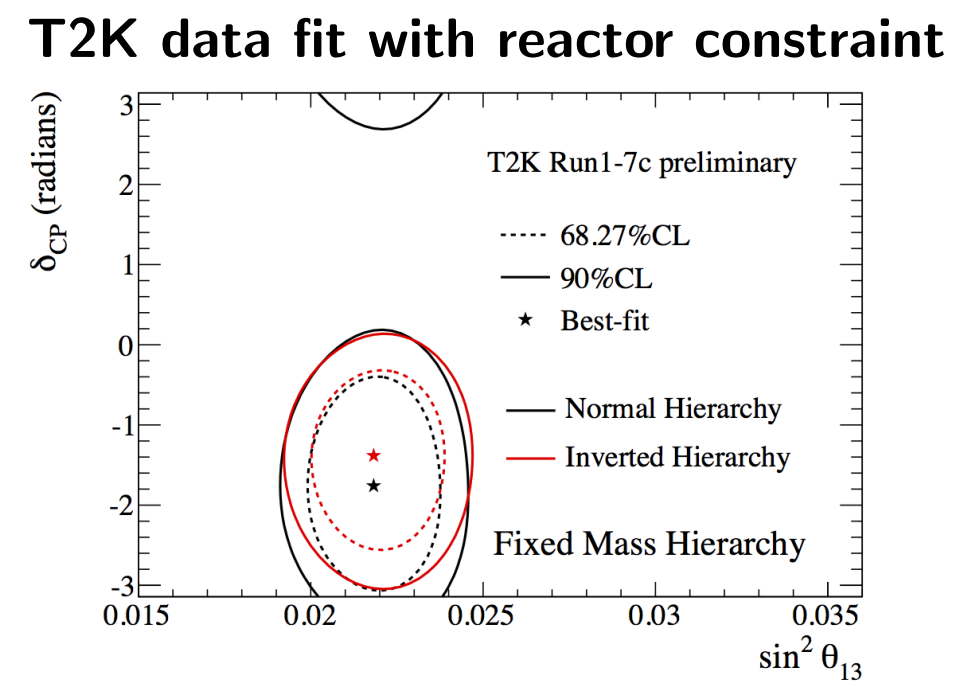
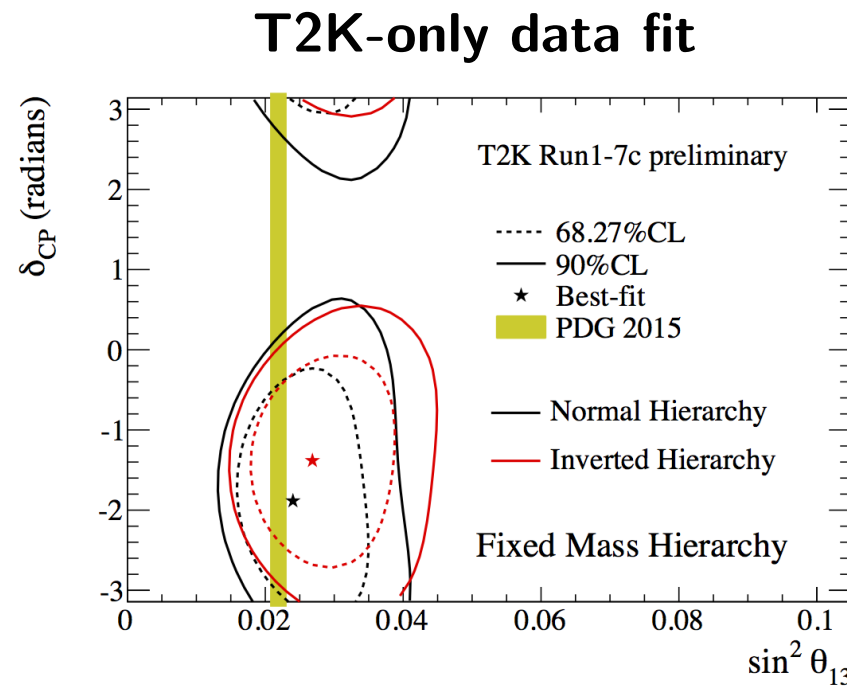


- Consistent with **maximal mixing**.
- Some tension with NOvA results.

Best-fit parameter	NH	IH
$\sin^2\theta_{23}$	0.532	0.534
$ \Delta m_{32}^2  (\times 10^{-3} \text{ eV}^2)$	2.545	2.510

# T2K joint 3-flavour analysis: $\theta_{13}$ and $\delta_{CP}$

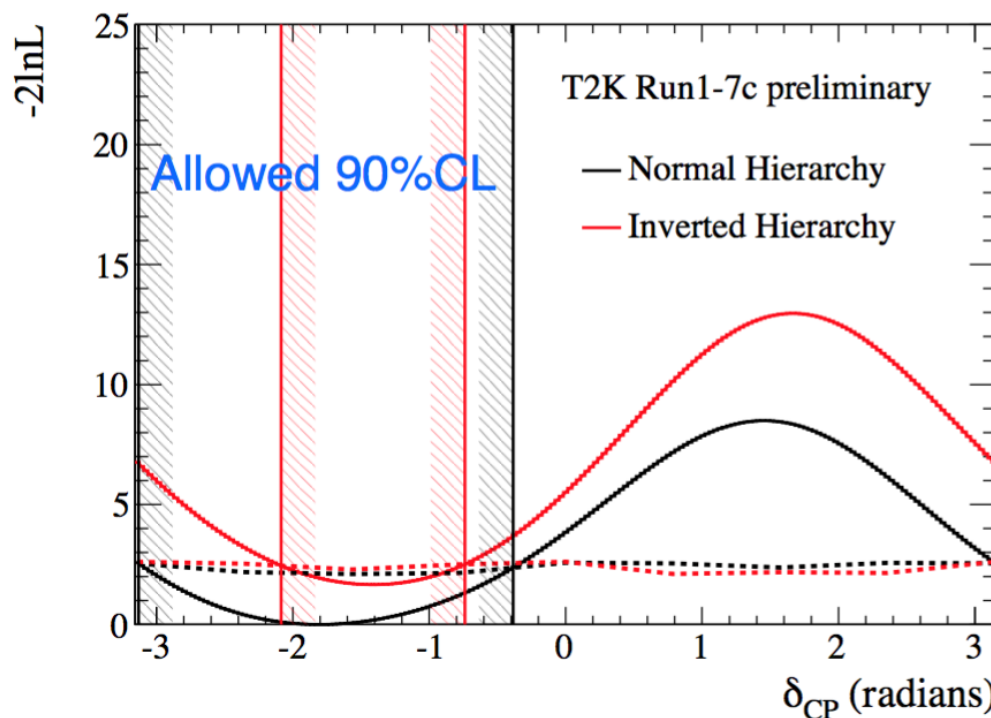
- Good agreement with the reactor measurement of  $\theta_{13}$ 
  - $\sin^2 2\theta_{13} = 0.085 \pm 0.005$  [PDG2015]
- T2K-only data **disfavor the region of  $\delta_{CP}$  around  $\pi/2$ .**
- T2K **prefers  $-\pi/2$**  for both NH and IH.



Mass hierarchy is fixed to either normal or inverted. Contours with constant  $\Delta\chi^2$  method (gaussian approximation)

# T2K joint 3-flavour analysis: $\delta_{CP}$

- Best-fit:  $\delta_{CP} = -1.885$ , NH
- $\delta_{CP} = 0$  is excluded at  $2\sigma$  C.L., while  $\delta_{CP} = \pi$  is excluded at 90% C.L.
- Allowed 90% C.L. regions:  $[-3.13, 0.39]$  (NH),  $[-2.09, -0.74]$  (IH)



Confidence intervals computed with Feldman-Cousins method to guarantee frequentist coverage.

# Dependence on cross-section model choices

Near detector data reduce dependence on interaction simulations.

To what extend?

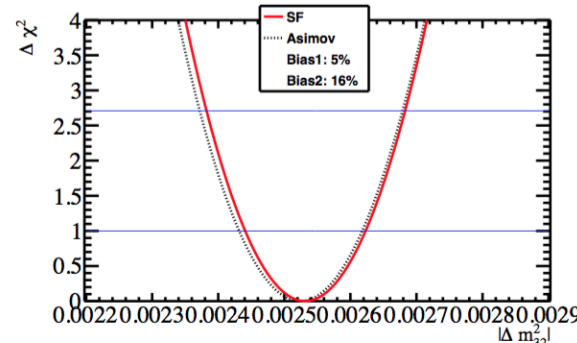
Several studies were made using "alternative" models testing effect of:

- Spectral Function model
- Shape and strength of RPA correction
- Differences between Martini and Nieves 2p-2h
- Effect of 2p-2h models on lepton kinematics
- Differences between nominal and Nieves 1p-1h

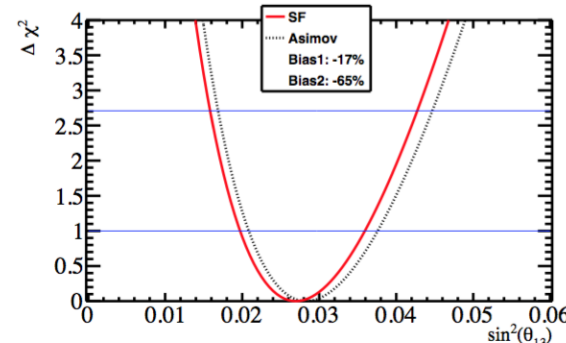
More details in Asher's talk next

# Dependence on cross-section model choices (example)

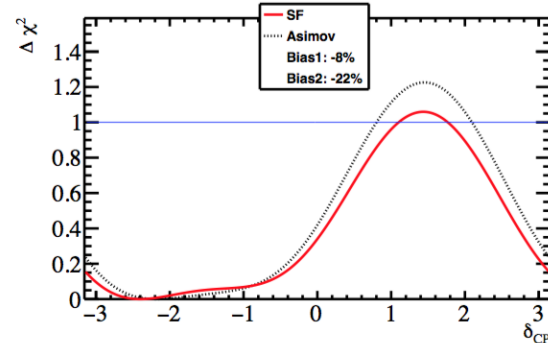
Effect of Spectral Function model:



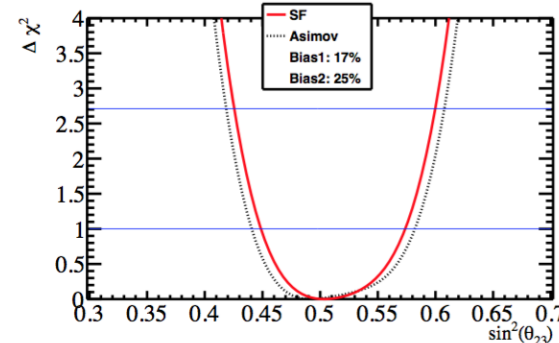
(a)  $|\Delta m_{32}^2|$



(b)  $\sin^2(\theta_{13})$



(c)  $\delta_{CP}$



(d)  $\sin^2(\theta_{23})$

Using:  $\delta_{CP} = -1.601$ ,  $\sin^2\theta_{23} = 0.528$ ,  $\sin^2\theta_{13} = 0.025$ ,  $\sin^2\theta_{12} = 0.306$ ,  $\Delta m_{32}^2$  ( $\Delta m_{13}^2$ ) =  $2.509 \times 10^{-3} \text{ eV}^2/c^4$ , and  $\Delta m_{31}^2 = 7.5 \times 10^{-5} \text{ eV}^2/c^4$ .

# Dependence on cross-section model choices

Maximum bias seen for any set of true oscillation parameters considered  
(Current exposure)

Fake data	Maximum absolute bias on parameter ( $\sigma$ )			
	$\Delta m_{23}^2$	$\sin^2 \theta_{23}$	$\sin^2 \theta_{13}$	$\delta_{CP}$
SF	0.09	0.17	0.17	0.10
ERPA	0.00	0.06	0.00	0.04
Martini 2p-2h	0.04	0.12	0.06	0.11
Martini 2p-2h with $\bar{\nu}$ 2p-2h parameter with reactor constraint	0.10	0.08 0.13	0.10	0.75 0.03
PDD-like 2p-2h with reactor constraint	0.09	0.02 0.03	0.03	0.07 0.13
NonPDD-like 2p-2h with reactor constraint	0.20	0.13 0.20	0.06	0.05 0.07
Nieves-NEUT 1p-1h with reactor constraint	0.45	0.02 0.00	0.09	0.51 0.31
Nieves-NEUT 1p-1h with ND280 error with reactor constraint	0.30	0.02 0.06	0.10	0.55 0.36

# Dependence on cross-section model choices

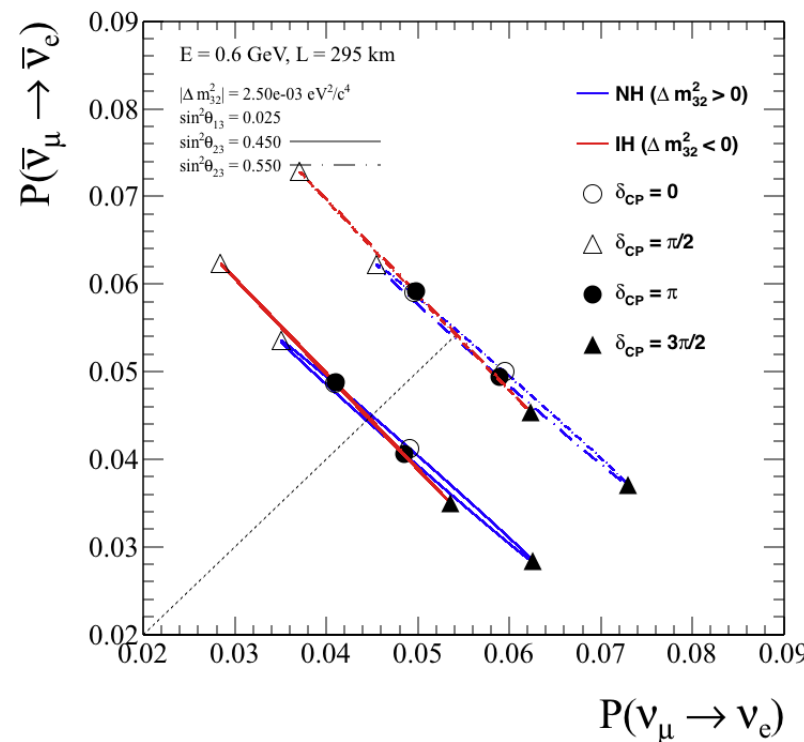
Difference between the number of events at SK predicted by a) ND280 fake data fit, and b) actual SK fake data (Current exposure)

Fake data	$1R_\mu$	$1R_e$	RHC $1R_\mu$	RHC $1R_e$
SF	3.91	5.58	3.92	3.55
ERPA	0.30	2.19	-1.02	-1.21
Martini $2p\text{-}2h$	2.27	-0.83	4.67	5.97
Martini with $\bar{\nu}$ $2p\text{-}2h$ parameter	2.86	1.94	1.19	0.69
PDD-like $2p\text{-}2h$	-0.04	-0.72	1.32	3.48
NonPDD-like $2p\text{-}2h$	3.31	3.49	3.33	1.39
Nieves-NEUT $1p\text{-}1h$	3.48	2.50	4.33	3.08
Nieves-NEUT $1p\text{-}1h$ with ND280 error	2.69	3.37	3.31	3.27

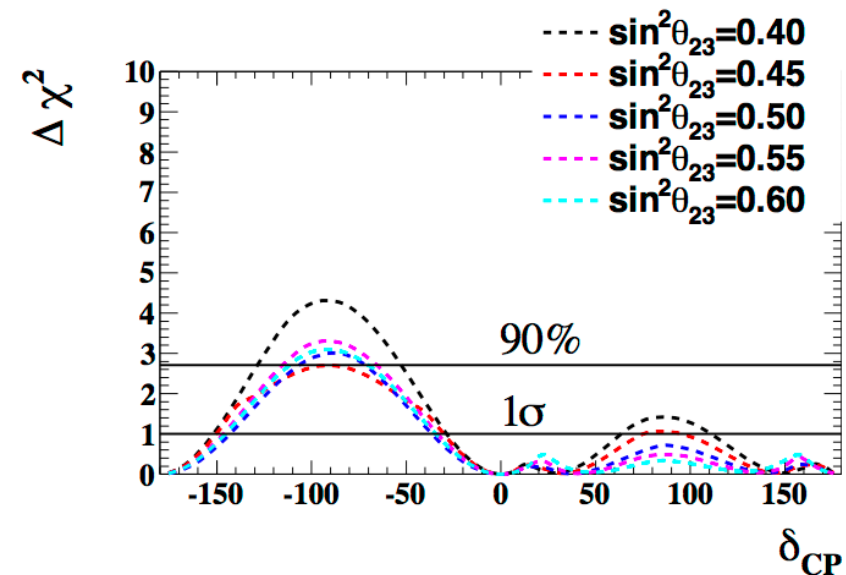
Numbers shown are percentages and positive when the ND280-driven prediction is larger than the SK fake data.

# Current → Future long-baseline oscillation programme

- T2K statistics limited
- Systematic error starts to be dominated by SuperK detector errors
- Limited CP sensitivity outside "sweet spots"

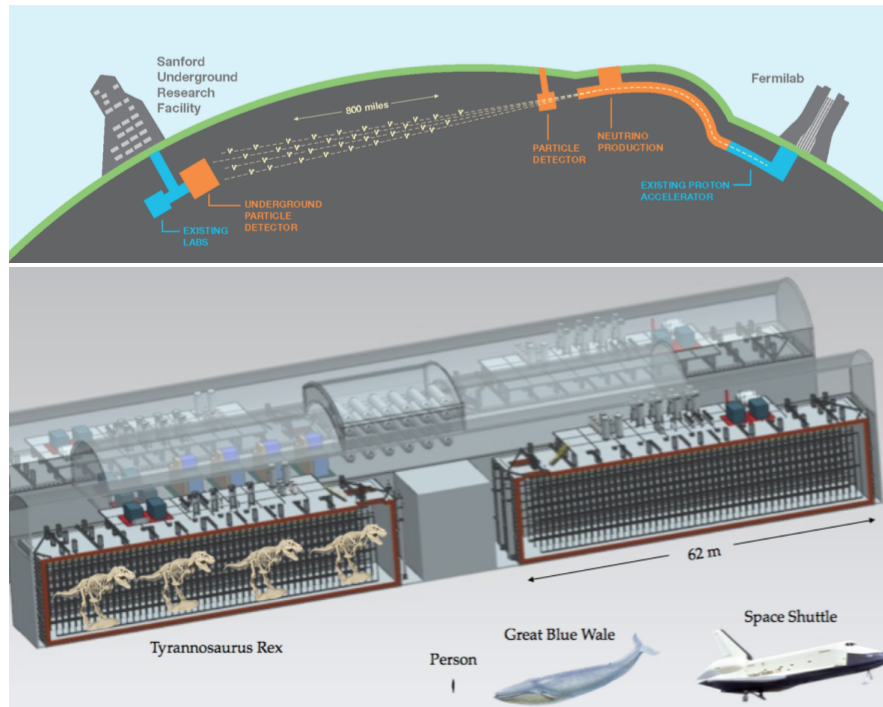


True MH: NH, Full T2K exposure,  
50%  $\nu$  - 50%  $\bar{\nu}$



The question of how physics systematics impact oscillation measurements becomes (more) pertinent for the next generation of LBL experiments.

# Future long-baseline oscillation programme

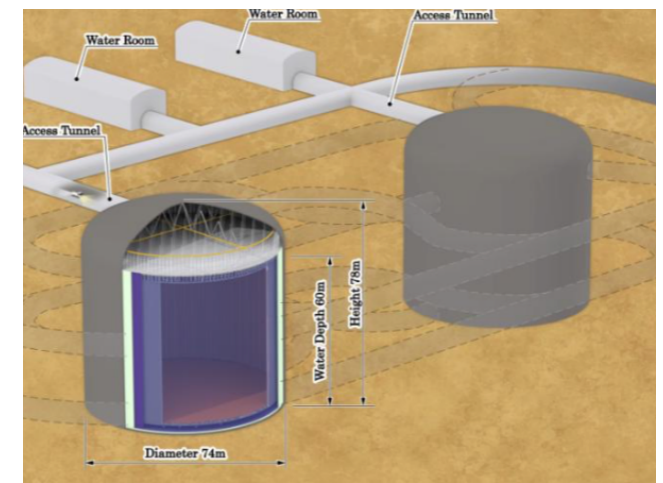


## DUNE:

- New **wide-band**  $\nu_\mu/\bar{\nu}_\mu$  beam at FNAL pointing towards SURF (**1300 km** away)
  - 1.2 MW protons from PIP-II by 2026.
  - Upgradeable to **2.4 MW by 2030!**
- **40-kt fiducial mass LAr TPC** located deep underground at SURF **4850-ft** level
  - first 10-kt module deployed in 2024!
- **High-resolution/fine-grained near detector**

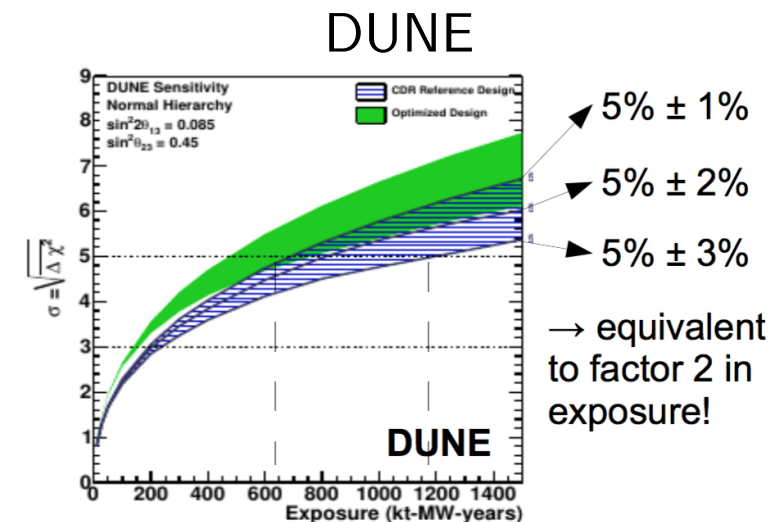
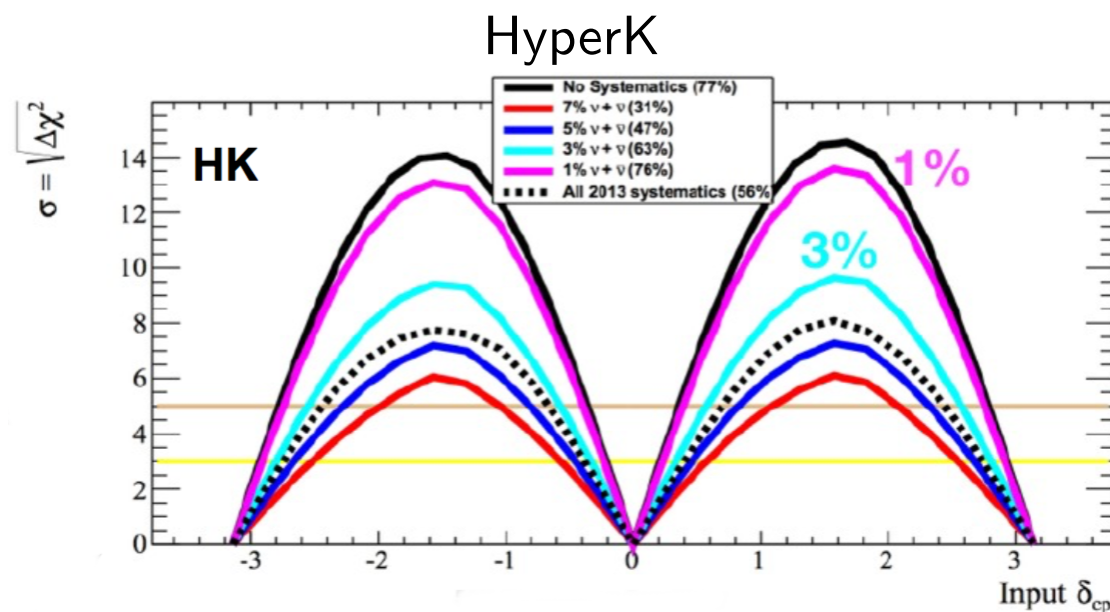
## HyperK:

- Upgraded narrow-band  $\nu_\mu/\bar{\nu}_\mu$  beam from the 30-GeV proton beam at J-PARC, reaching power of  $> 1.3$  MW.
- Upgraded near detector at 280 m and new intermediate WCkv detector at 1-2 km to constrain systematics.
- New 0.52 Mt (0.38 Mton fiducial) WCkv detector, 2.5° off-axis, 295 km away, instrumented with 80k PMTs (40% photo-coverage)



# Systematic error requirements for future LBL

Systematic error requirements for DUNE and HyperK well understood.



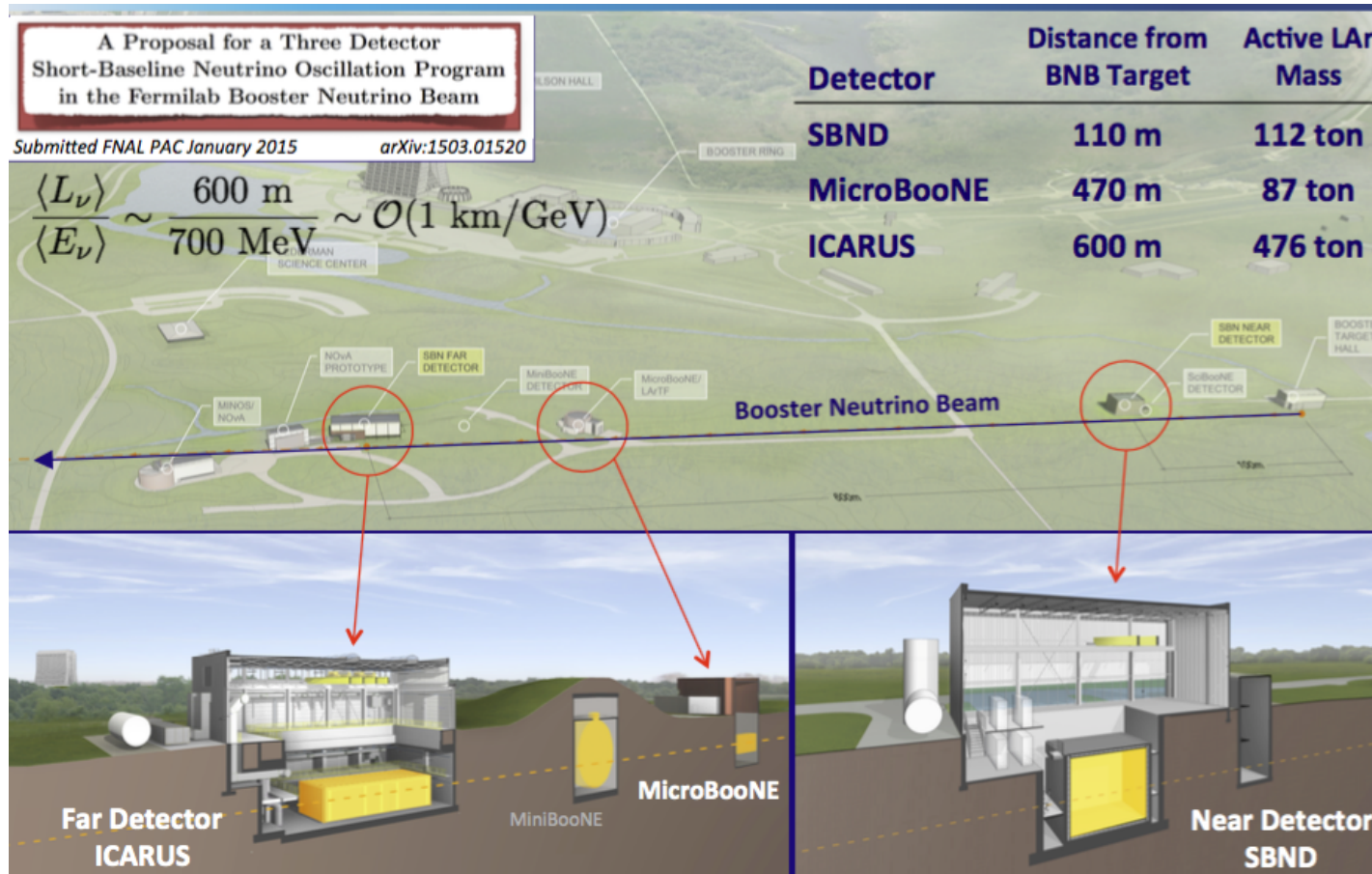
# Mitigating effects of cross-section systematics

DUNE, HyperK could be taking first beam data at 2026!!

Several efforts to mitigate the effects of cross-section uncertainties:

- **New cross-section measurements** (before 2026)
  - Upgraded ND280, MINERvA, NOvA,...
  - **SBN(D)**: Generational advance in cross-section studies!
- **New theoretical work**
- **Continued upgrade of our comprehensive MCs**
  - GENIE Incubator - Main community/generator interface
- **Global neutrino cross-section fits**
  - Effort to interface GENIE with Professor (used for general purpose MC tuning at the LHC) supported via an IPPP Associateship award.  
*Presentation by Marco Roda in this meeting.*
  - Nuisance effort  
*Presentation by Patrick Stowell in this meeting.*
- **Design and build highly-capable DUNE and HyperK NDs**

# Near-future measurements @ SBN



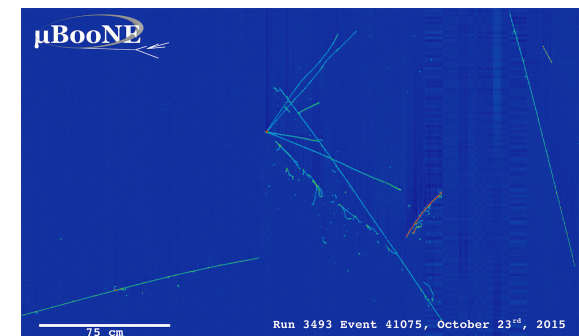
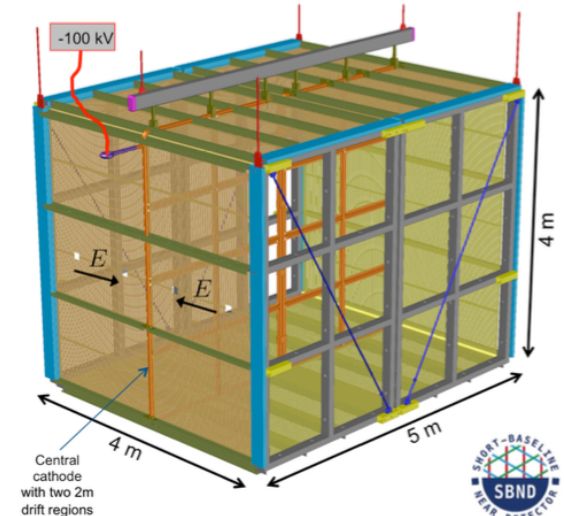
Physics data-taking: SBND: Early 2019,  $\mu$ BooNE: now, ICARUS: 2018.

# Near-future measurements @ SBN

O(100 tonnes) liquid Argon TPCs with "bubble chamber"-like imaging capabilities: O(100k) - O(1M) event samples for key samples!

## SBND event rates for an exposure of $6.6 \times 10^{20}$ POT

Process	No. Events	
<i><math>\nu_\mu</math> Events (By Final State Topology)</i>		
CC Inclusive	5,212,690	
CC 0 $\pi$	$\nu_\mu N \rightarrow \mu + Np$ · $\nu_\mu N \rightarrow \mu + 0p$ · $\nu_\mu N \rightarrow \mu + 1p$ · $\nu_\mu N \rightarrow \mu + 2p$ · $\nu_\mu N \rightarrow \mu + \geq 3p$	3,551,830 793,153 2,027,830 359,496 371,347
CC 1 $\pi^\pm$	$\nu_\mu N \rightarrow \mu + \text{nucleons} + 1\pi^\pm$	1,161,610
CC $\geq 2\pi^\pm$	$\nu_\mu N \rightarrow \mu + \text{nucleons} + \geq 2\pi^\pm$	97,929
CC $\geq 1\pi^0$	$\nu_\mu N \rightarrow \mu + \text{nucleons} + \geq 1\pi^0$	497,963
NC Inclusive	1,988,110	
NC 0 $\pi$	$\nu_\mu N \rightarrow \text{nucleons}$	1,371,070
NC 1 $\pi^\pm$	$\nu_\mu N \rightarrow \text{nucleons} + 1\pi^\pm$	260,924
NC $\geq 2\pi^\pm$	$\nu_\mu N \rightarrow \text{nucleons} + \geq 2\pi^\pm$	31,940
NC $\geq 1\pi^0$	$\nu_\mu N \rightarrow \text{nucleons} + \geq 1\pi^0$	358,443
<i><math>\nu_e</math> Events</i>		
CC Inclusive	36798	
NC Inclusive	14351	
Total $\nu_\mu$ and $\nu_e$ Events	7,251,948	

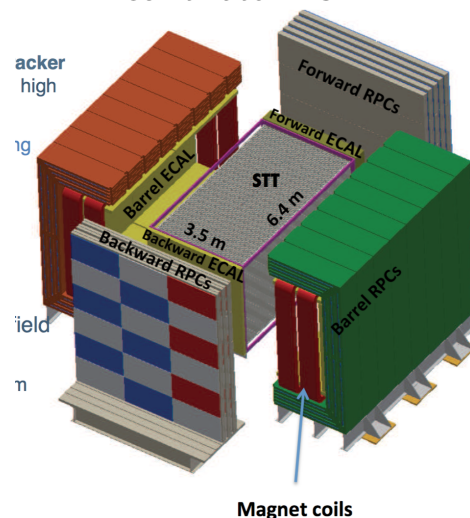


# Near detectors at future LBL experiments

Several exciting and highly capable ND systems proposed for future LBL experiments, in particular for DUNE:

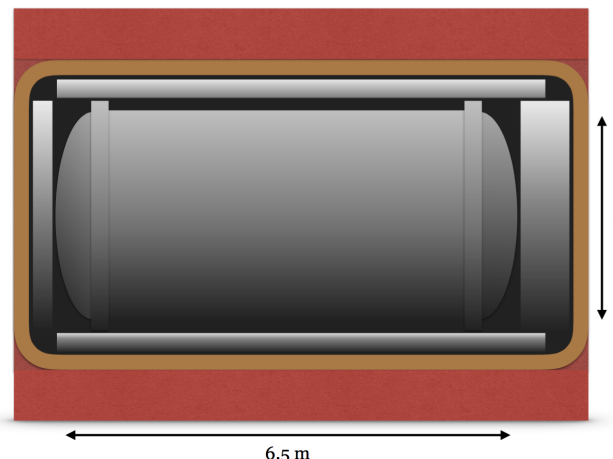
## Fine-Grained Tracker

Active low-density straw-tube tracker in 0.4 T B field with embedded high pressure argon gas targets. Target mass  $\sim 7$  tonnes. In  $4\pi$  plastic scintillator ECAL.



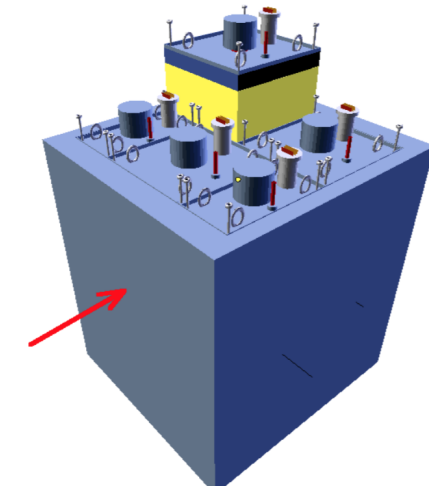
## Gas Argon TPC

1 tonne of gas Argon at 10 bar pressure in a titanium alloy vessel. In a 0.4 T B field and surrounded by a  $4\pi$  plastic scintillator ECAL.



## Liquid Argon TPC

Magnetized, modular LAr TPC sharing common cryostats. Shorter drift times and contained scintillation light in each module. Pixelated charge readout for 3-D reconstruction.



- Do proposed detectors meet the DUNE systematic error requirements?
- How to best optimize the DUNE near detector system?

# ND performance evaluation considerations

- ND **performance evaluation was debated extensively** in DUNE.
- multi-dimensional optimization problem.
- We took a very **broad and inclusive approach**.
- At the systematic error regime of DUNE, **any of a large number of systematics** can limit the sensitivity substantially.  
For each proposed ND concept:
  - Demonstrate adequate error reduction across the board.
  - → Employ a multi-channel analysis (VALOR)
- Not sufficient to just optimise a resolution or efficiency
  - Use **oscillation physics driven metrics**.
- Use **mock-up reconstruction**.
  - '*Cheating but not lying*' (Steve Brice)
  - Try to reflect the ultimate performance of reconstruction tools after years of experience of operating each detector.

# Analysis method

**Likelihood fit of physics systematics** to kinematical distributions of 46 DUNE ND samples.  
The following 23 samples are used for the neutrino-enhanced (FHC) beam configuration:

- $\nu_\mu$  CC

- 1 1-track  $0\pi$  ( $\mu^-$  only)
- 2 2-track  $0\pi$  ( $\mu^-$  + nucleon)
- 3 N-track  $0\pi$  ( $\mu^-$  + ( $>1$ ) nucleons)
- 4 3-track  $\Delta$ -enhanced ( $\mu^- + \pi^+ + p$ ,  $W_{reco} \approx 1.2$  GeV)
- 5  $1\pi^\pm$  ( $\mu^- + 1\pi^\pm + X$ )
- 6  $1\pi^0$  ( $\mu^- + 1\pi^0 + X$ )
- 7  $1\pi^\pm + 1\pi^0$  ( $\mu^- + 1\pi^\pm + 1\pi^0 + X$ )
- 8 Other

- Wrong-sign  $\nu_\mu$  CC

- 9  $0\pi$  ( $\mu^+ + X$ )
- 10  $1\pi^\pm$  ( $\mu^+ + \pi^\pm + X$ )
- 11  $1\pi^0$  ( $\mu^+ + \pi^0 + X$ )
- 12 Other

- $\nu_e$  CC

- 13  $0\pi$  ( $e^- + X$ )
- 14  $1\pi^\pm$  ( $e^- + \pi^\pm + X$ )
- 15  $1\pi^0$  ( $e^- + \pi^0 + X$ )
- 16 Other

- Wrong-sign  $\nu_e$  CC

- 17 Inclusive

- NC

- 18  $0\pi$  (nucleon(s))
- 19  $1\pi^\pm$  ( $\pi^\pm + X$ )
- 20  $1\pi^0$  ( $\pi^0 + X$ )
- 21 Other

- $\nu$ -e

- 22  $\nu_e + e^-$  elastic
- 23 Inverse  $\mu$  decay  $\nu_\mu + e^- \rightarrow \mu^- + \nu_e$  and  $\bar{\nu}_e + e^- \rightarrow \mu^- + \bar{\nu}_\mu$  (annih.)

and a similar set of 23 samples for the antineutrino enhanced (RHC) beam configuration.

# Physics systematics in the VALOR fit

- **208 neutrino flux systematics:**  
Normalization factors for "bins" in the 4-D space of (detector hall, beam configuration, neutrino species, energy range).
- **43 neutrino interaction systematics:**  
See next page.
- **310 detector systematics**

# Neutrino interaction systematics in the VALOR fit

## Neutrino cross-section systematics:

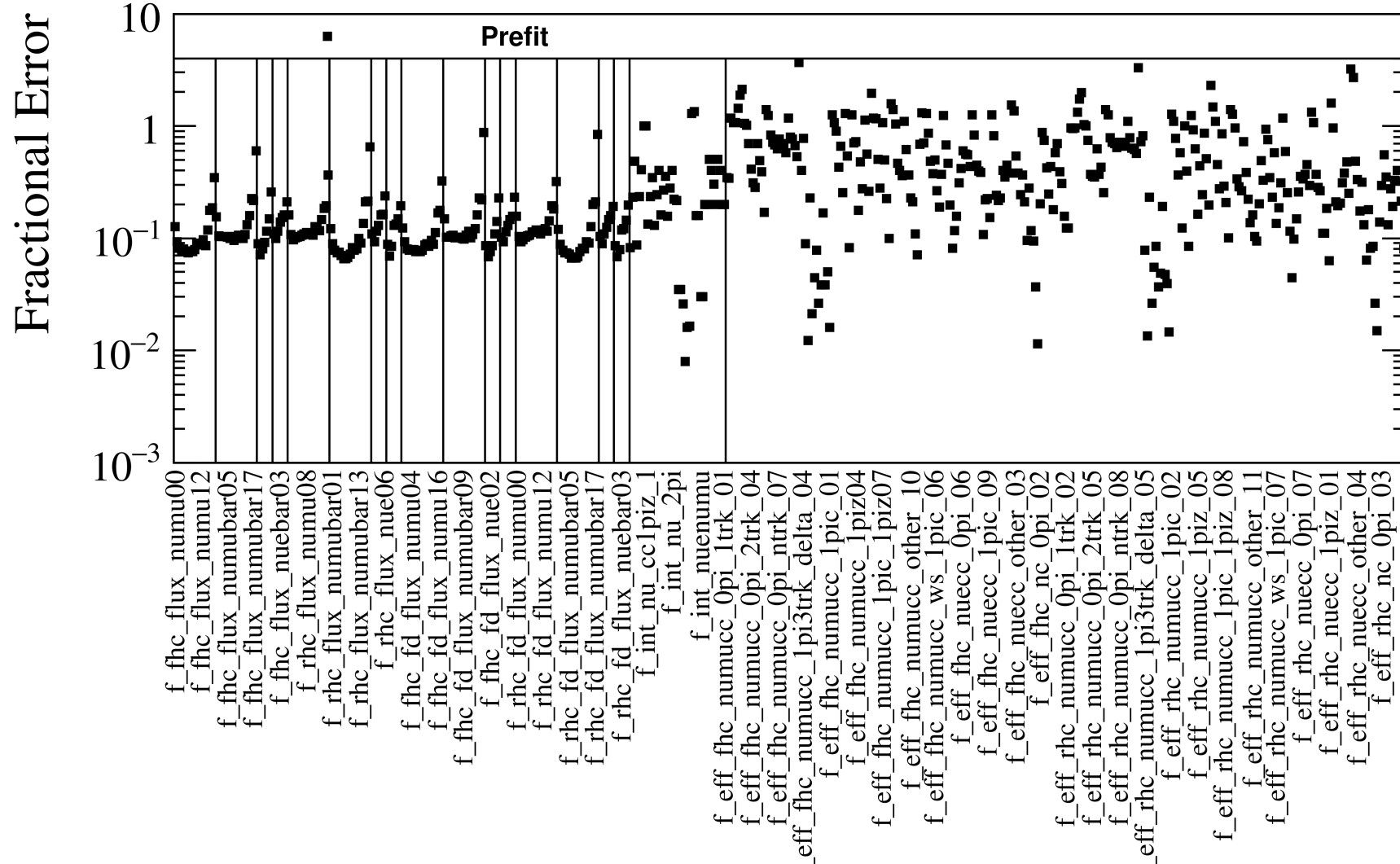
- 6  $Q^2$ -dependent systematics for  $\nu$  and  $\bar{\nu}$  CC QE,
- 2 systematics for  $\nu$  and  $\bar{\nu}$  CC MEC,
- 6  $Q^2$ -dependent systematics for  $\nu$  and  $\bar{\nu}$  CC  $1\pi^\pm$ ,
- 6  $Q^2$ -dependent systematics for  $\nu$  and  $\bar{\nu}$  CC  $1\pi^0$ ,
- 2 systematics for  $\nu$  and  $\bar{\nu}$  CC  $2\pi$
- 6 energy-dependent systematics for  $\nu$  and  $\bar{\nu}$  CC DIS ( $> 2\pi$ )
- 2 systematics for  $\nu$  and  $\bar{\nu}$  CC coherent production of pions,
- 2 overall systematics for  $\nu$  and  $\bar{\nu}$  NC, and
- 1  $\nu_e/\nu_\mu$  cross-section ratio systematic.

## Hadronic re-interaction (FSI) systematics:

- 2 systematics on the overall re-interaction rate for pions and nucleons, and
- 8 systematics on the relative strength of different rescattering mechanisms (chg. exch., inelastic, absorption, pion production) for pions and nucleons.

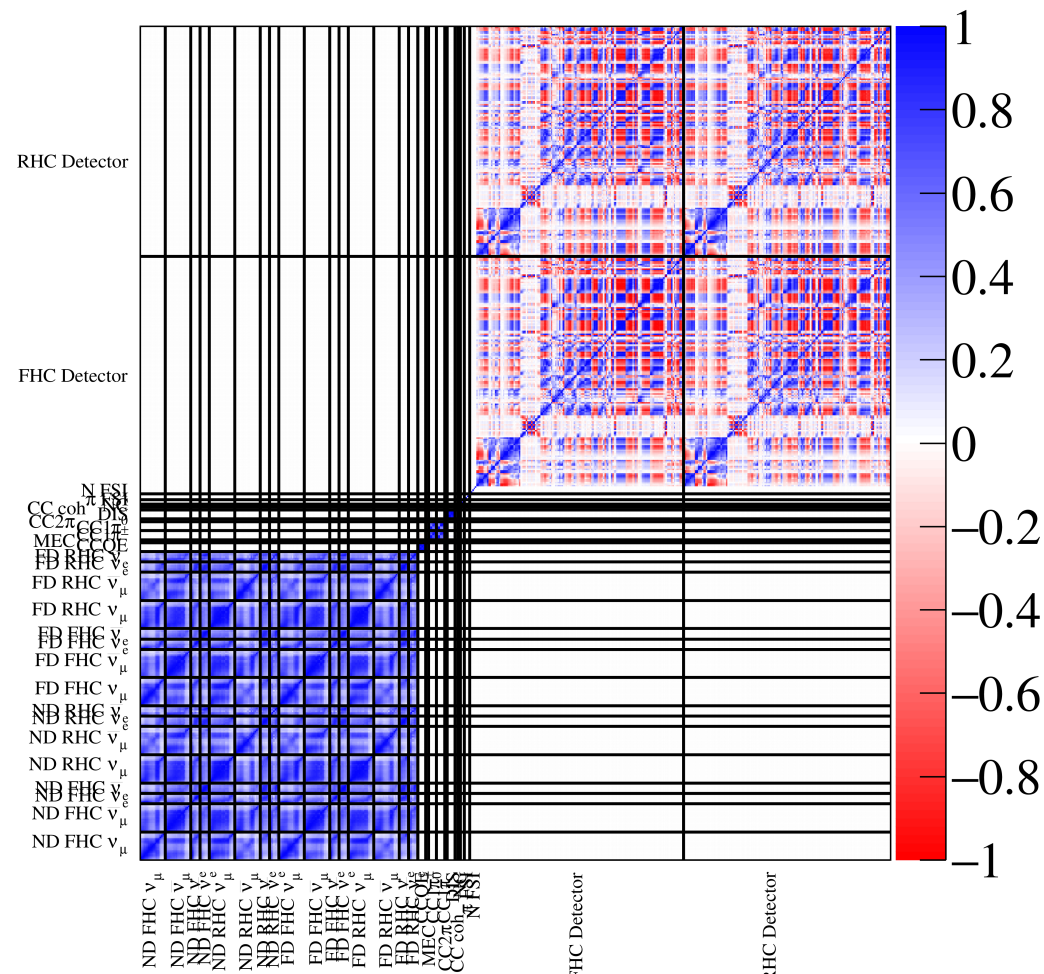
# Prior uncertainties

$1\sigma$  fractional error for all  $\approx 250$  physics and  $\approx 300$  detector systematics.



# Prior uncertainties

A block-diagonal correlation matrix:  
Flux ( $208 \times 208$ ) + Interaction ( $43 \times 43$ ) +  
Detector ( $310 \times 310$ )

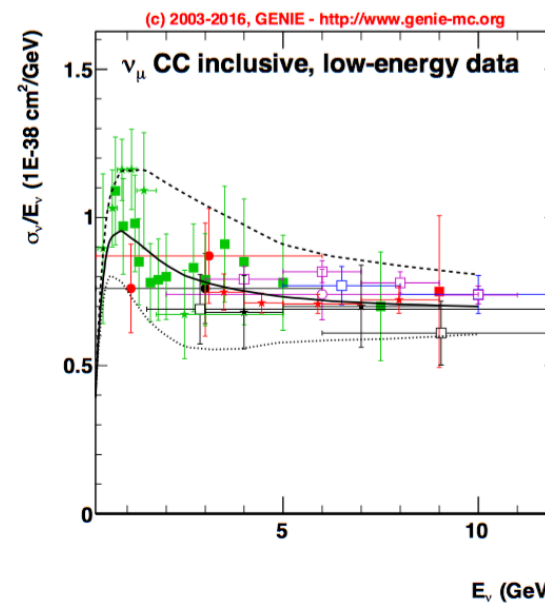
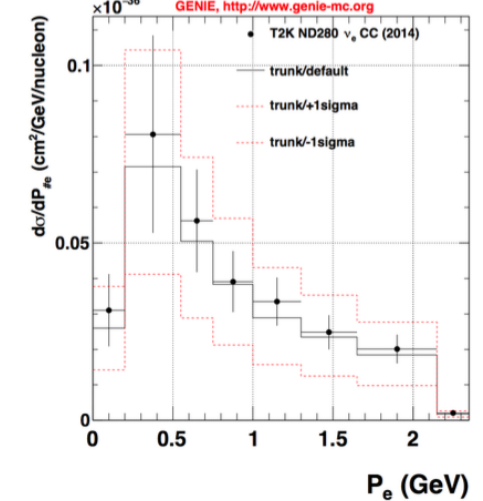
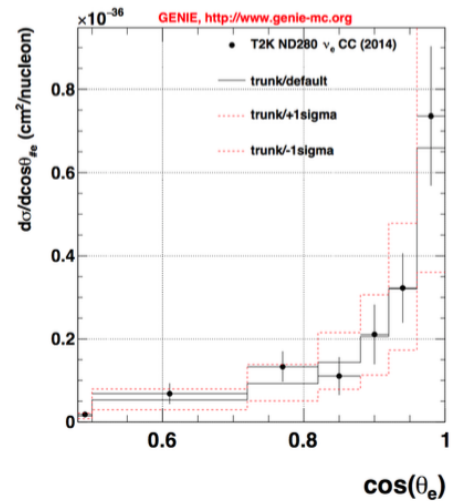
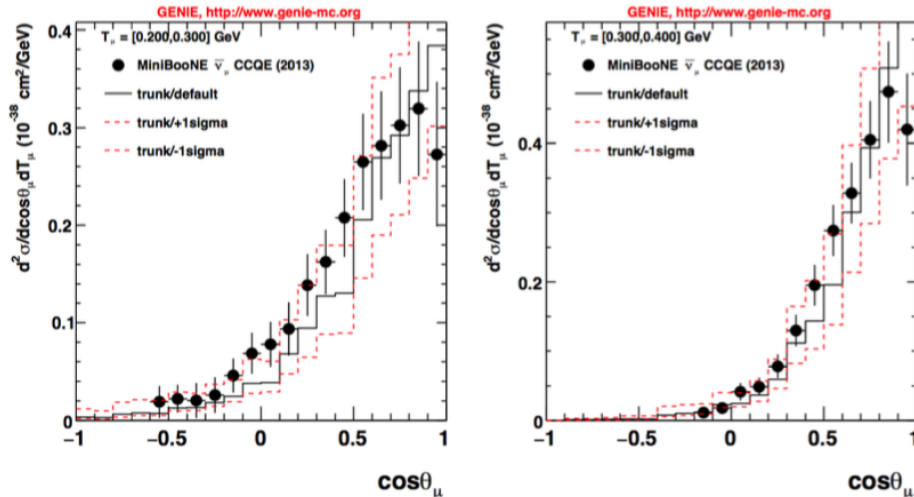
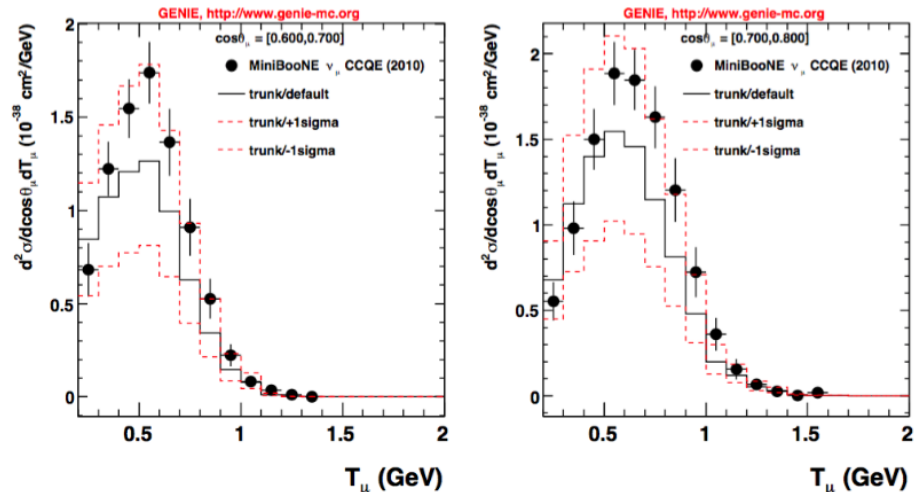


Substantial effort to quantify prior flux, cross-section and detector uncertainties for DUNE using

- published hadro-production data and LBNF flux simulations,
- published cross-section data and GENIE simulations,
- informed choices regarding the detector performance.

# Prior uncertainties: Cross-sections

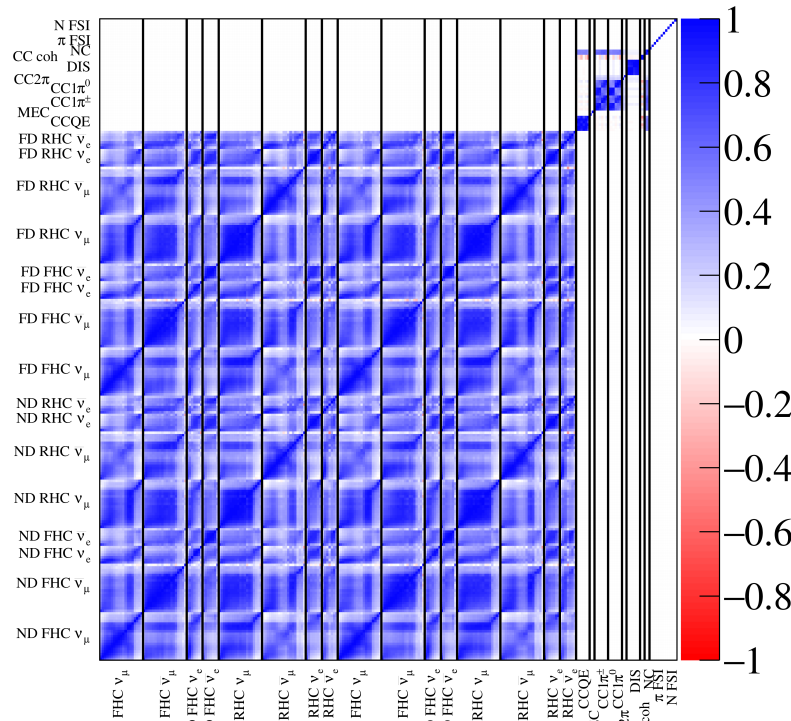
**Conservative prior neutrino interaction systematics assignments were supported by a series of data / GENIE MC comparisons. More studies are in progress.**



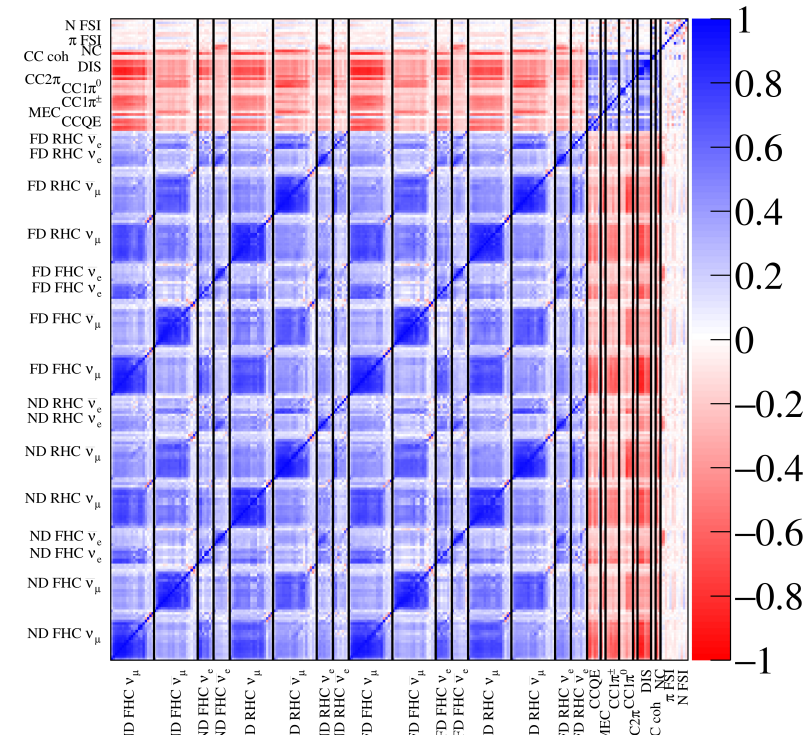
(c) 2003-2016, GENIE - <a href="http://www.genie-mc.org">http://www.genie-mc.org</a>	
<b>CC inclusive, low-energy data</b>	
ANL_12FT,2 [Barish et al., Phys.Lett.B66:291 (1977)]	●
ANL_12FT,4 [Barish et al., Phys.Rev.D19:2521 (1979)]	●
BNL_7FT,0 [Bally et al., Phys.Rev.Lett.44:916 (1980)]	■
BNL_7FT,4 [Baker et al., Phys.Rev.D25:817 (1982)]	■
Gargamelle,0 [Eichten et al., Phys.Lett.B46:274 (1973)]	○
Gargamelle,10 [Cimpolillo et al., Phys.Lett.B94:291 (1980)]	□
IHEP_JTEP,2 [Vovchenko et al., Sov.J.Nucl.Phys.30:328 (1975)]	□
IHEP_JINR,0 [Anikeev et al., Zeit.Phys.C70:39 (1996)]	□
SKAT,0 [Beranov et al., Phys.Rev.B81:255 (1979)]	★
MINOS,0 [Adamson et al., Phys.Rev.D81:072002 (2010)]	★
SciBooNE,0 [Nakajima et al., Phys.Rev.D83:012005 (2011)]	★
GENIE vtrunk / nominal	—
GENIE vtrunk / +1sigma	- - -
GENIE vtrunk / -1sigma	.....

# Prior vs VALOR/DUNE post-fit uncertainties

Joint multi-channel fit **breaks systematic parameter correlations**.  
As expected (experimental constraint is an event rate), flux and cross-section parameters become anti-correlated.

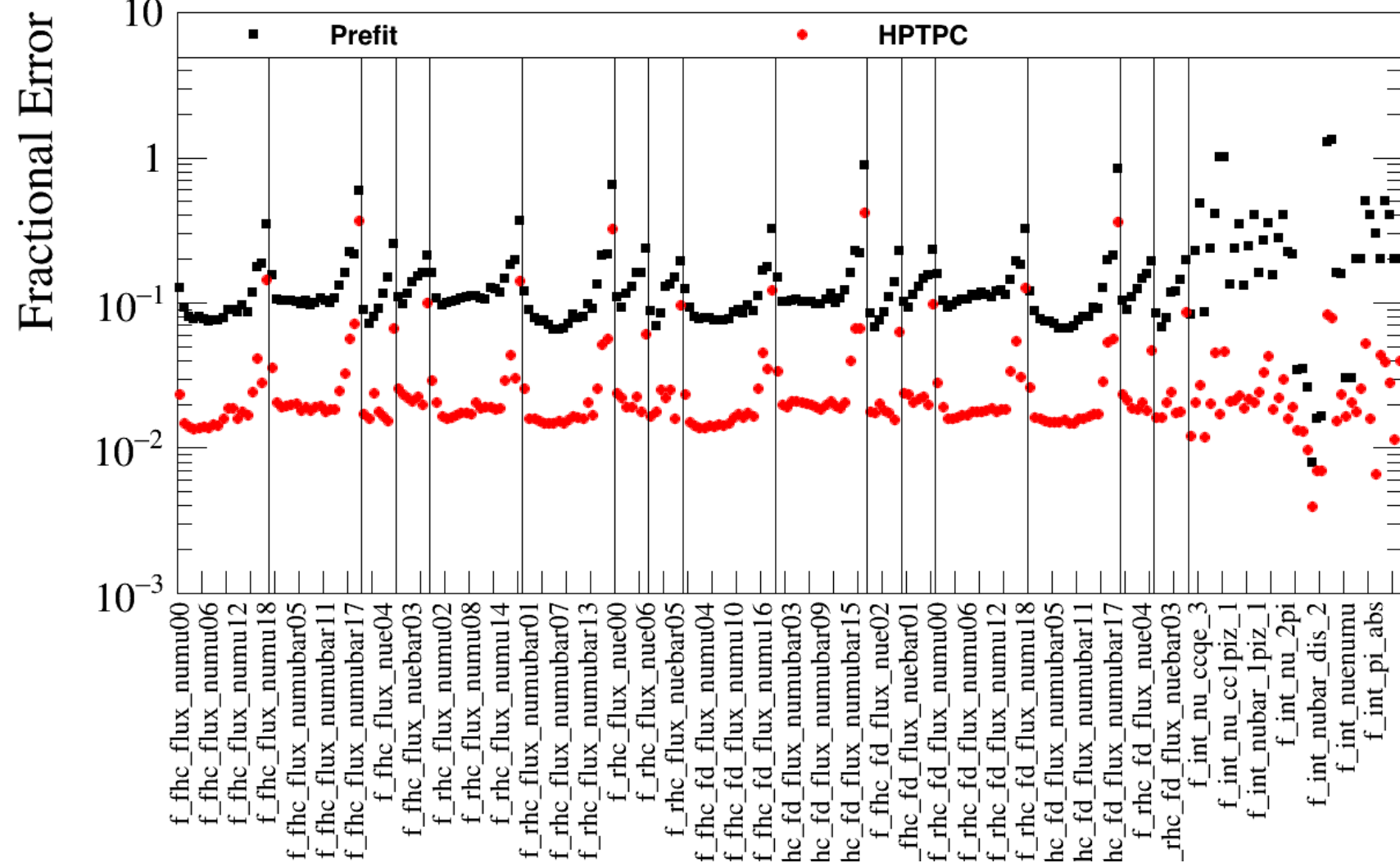


Pre-fit correlations

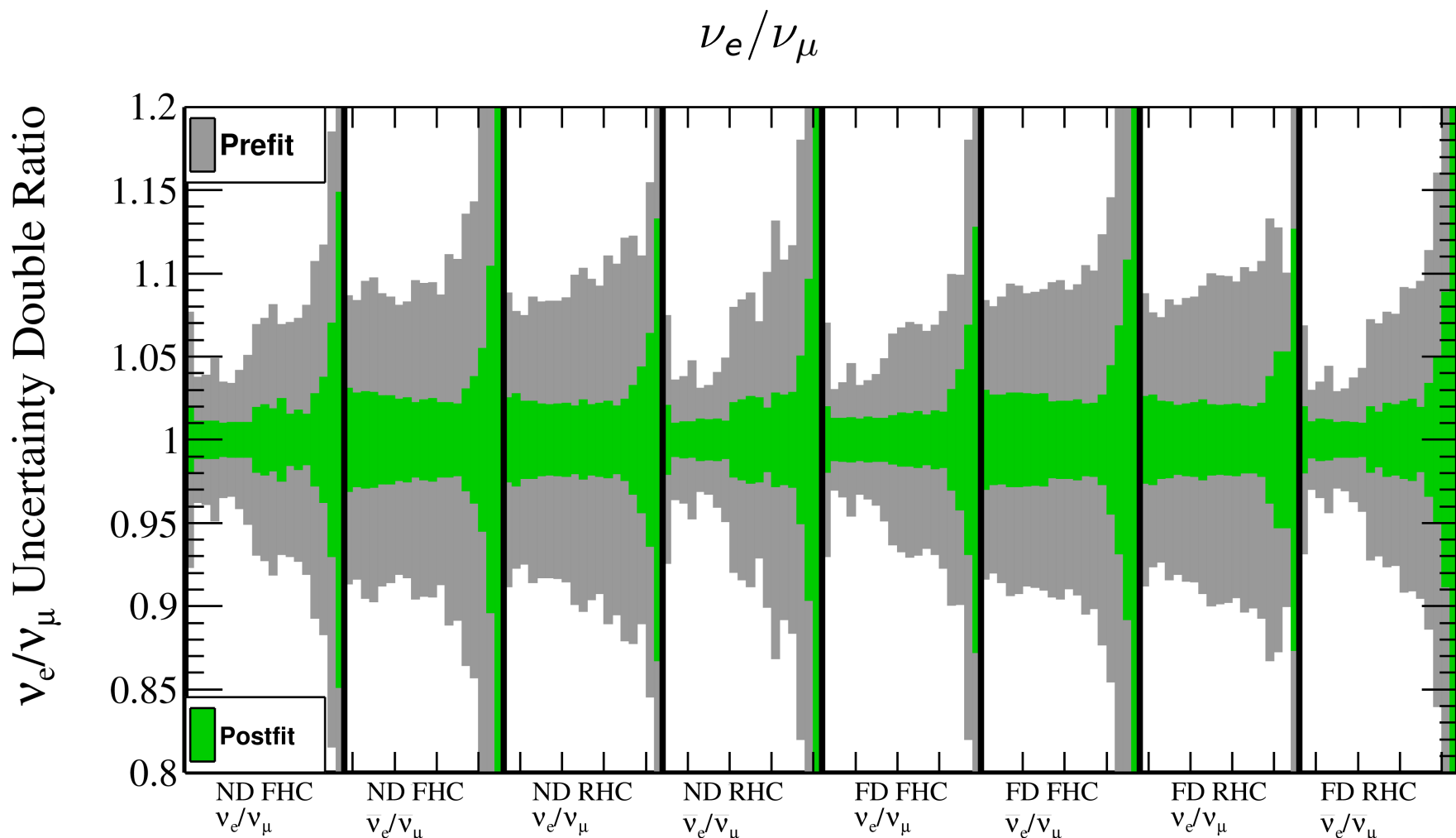


Post-fit correlations

# Systematic error reduction with VALOR/DUNE fit



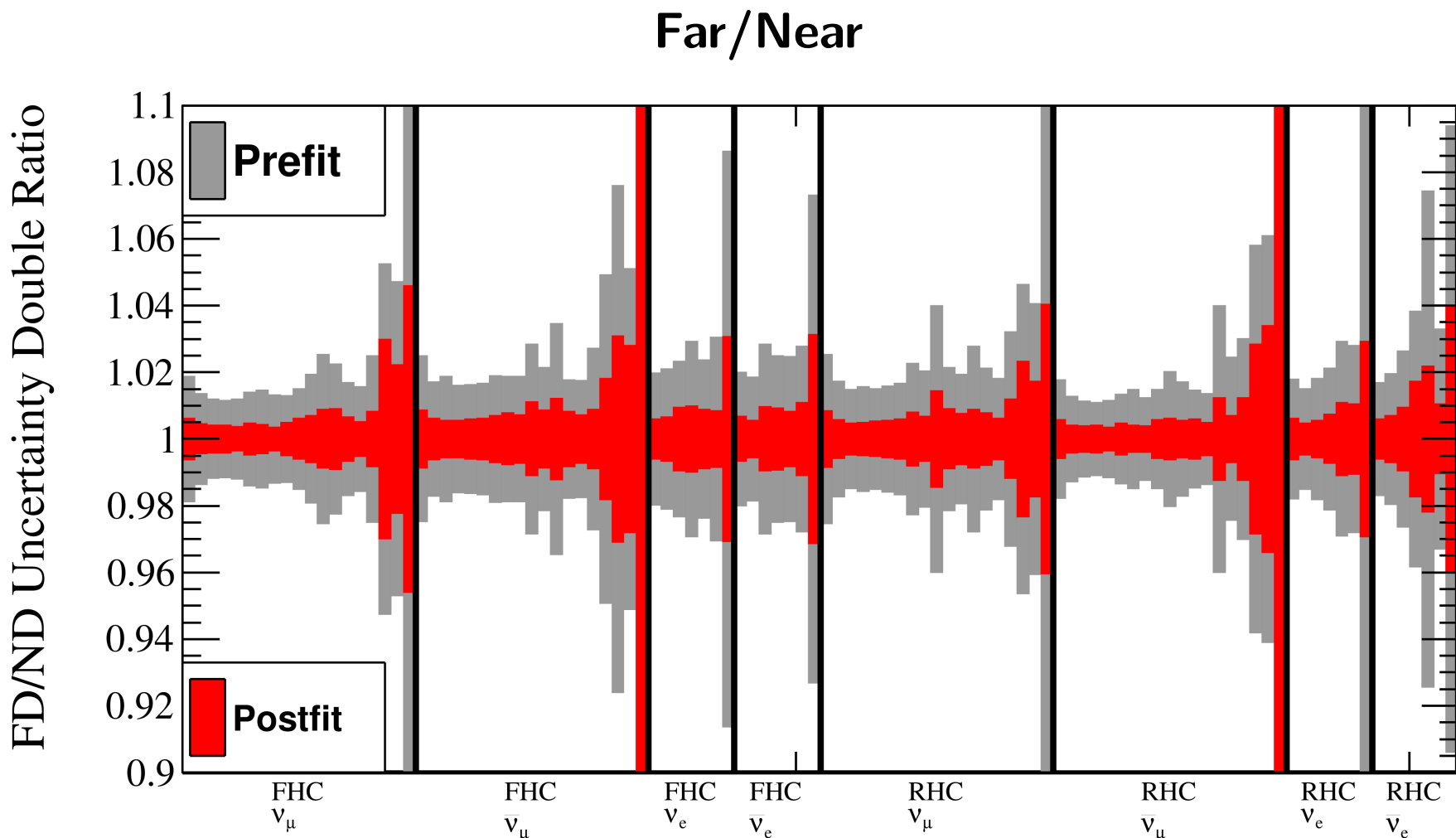
# Relative flux constraints (uncorrelated error)



1-2% level in oscillation region



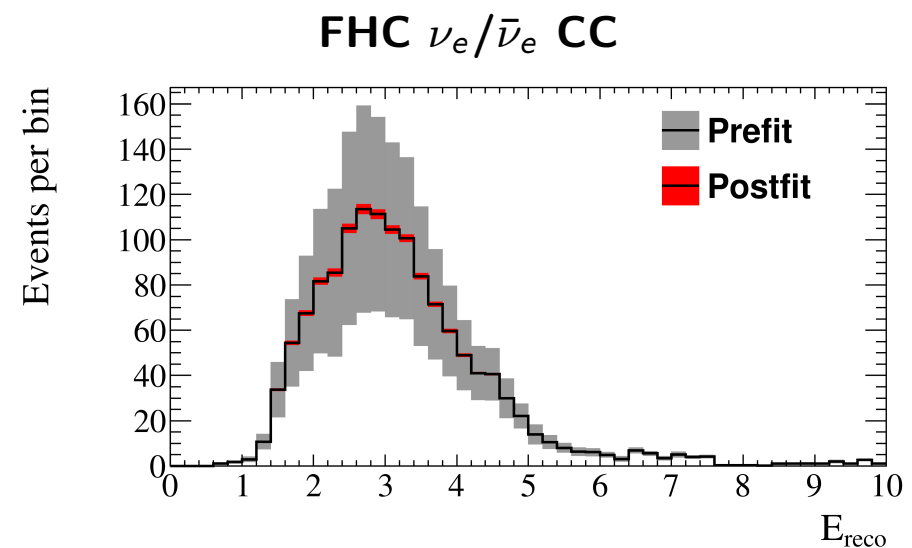
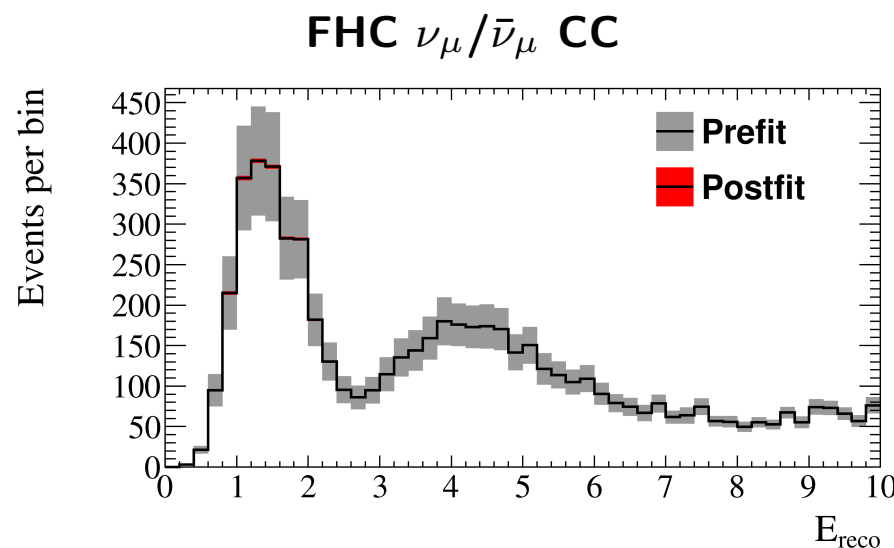
# Relative flux constraints (uncorrelated error)



1-2% level in oscillation region

# Impact on FD event rate predictions

	FHC		RHC	
	$\mu$ -like	e-like	$\mu$ -like	e-like
Flux + interaction w/o ND	16.8%	36.3%	15.0%	28.3%
Flux + interaction w ND	1.0%	2.4%	0.9%	1.5%
Flux w/ ND	1.9%	1.9%	1.8%	1.7%
Interaction w/ ND	2.0%	3.9%	1.6%	2.7%



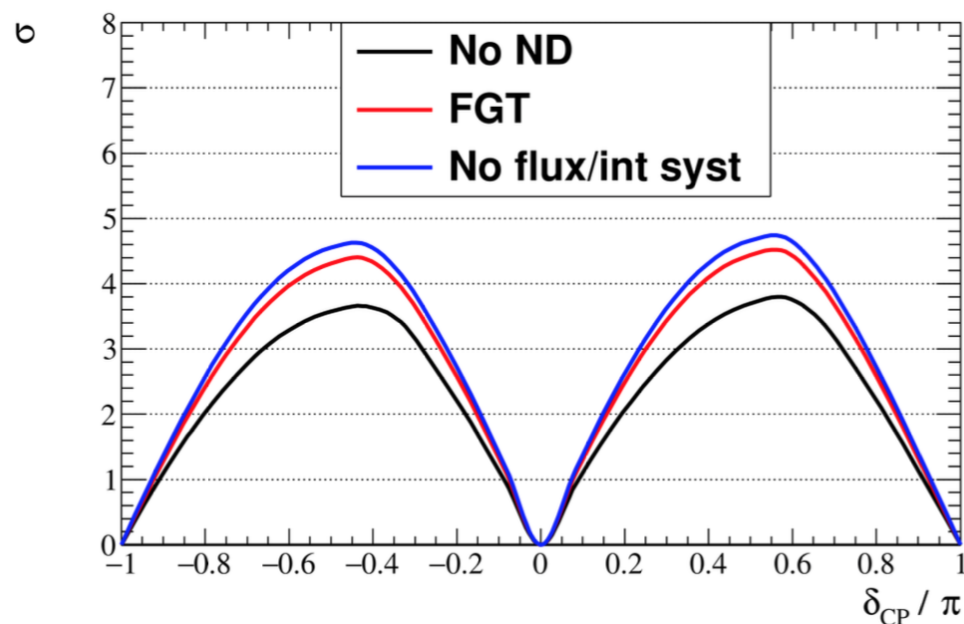
# Impact on the DUNE CP sensitivity

## DUNE CP discovery sensitivity (for NuFit2016 best-fit parameters)

Exposure:  $\approx 10\text{-yr FHC} + 10\text{-yr RHC running } (1.47 \times 10^{21} \text{ POT/yr})$  with 40-kt fiducial FD)

First sensitivities from an **end-to-end analysis** including both ND and FD!

- Evidence for "adequate" physics systematics constraints from proposed NDs
- More studies needed.
- FD uncertainties (not evaluated yet) likely to be main limitation to sensitivity



Note: Using **real FD reconstruction** (in its current state), hence reduced absolute sensitivity due to NC backgrounds. Actual expected sensitivity substantially higher!

# Summary

- Poor understanding of  $\nu$  interactions limits sensitivity to new physics.
- Two-detector LBL experiment paradigm powerful!
  - Well-founded concerns over model dependencies.
- Issues pertinent with full-statistics T2K/NOvA and future LBL
- Not an intractable problem! Risk to LBL programme mitigated by
  - New precise measurements at SBN and elsewhere
  - New model development, MC generator upgrades and global tunes
  - New highly-capable LBL NDs currently being designed
- Also, 3-flavour paradigm extremely powerful!
  - It is a strong constraint that alleviates the effects of uncertainties.
- Systematic error requirements for physics beyond the 3-flavour scheme not well established!

# Backup slides

# The VALOR group



**VALOR is a well-established neutrino fitting group.**  
(2010 - present); <https://valor.pp.rl.ac.uk>

Costas Andreopoulos<sup>1,2</sup>, Chris Barry<sup>1</sup>, Francis Bench<sup>1</sup>, Andy Chappell<sup>3</sup>,  
Thomas Dealtry<sup>4</sup>, Steve Dennis<sup>1</sup>, Lorena Escudero<sup>5</sup>, Rhiannon Jones<sup>1</sup>,  
Nick Grant<sup>3</sup>, Marco Roda<sup>1</sup>, Davide Sgalaberna<sup>6</sup>, Raj Shah<sup>2,7</sup>

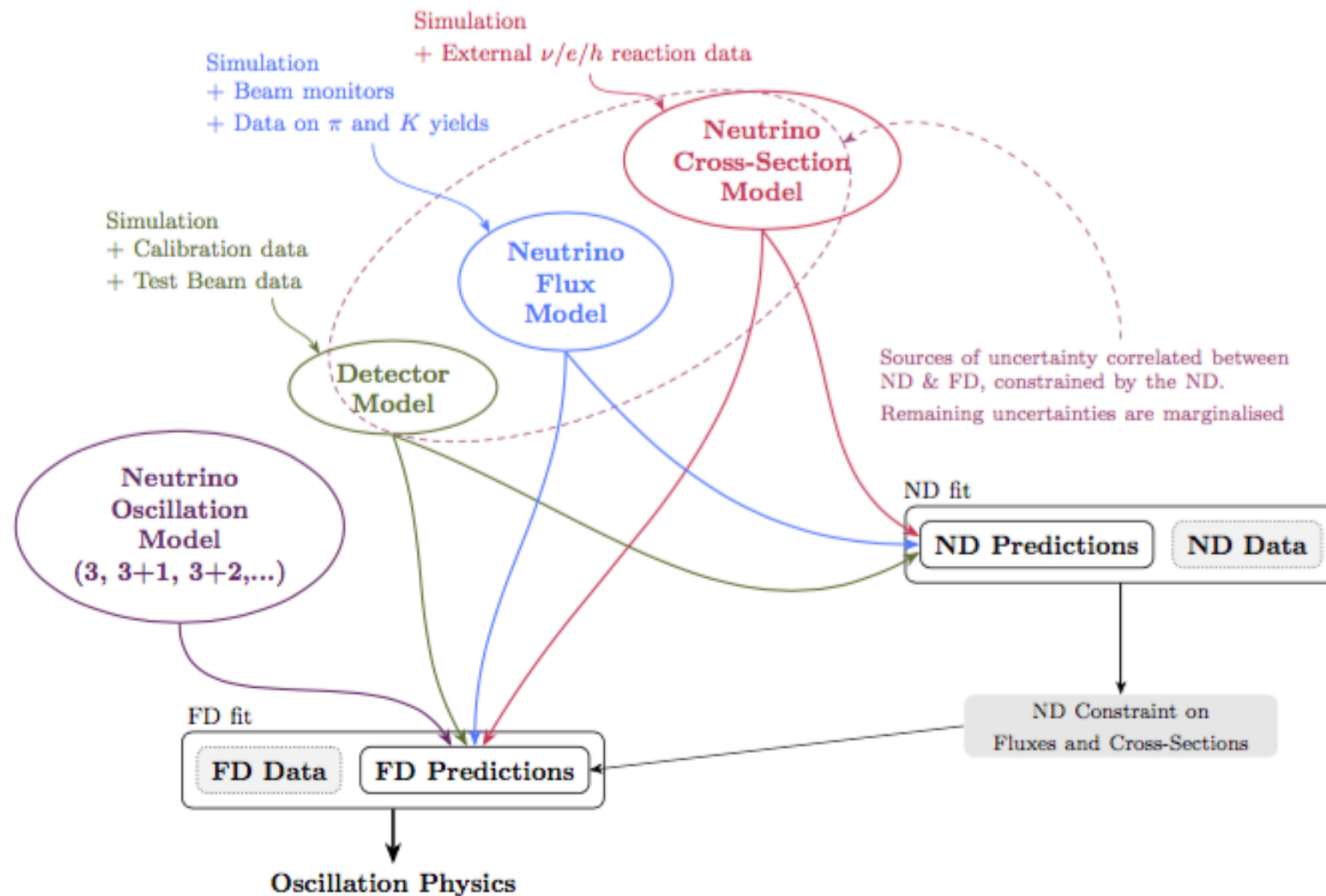
[ Faculty, Postdocs (former PhD students with VALOR T2K PhD theses), Postdocs, Current PhD students ]



<sup>1</sup> University of Liverpool, <sup>2</sup> STFC Rutherford Appleton Laboratory, <sup>3</sup> University of Warwick,  
<sup>4</sup> Lancaster University, <sup>5</sup> University of Cambridge, <sup>6</sup> University of Geneva, <sup>7</sup> University of Oxford

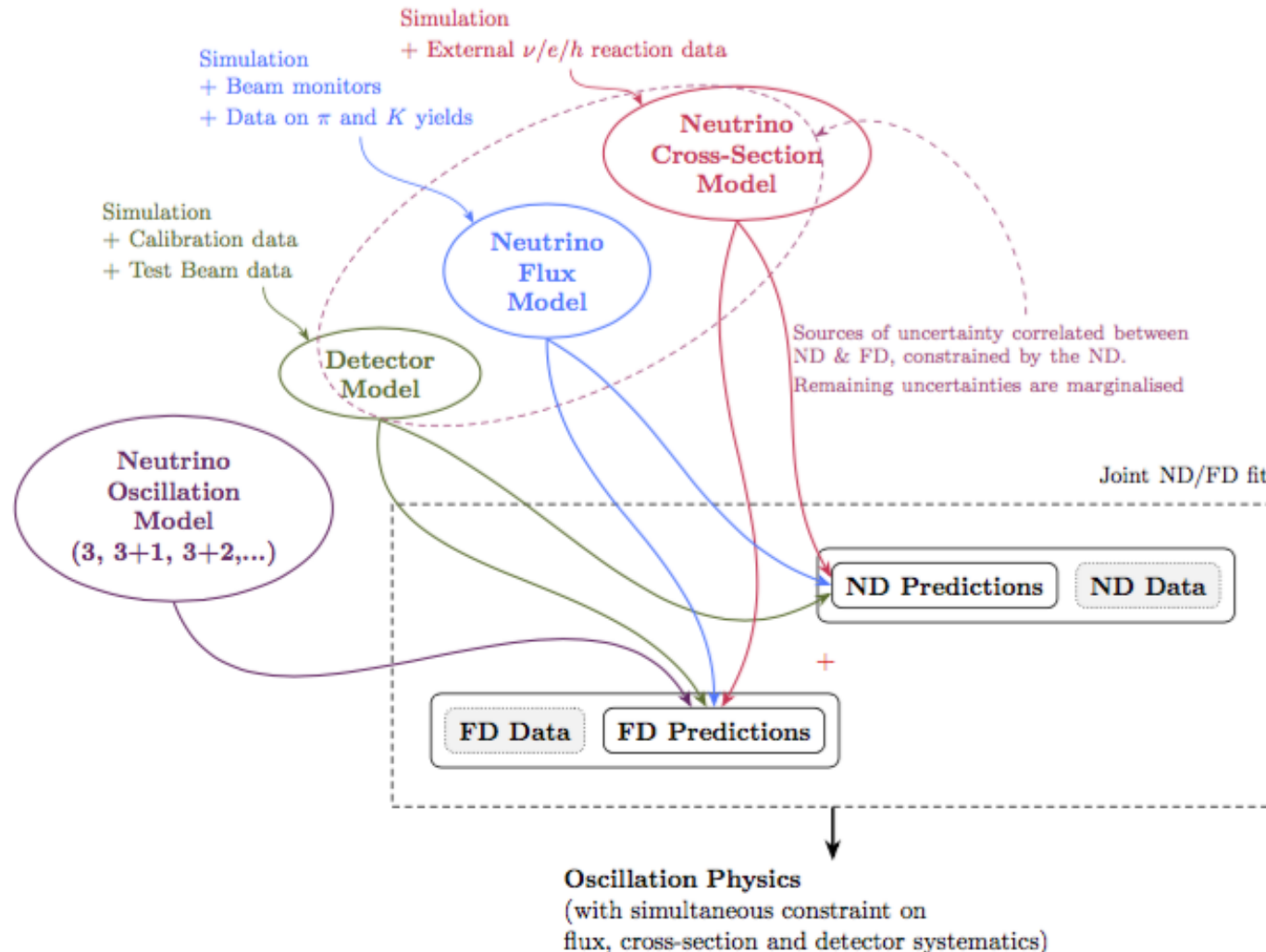
# Oscillation analysis strategy implemented in VALOR

A two-step procedure used in T2K: ND constraint followed by FD oscillation fit



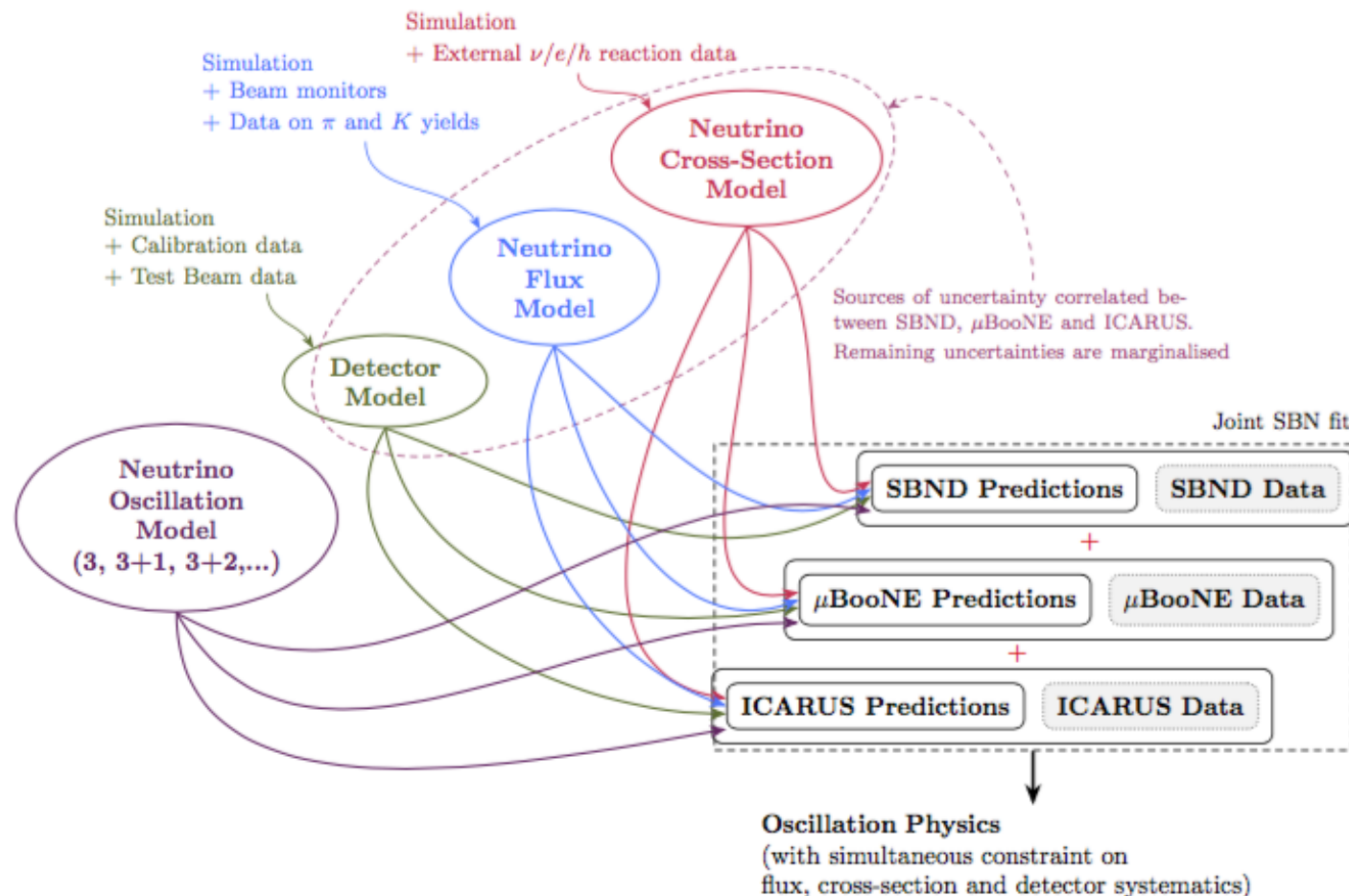
# Oscillation analysis strategy implemented in VALOR

VALOR analysis for DUNE: In the DUNE systematic error regime, a 2-step fit is unwarranted. A joint oscillation and systematics constraint fit was implemented.



# Oscillation analysis strategy implemented in VALOR

VALOR analysis for SBN: A joint oscillation and systematics constraint fit to several exclusive samples from SBND, MicroBooNE and ICARUS.



# **VALOR fit**

# **Physics parameterization**



# VALOR fit: Construction of likelihood

A joint VALOR fit considers simultaneously:

- A flexibly-defined **set of detectors**  $\mathbf{d}$ . E.g.  $d \in \{\text{SBND}, \mu\text{BooNE}, \text{ICARUS}\}$ .
- A flexibly-defined **set of beam configurations**  $\mathbf{b}$  (for each  $d$ ). E.g.  $b \in \{\text{FHC}, \text{RHC}, \dots\}$
- A flexibly-defined **set of event selections**  $\mathbf{s}$  (for each  $d$  and  $b$ ). E.g. see page 11.

For each  $(d, b, s)$ :

- Experimental information is recorded in a number of **multi-dim. reco. kinematical bins**  $\mathbf{r}$   
E.g.  $r \equiv \{E_{\nu;\text{reco}}\}, \{E_{\nu;\text{reco}}, y_{\text{reco}}\}, \{p_{\ell;\text{reco}}, \theta_{\ell;\text{reco}}\}, \{E_{\text{vis};\text{reco}}\}, \dots$

Our predictions for

- a set of **interesting physics params**  $\vec{\theta}$  (e.g.  $\{\theta_{23}, \delta_{CP}, \Delta m^2_{31}\}$  or  $\{\theta_{\mu e}, \theta_{\mu\mu}, \Delta m^2_{41}\}$  ), and
- a set of  $O(10^2)$ - $O(10^3)$  **systematic (nuisance) params**  $\vec{f}$

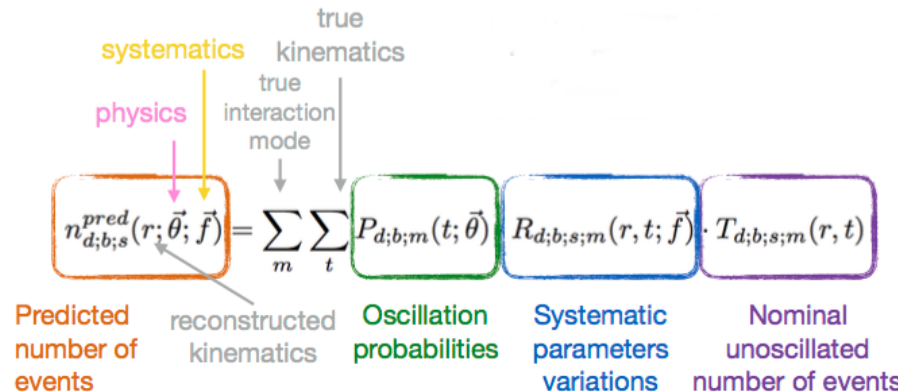
are constructed as follows:

The diagram illustrates the formula for the predicted number of events,  $n_{d;b;s}^{pred}(r; \vec{\theta}; \vec{f})$ , which is the sum of three terms:  $P_{d;b;m}(t; \vec{\theta})$ ,  $R_{d;b;s;m}(r, t; \vec{f}) \cdot T_{d;b;s;m}(r, t)$ , and  $T_{d;b;s;m}(r, t)$ . The inputs to the formula are categorized as follows:

- physics**:  $\vec{\theta}$  (represented by a pink arrow pointing to the first term)
- systematics**:  $\vec{f}$  (represented by a yellow arrow pointing to the second term)
- true kinematics**:  $r$  (represented by a grey arrow pointing to the third term)
- true interaction mode**:  $t$  (represented by a grey arrow pointing to the second term)
- Predicted number of events**:  $n_{d;b;s}^{pred}(r; \vec{\theta}; \vec{f})$  (boxed in orange)
- reconstructed kinematics**:  $t$  (grey text)
- Oscillation probabilities**:  $P_{d;b;m}(t; \vec{\theta})$  (boxed in green)
- Systematic parameters variations**:  $\vec{f}$  (grey text)
- Nominal unoscillated number of events**:  $T_{d;b;s;m}(r, t)$  (boxed in purple)

# VALOR fit: Construction of likelihood

Predictions are built using **MC templates**  $T_{d;b;s;m}(r, t)$  constructed by applying event selection code to the output of a full event simulation and reconstruction chain.



- $\nu_\mu$  CC QE
- $\nu_\mu$  CC MEC
- $\nu_\mu$  CC  $1\pi^\pm$
- $\nu_\mu$  CC  $1\pi^0$
- $\nu_\mu$  CC  $2\pi^\pm$
- $\nu_\mu$  CC  $2\pi^0$
- $\nu_\mu$  CC  $1\pi^\pm + 1\pi^0$
- $\nu_\mu$  CC coherent
- $\nu_\mu$  CC other
- $\nu_\mu$  NC  $1\pi^\pm$
- $\nu_\mu$  NC  $1\pi^0$
- $\nu_\mu$  NC coherent
- $\nu_\mu$  NC other
- similarly for  $\bar{\nu}_\mu$
- similarly for  $\nu_e$
- similarly for  $\bar{\nu}_e$

For each  $(d,b,s)$ , MC templates are constructed for a set of **true reaction modes m**.

- Currently, templates are constructed for the 52 true reaction modes shown on the right.

The templates store the mapping between reconstructed and truth information (as derived from full simulation and reconstruction).

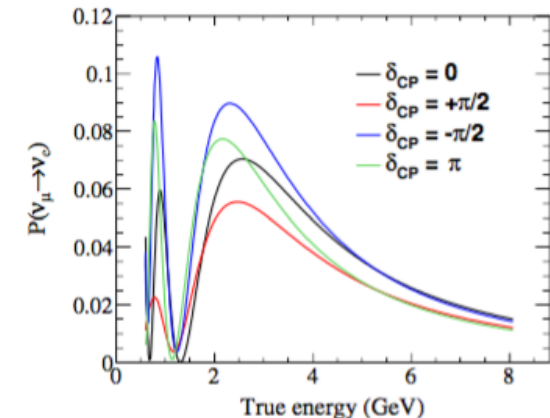
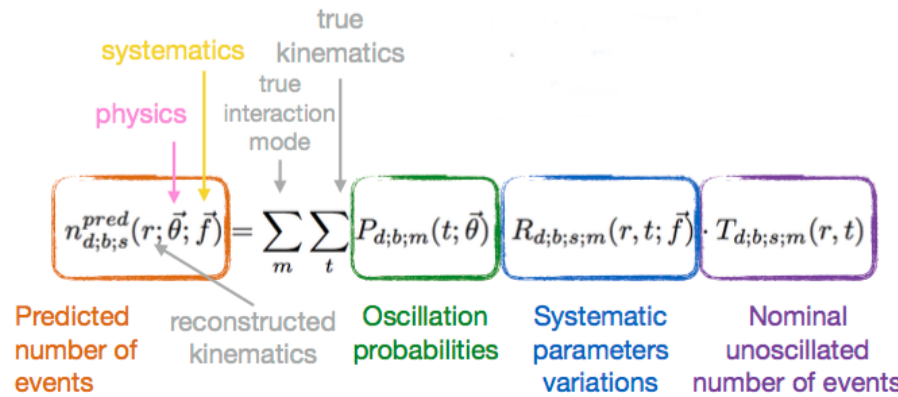
- E.g.  $\{E_{\nu;true}, Q_{true}^2, W_{true}\} \leftrightarrow \{p_{\ell;reco}, \theta_{\ell;reco}\}$

The choice of true kinematical space  $\{t\}$  and true reaction modes m is **highly configurable** for each  $(d,b,s)$  independently.

- Main consideration: **Sufficient granularity to apply desired physics and systematic effects** (function of truth quantities).

# VALOR fit: Construction of likelihood

Finally, the effect of **neutrino oscillations** is included in  $P_{d;b;m}(t; \vec{\theta})$ .

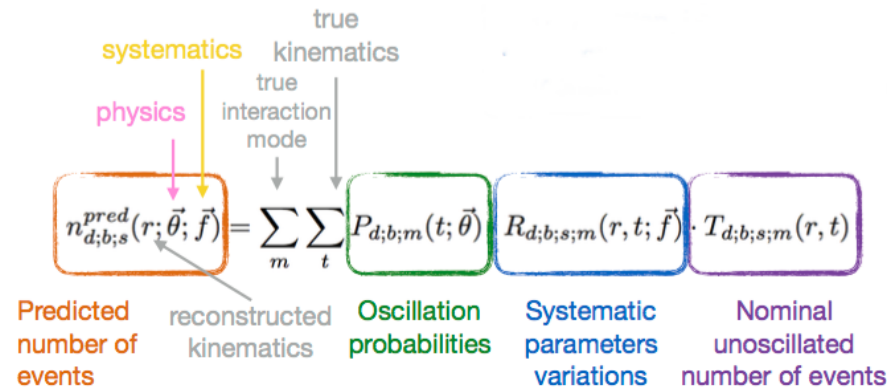


- Using bespoke library for calculation of osc. probabilities.
- Very fast!**
- Extensively validated** against GloBES and Prob3++.
- Supports 3-flavour calculations (incl. standard matter / NSI effects) and, also, calculations in 3+1, 3+2, 1+3+1 schemes.
- Flexibility** provided by bespoke library is immensely useful (tuning performance, moving between different parameter conventions, trying out different oscillation frameworks).

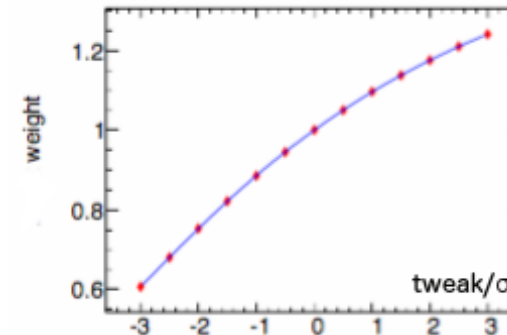
- $\sin^2(\theta_{12}) = 0.3$
- $\sin^2(\theta_{13}) = 0.025$
- $\sin^2(\theta_{23}) = 0.5$
- $\Delta m_{21}^2 = 7.5 \times 10^{-5} \text{ eV}^2/\text{c}^4$
- $\Delta m_{32}^2 = 2.5 \times 10^{-3} \text{ eV}^2/\text{c}^4$
- Normal ordering
- Earth matter density = 2.7 g/cm<sup>3</sup>
- Baseline = 1300 km

# VALOR fit: Construction of likelihood

Systematic variations are applied using the **response functions**  $R_{d;b;s;m}(r, t; \vec{f})$ .



Example of a non-linear response function.



Typically, but not always, the response  $R_{d;b;s;m}(r, t; \vec{f})$  factorises and it can be written as

$$R_{d;b;s;m}(r, t; \vec{f}) = \prod_{i=0}^{N-1} R_{d;b;s;m}^i(r, t; f_i)$$

For several systematics the response is linear and, therefore,

$$R_{d;b;s;m}^i(r, t; f_i) \propto f_i$$

For non linear systematics, the response function  $R_{d;b;s;m}^i(r, t; f_i)$  is pre-computed (for every detector, beam, sample, mode, true kinematical bin and reconstructed kinematical bin) using event reweighting libraries in the  $[-5\sigma, +5\sigma]$  range of the parameter  $f_i$  and it is represented internally using an Akima spline.

# VALOR fit: Construction of likelihood

Once we have estimates of  $n_{d;b;s}^{pred}(r; \vec{\theta}; \vec{f})$ , VALOR computes a **likelihood ratio**:

$$\ln \lambda_{d;b;s}(\vec{\theta}; \vec{f}) = - \sum_r \left\{ \left( n_{d;b;s}^{pred}(r; \vec{\theta}; \vec{f}) - n_{d;b;s}^{obs}(r) \right) + n_{d;b;s}^{obs}(r) \cdot \ln \frac{n_{d;b;s}^{obs}(r)}{n_{d;b;s}^{pred}(r; \vec{\theta}; \vec{f})} \right\}$$

$$\lambda_{SBN}(\vec{\theta}; \vec{f}) = \prod_d \prod_b \prod_s \lambda_{d;b;s}(\vec{\theta}; \vec{f})$$

Most parameters in the fit come with prior constraints from external data. Where needed, the following Gaussian penalty term is computed:

$$\ln \lambda_{prior}(\vec{\theta}; \vec{f}) = -\frac{1}{2} \left\{ (\vec{\theta} - \vec{\theta}_0)^T C_{\theta}^{-1} (\vec{\theta} - \vec{\theta}_0) + (\vec{f} - \vec{f}_0)^T C_f^{-1} (\vec{f} - \vec{f}_0) \right\}$$

and combined likelihood ratio is given by:

$$\lambda(\vec{\theta}; \vec{f}) = \lambda_{SBN}(\vec{\theta}; \vec{f}) \cdot \lambda_{prior}(\vec{\theta}; \vec{f})$$

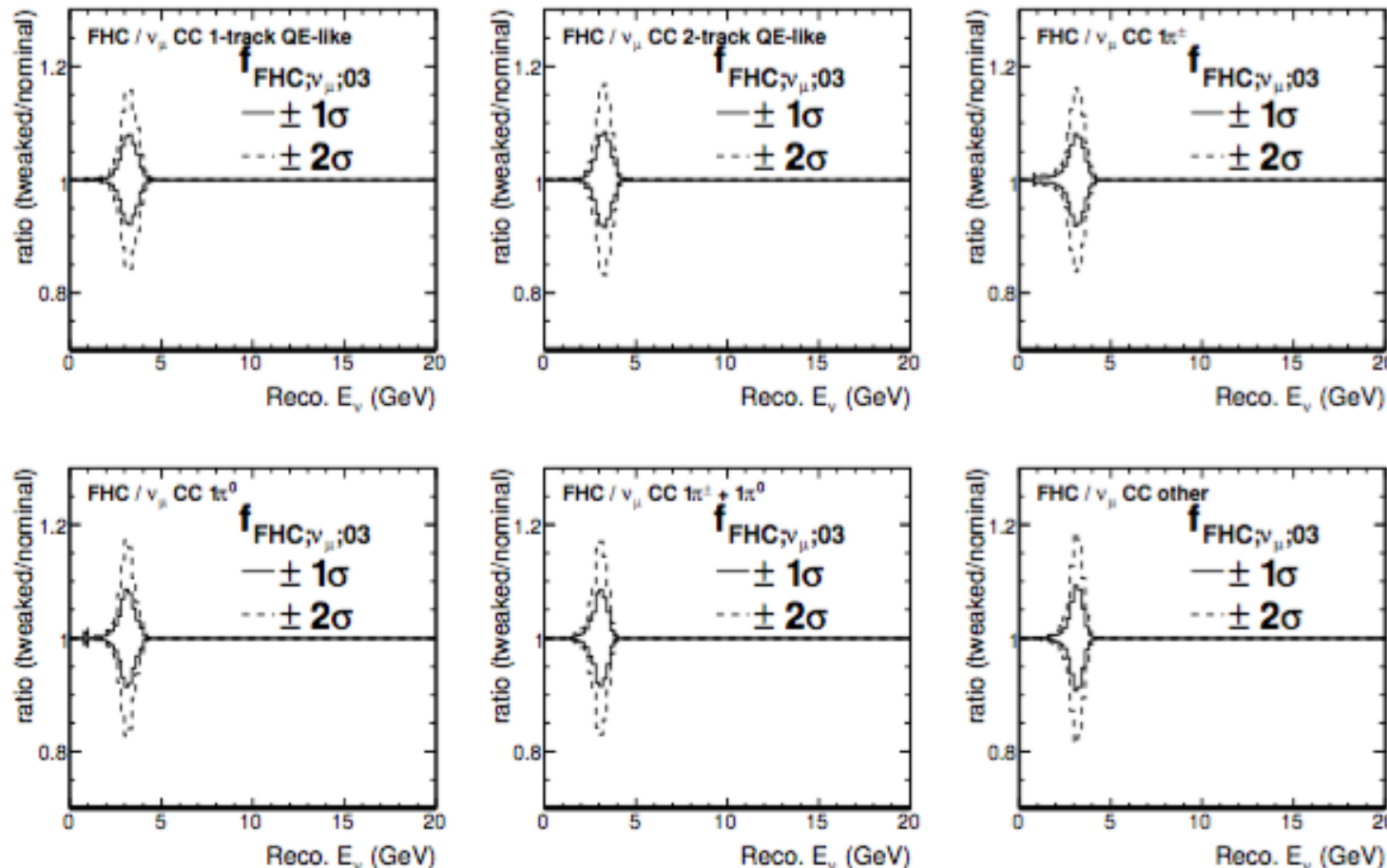
---

In the large-sample limit, the quantity  $-2\lambda(\vec{\theta}; \vec{f})$  has a  $\chi^2$  distribution and it can therefore be used as a goodness-of-fit test.

# Systematics in the VALOR/DUNE fit - Example variation

Pre-fit effect of a flux systematic [ $\nu_\mu$  FHC at 3.0-3.5 GeV] on selected VALOR/DUNE samples.

The ratios of tweaked/nominal spectra for  $\pm 1\sigma$  and  $\pm 2\sigma$  variations are shown.



# Physics systematics in the VALOR/DUNE fit I

Idx	Name	Physics quantity
0-18	$f_{ND;FHC;\nu_\mu;00}$ $f_{ND;FHC;\nu_\mu;18}$	FHC $\nu_\mu$ flux at the ND hall in the 18 true energy bins defined by the following bin edges: (0.0, 0.5, 1.0, 1.5, 2.0, 2.5, 3.0, 3.5, 4.0, 4.5, 5.0, 5.5, 6.0, 7.0, 8.0, 12.0, 16.0, 20.0, 40.0, 100.0) GeV.
19-37	$f_{ND;FHC;\bar{\nu}_\mu;00}$ $f_{ND;FHC;\bar{\nu}_\mu;18}$	FHC $\bar{\nu}_\mu$ flux at the ND hall in same 18 true energy bins listed above.
38-44	$f_{ND;FHC;\nu_e;00}$ $f_{ND;FHC;\nu_e;06}$	FHC $\nu_e$ flux at the ND hall in the 7 true energy bins defined by the following bin edges: (0.0, 2.0, 4.0, 6.0, 8.0, 10.0, 20.0, 100.0) GeV.
45-51	$f_{ND;FHC;\bar{\nu}_e;00}$ $f_{ND;FHC;\bar{\nu}_e;06}$	FHC $\bar{\nu}_e$ flux at the ND hall in same 7 true energy bins listed above.
52-70	$f_{ND;RHC;\nu_\mu;00}$ $f_{ND;RHC;\nu_\mu;18}$	RHC $\nu_\mu$ flux at the ND hall in the 18 true energy bins defined by the following bin edges: (0.0, 0.5, 1.0, 1.5, 2.0, 2.5, 3.0, 3.5, 4.0, 4.5, 5.0, 5.5, 6.0, 7.0, 8.0, 12.0, 16.0, 20.0, 40.0, 100.0) GeV.
71-89	$f_{ND;RHC;\bar{\nu}_\mu;00}$ $f_{ND;RHC;\bar{\nu}_\mu;18}$	RHC $\bar{\nu}_\mu$ flux at the ND hall in same 18 true energy bins listed above.
90-96	$f_{ND;RHC;\nu_e;00}$ $f_{ND;RHC;\nu_e;06}$	RHC $\nu_e$ flux at the ND hall in the 7 true energy bins defined by the following bin edges: (0.0, 2.0, 4.0, 6.0, 8.0, 10.0, 20.0, 100.0) GeV.
97-103	$f_{ND;RHC;\bar{\nu}_e;00}$ $f_{ND;RHC;\bar{\nu}_e;06}$	RHC $\bar{\nu}_e$ flux at the ND hall in same 7 true energy bins listed above.
104-122	$f_{FD;FHC;\nu_\mu;00}$ $f_{FD;FHC;\nu_\mu;18}$	FHC $\nu_\mu$ flux at the FD hall in the 18 true energy bins defined by the following bin edges: (0.0, 0.5, 1.0, 1.5, 2.0, 2.5, 3.0, 3.5, 4.0, 4.5, 5.0, 5.5, 6.0, 7.0, 8.0, 12.0, 16.0, 20.0, 40.0, 100.0) GeV.
123-141	$f_{FD;FHC;\bar{\nu}_\mu;00}$ $f_{FD;FHC;\bar{\nu}_\mu;18}$	FHC $\bar{\nu}_\mu$ flux at the FD hall in same 18 true energy bins listed above.
142-148	$f_{FD;FHC;\nu_e;00}$ $f_{FD;FHC;\nu_e;06}$	FHC $\nu_e$ flux at the FD hall in the 7 true energy bins defined by the following bin edges: (0.0, 2.0, 4.0, 6.0, 8.0, 10.0, 20.0, 100.0) GeV.

# Physics systematics in the VALOR/DUNE fit II

149-155	$f_{FD;FHC;\bar{\nu}_e;00}$ $f_{FD;FHC;\bar{\nu}_e;06}$	-	FHC $\bar{\nu}_e$ flux at the FD hall in same 7 true energy bins listed above.
156-174	$f_{FD;RHC;\nu_\mu;00}$ $f_{FD;RHC;\nu_\mu;18}$	-	RHC $\nu_\mu$ flux at the FD hall in the 18 true energy bins defined by the following bin edges: (0.0, 0.5, 1.0, 1.5, 2.0, 2.5, 3.0, 3.5, 4.0, 4.5, 5.0, 5.5, 6.0, 7.0, 8.0, 12.0, 16.0, 20.0, 40.0, 100.0) GeV.
175-193	$f_{FD;RHC;\bar{\nu}_\mu;00}$ $f_{FD;RHC;\bar{\nu}_\mu;18}$	-	RHC $\bar{\nu}_\mu$ flux at the FD hall in same 18 true energy bins listed above.
194-200	$f_{FD;RHC;\nu_e;00}$ $f_{FD;RHC;\nu_e;06}$	-	RHC $\nu_e$ flux at the FD hall in the 7 true energy bins defined by the following bin edges: (0.0, 2.0, 4.0, 6.0, 8.0, 10.0, 20.0, 100.0) GeV.
201-207	$f_{FD;RHC;\bar{\nu}_e;00}$ $f_{FD;RHC;\bar{\nu}_e;06}$	-	RHC $\bar{\nu}_e$ flux at the FD hall in same 7 true energy bins listed above.
208 - 210	$f_{\nu CCQE;1}$ $f_{\nu CCQE;3}$	-	$\nu_\mu$ CC QE cross-section for the 3 true $Q^2$ bins defined by the following bin edges: (0, 0.2, 0.55, $\infty$ ) GeV $^2$ .
211 - 213	$f_{\bar{\nu} CCQE;1}$ $f_{\bar{\nu} CCQE;3}$	-	$\bar{\nu}_\mu$ CC QE cross-section for the same 3 true $Q^2$ bins defined above.
214	$f_{\nu CCMEC}$		$\nu_\mu$ CC MEC cross-section
215	$f_{\bar{\nu} CCMEC}$		$\bar{\nu}_\mu$ CC MEC cross-section
216 - 218	$f_{\nu CC1\pi^0;1}$ $f_{\nu CC1\pi^0;3}$	-	$\nu$ CC1 $\pi^0$ cross-section for the 3 true $Q^2$ bins defined by the following bin edges: (0, 0.35, 0.9, $\infty$ ) GeV $^2$ .
219 - 221	$f_{\nu CC1\pi^\pm;1}$ $f_{\nu CC1\pi^\pm;3}$	-	$\nu$ CC1 $\pi^\pm$ cross-section for the 3 true $Q^2$ bins defined by the following bin edges: (0, 0.3, 0.8, $\infty$ ) GeV $^2$ .
222 - 224	$f_{\bar{\nu} CC1\pi^0;1}$ $f_{\bar{\nu} CC1\pi^0;3}$	-	$\bar{\nu}$ CC1 $\pi^0$ cross-section for the same 3 true $Q^2$ bins used for $\nu$ CC1 $\pi^0$ .

# Physics systematics in the VALOR/DUNE fit III

225 - 227	$f_{\bar{\nu}CC1\pi^\pm;1}$ $f_{\bar{\nu}CC1\pi^\pm;3}$	-	$\bar{\nu}$ CC1 $\pi^\pm$ cross-section for the same 3 true $Q^2$ bins used for $\nu$ CC1 $\pi^\pm$ .
228	$f_{\nu CC2\pi}$		$\nu$ CC2 $\pi$ cross-section.
229	$f_{\bar{\nu}CC2\pi}$		$\bar{\nu}$ CC2 $\pi$ cross-section.
230 - 232	$f_{\nu CCDIS;1}$ $f_{\nu CCDIS;3}$	-	CCDIS ( $> 2\pi$ ) cross-section for the 3 true neutrino energy bins defined by the following bin edges: (0, 7.5, 15.0, $\infty$ ) GeV.
233 - 235	$f_{\bar{\nu}CCDIS;1}$ $f_{\bar{\nu}CCDIS;3}$	-	$\bar{\nu}$ CCDIS ( $> 2\pi$ ) cross-section for the 3 true neutrino energy bins defined above.
236	$f_{\nu CCCoh}$		$\nu$ CC coherent $\pi$ production cross-section.
237	$f_{\bar{\nu}CCCoh}$		$\bar{\nu}$ CC coherent $\pi$ production cross-section.
238	$f_{\nu NC}$		$\nu$ NC inclusive cross-section.
239	$f_{\bar{\nu}NC}$		$\bar{\nu}$ NC inclusive cross-section.
240	$f_{\nu_e/\nu_\mu}$		$\nu_e/\nu_\mu$ cross-section ratio.
241	$f_{FSI;\pi;MFP}$		$\pi$ mean free path in nucleus.
242	$f_{FSI;N;MFP}$		nucleon mean free path in nucleus.
243	$f_{FSI;\pi;CEx}$		$\pi$ -nucleus charge exchange cross-section fraction.
244	$f_{FSI;\pi;Inel}$		$\pi$ -nucleus inelastic cross-section fraction.
245	$f_{FSI;\pi;Abs}$		$\pi$ -nucleus absorption cross-section fraction.
246	$f_{FSI;\pi;\pi Prod}$		$\pi$ -nucleus $\pi$ production cross-section fraction.
247	$f_{FSI;N;CEx}$		nucleon-nucleus charge exchange cross-section fraction.
248	$f_{FSI;N;Inel}$		nucleon-nucleus inelastic cross-section fraction.
249	$f_{FSI;N;Abs}$		nucleon-nucleus absorption cross-section fraction.
250	$f_{FSI;N;\pi Prod}$		nucleon-nucleus $\pi$ production cross-section fraction.

# VALOR fit Statistical treatment

All physics is included in the definition of  $\lambda(\vec{\theta}; \vec{f})$  (see previous page).

What follows describes (briefly) the procedures used for nuisance parameter elimination, point and interval estimation, and hypothesis testing.

VALOR draws in a pragmatic way on both Bayesian and Frequentist methods. The methodology follows best HEP traditions and it was exercised repeatedly by the group in precision neutrino measurements (T2K).

*E.g. see several talks and posters by group members during PHYSTAT- $\nu$  at IPMU and FNAL.*



# VALOR fit: Parameter elimination

The likelihood ratio  $\lambda(\vec{\theta}; \vec{f})$  built for the **VALOR multi-detector, multi-channel, joint oscillation and systematics constraint fit** a function of  $O(10^2 - O(10^3)$  interesting physics and nuisance parameters!

Both **marginalization** and **profiling** are used for parameter elimination.

- Most parameters  $\vec{f}'$  (any subset of  $(\vec{\theta}; \vec{f})$ ) would have a **well-established prior**  $\pi(\vec{f}')$  (from hadron-production measurements, external neutrino cross-section measurements, electron scattering data, calibration data etc.).
  - Eliminated by marginalization. The **marginal likelihood**  $\lambda_{marg}(\vec{\theta}')$  is:

$$\lambda_{marg}(\vec{\theta}') = \int \lambda(\vec{\theta}'; \vec{f}') \pi(\vec{f}') d\vec{f}'$$

- For other parameters ( $\theta_{\mu e}$ ,  $\theta_{\mu \mu}$ ,  $\Delta m_{41}^2$ ) use of a prior may be undesirable and an uninformative prior may be problematic: Flat priors in  $\theta_{\mu e}$ ,  $\sin\theta_{\mu e}$ ,  $\sin^2\theta_{\mu e}$ ,  $\sin^2 2\theta_{\mu e}$ , would yield different results!
  - Eliminated by profiling (free-floating parameters included in the fit).

# VALOR fit: Parameter estimation

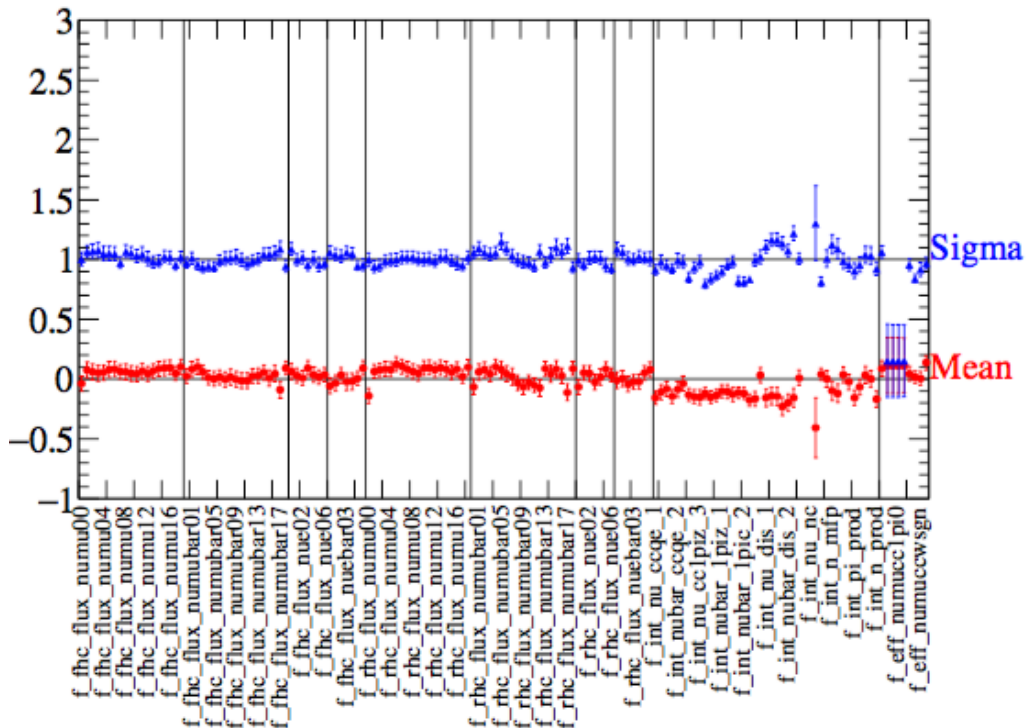
To extremize the test-statistic VALOR uses the **MINUIT/MIGRAD** algorithm.

Several other methods available within VALOR via a **VALOR/GSL** interface:

Simulated annealing, Levemberg-Marquardt, Fletcher-Reeves conjugate gradient, Polak-Ribiere conjugate gradient and Vector Broyden-Fletcher-Goldfarb-Shanno.

Marginalization of systematic parameters reduces the dimensionality of the likelihood ratio dramatically. Nevertheless, would like to make the point here that much more complex fits work beautifully within VALOR:

Pulls from a O(150) parameter fit.



$$pull = \frac{f_{bf} - f_0}{\sqrt{\sigma_{prior}^2 - \sigma_{post-fit}^2}}$$

- $f_{bf}$ : best-fit value of systematic parameter  $f$
- $f_0$ : nominal value
- $\sigma_{prior}$ : prior error on  $f$
- $\sigma_{post-fit}$ : fit (MIGRAD) error on  $f$

# VALOR fit: Interval estimation

After the fit is completed, the full  $\chi^2$  ( $= -2\lambda(\vec{\theta}')$ ) distribution is shifted with respect to  $\chi^2(\vec{\theta}'_{bf})$ :

$$\Delta\chi^2(\vec{\theta}') = \chi^2(\vec{\theta}') - \chi^2(\vec{\theta}'_{bf})$$

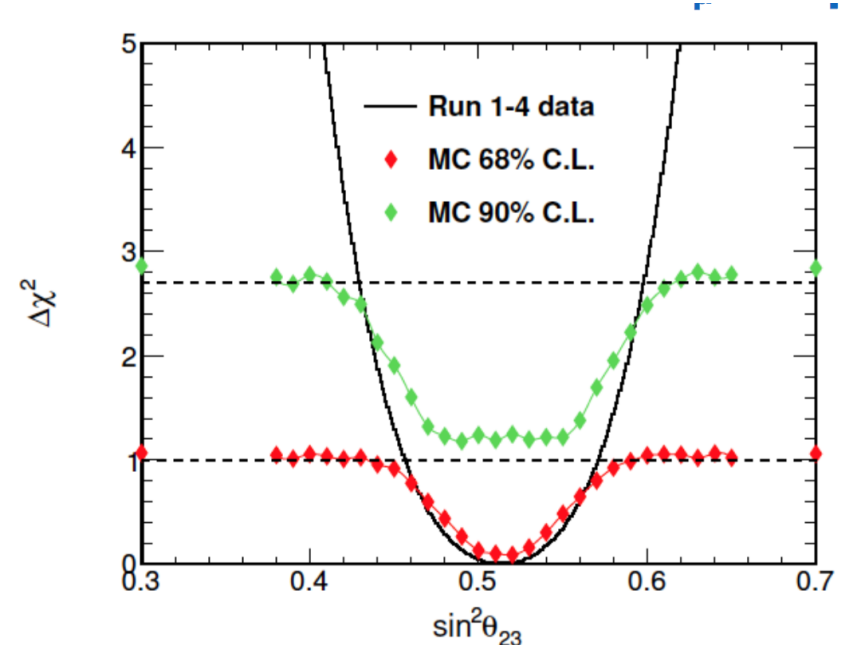
Confidence intervals at X% C.L. are set on  $\Delta\chi^2(\vec{\theta}')$ .

$$\Delta\chi^2(\vec{\theta}') < \Delta\chi^2_{crit;X}$$

where  $\Delta\chi^2_{crit;X}$  the corresponding critical value.

In the Gaussian approximation constant values of  $\Delta\chi^2_{crit}$  can be used. Usually this approximation is not reliable and the Feldman - Cousins / Cousins - Highland method is used instead.

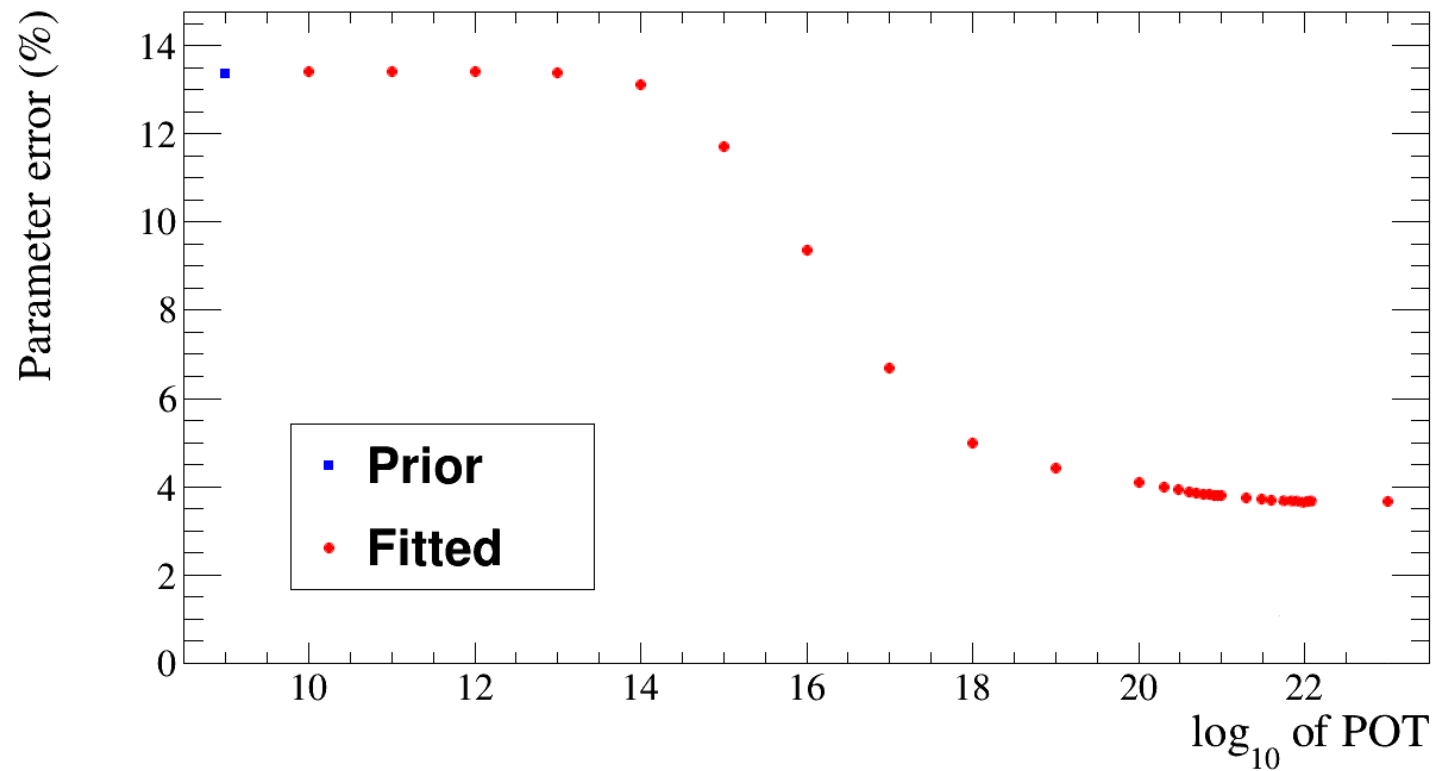
The VALOR group has developed several tools to probe the severity of coverage problems.  
If needed, it has the CPU muscle and efficient methods to compute corrections.



Example from T2K Run 1-4 disappearance analysis.  
Comparison of  $\Delta\chi^2_{crit;X}$  values from the FC method with the ones obtained under the Gaussian approximation.

# Illustration: Reduction of systematic uncertainties

Before closing, I would like to show you a beautiful example from the VALOR/DUNE analysis. It illustrates the power of a multi-channel analysis and ability to reduce systematic uncertainties.



# Neutrino oscillations

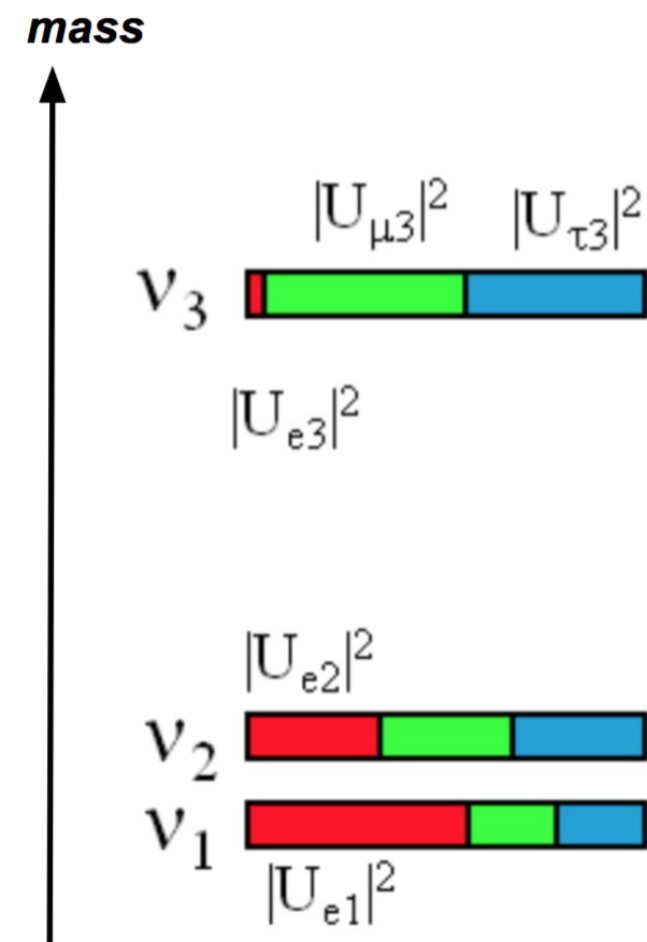
Each flavour eigenstate is a **superposition of mass eigenstates**.

$$\begin{pmatrix} \nu_e \\ \nu_\mu \\ \nu_\tau \end{pmatrix} = \underbrace{\begin{pmatrix} U_{e1} & U_{e2} & U_{e3} \\ U_{\mu 1} & U_{\mu 2} & U_{\mu 3} \\ U_{\tau 1} & U_{\tau 2} & U_{\tau 3} \end{pmatrix}}_{U_{PMNS}} \begin{pmatrix} \nu_1 \\ \nu_2 \\ \nu_3 \end{pmatrix}$$

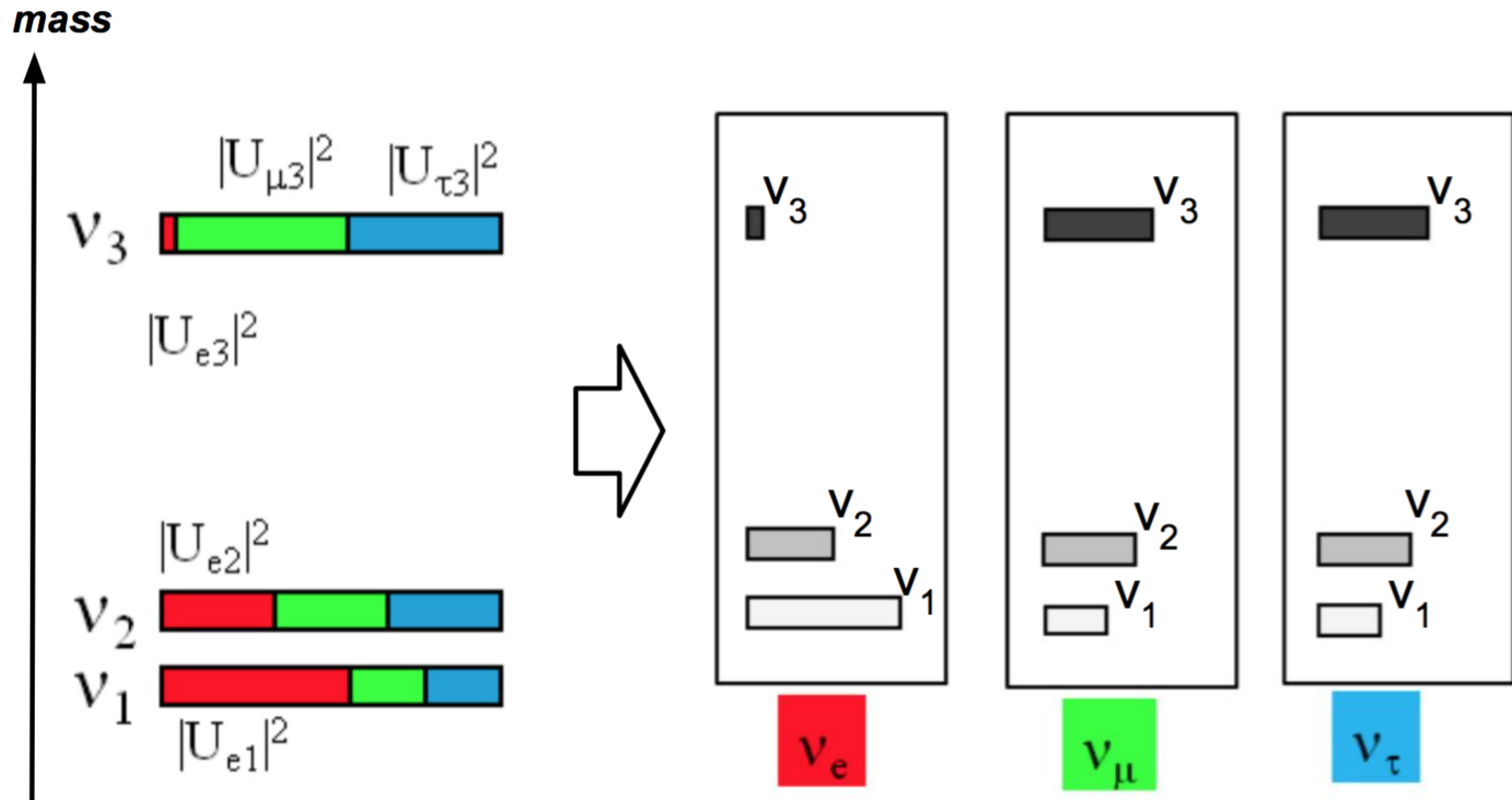
For antineutrinos:

$$U_{PMNS} \rightarrow U_{PMNS}^*$$

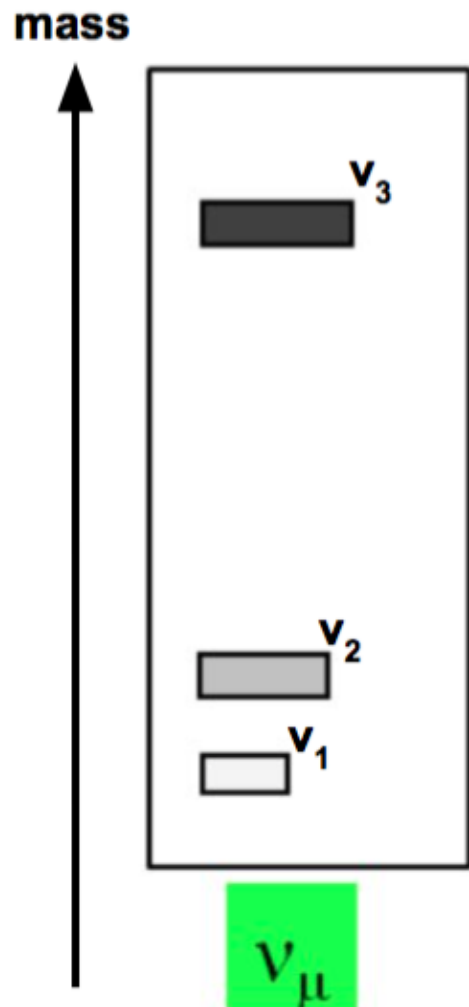
PMNS: Pontecorvo-Maki-Nakagawa-Sakata



# Neutrino oscillations

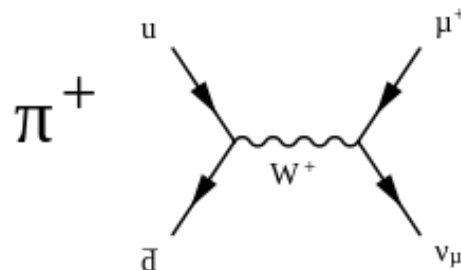


# Neutrino oscillations



A muon-neutrino, at the very moment it gets created, is described by the following state:

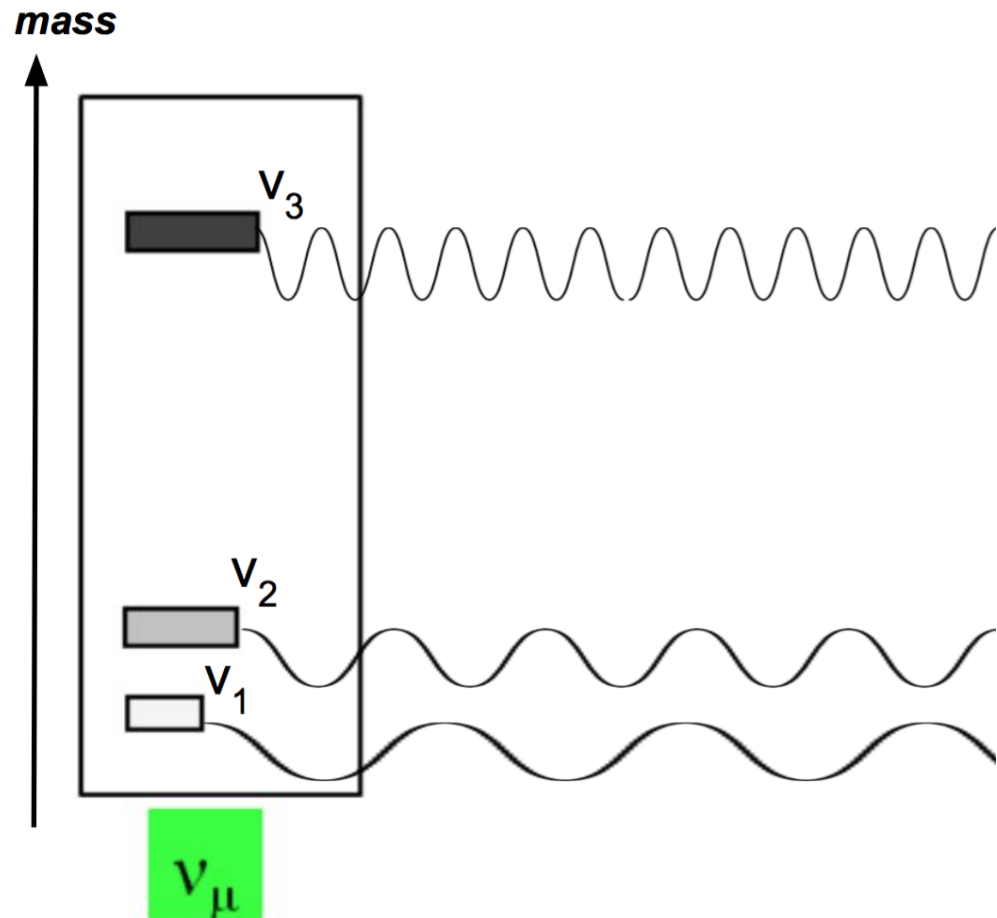
$$|\nu_\mu\rangle \approx 0.4 \cdot |\nu_1\rangle + 0.6 \cdot |\nu_2\rangle + 0.7 \cdot |\nu_3\rangle$$



So, at that time, a muon-neutrino is:

- $100 * (0.4)^2 \approx 15\% \nu_1$
- $100 * (0.6)^2 \approx 35\% \nu_2$
- $100 * (0.7)^2 \approx 50\% \nu_3$

# Neutrino oscillations



The propagation of each mass eigenstate  $i$  ( $i=1,2,3$ ) is described by a plane wave:

$$|\nu_i(L) \rangle = e^{-im_i^2 L/2E} \cdot |\nu_i(0) \rangle$$

Immediately after its creation, **the superposition** that makes up a flavour eigenstate **gets altered**.

The neutrino now has a **finite probability to be observed as a different flavour state**.

# What do we measure in neutrino oscillation experiments?

Probability for  $\nu_\alpha \rightarrow \nu_\beta$  ( $\alpha, \beta : e, \mu, \tau$ ) flavour oscillation:

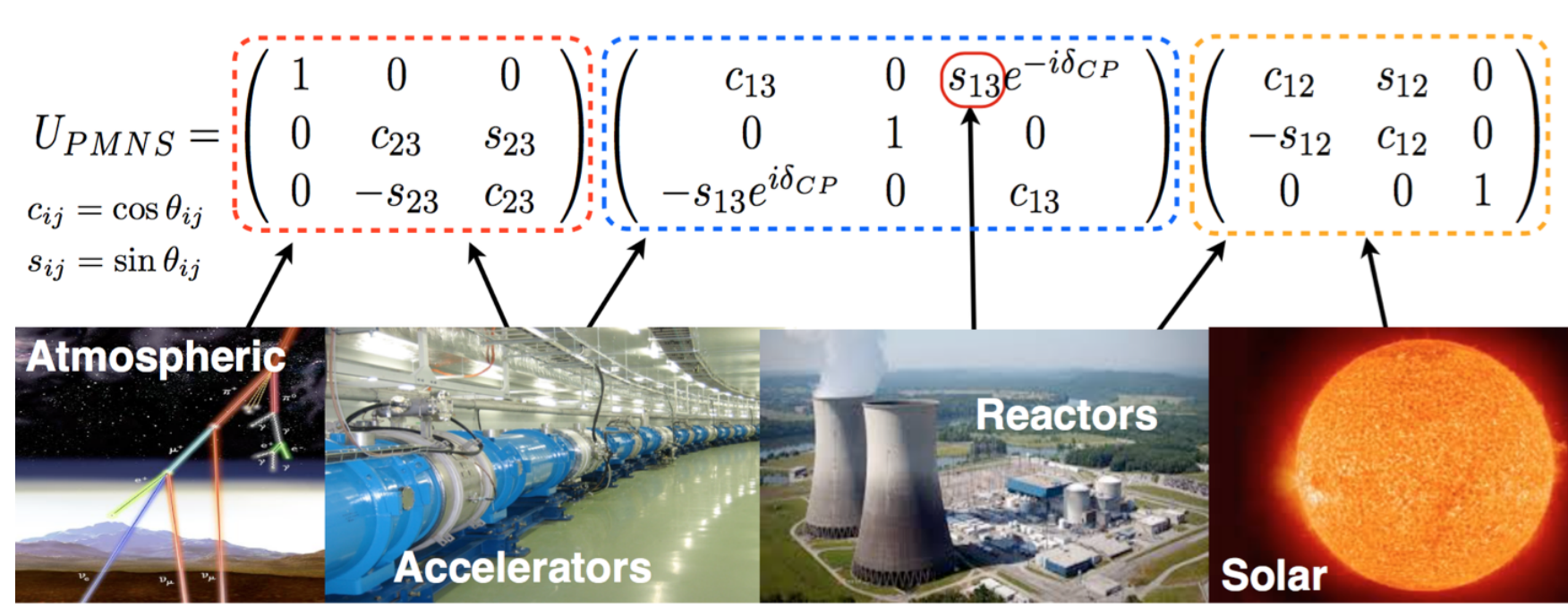
$$P_{\alpha\beta} = \delta_{\alpha\beta} - 4 \sum_{i>j} \text{Re}[\bar{U}_{\beta i} U_{\alpha i}^* \bar{U}_{\beta j}^* U_{\alpha j}] \sin^2\left(\frac{1}{4} \frac{L}{E} \Delta m_{ij}^2\right) \\ + 2 \sum_{i>j} \text{Im}[\bar{U}_{\beta i} U_{\alpha i}^* \bar{U}_{\beta j}^* U_{\alpha j}] \sin\left(\frac{1}{2} \frac{L}{E} \Delta m_{ij}^2\right)$$

Sensitivity to oscillations by tuning L/E (baseline to energy ratio)

For a purely phenomenological description of neutrino oscillations, assuming 3 active neutrinos, we need:

- Any 2 squared mass splittings (e.g.  $\Delta m_{21}^2, \Delta m_{32}^2$ )
- 3 mixing angles ( $\theta_{12}, \theta_{13}, \theta_{23}$ )
- 1 CP invariance violating phase ( $\delta_{CP}$ )

# What do we measure in neutrino oscillation experiments?



Parameter	best-fit ( $\pm 1\sigma$ )	$3\sigma$
$\Delta m_{21}^2$ [10 $^{-5}$ eV $^2$ ]	$7.54^{+0.26}_{-0.22}$	6.99 – 8.18
$ \Delta m^2 $ [10 $^{-3}$ eV $^2$ ]	$2.43 \pm 0.06$ ( $2.38 \pm 0.06$ )	$2.23 - 2.61$ ( $2.19 - 2.56$ )
$\sin^2 \theta_{12}$	$0.308 \pm 0.017$	$0.259 - 0.359$
$\sin^2 \theta_{23}, \Delta m^2 > 0$	$0.437^{+0.033}_{-0.023}$	$0.374 - 0.628$
$\sin^2 \theta_{23}, \Delta m^2 < 0$	$0.455^{+0.039}_{-0.031},$	$0.380 - 0.641$
$\sin^2 \theta_{13}, \Delta m^2 > 0$	$0.0234^{+0.0020}_{-0.0019}$	$0.0176 - 0.0295$
$\sin^2 \theta_{13}, \Delta m^2 < 0$	$0.0240^{+0.0019}_{-0.0022}$	$0.0178 - 0.0298$

$$U_{PMNS} \approx \begin{pmatrix} 0.80 & 0.55 & 0.15 \\ 0.40 & 0.60 & 0.70 \\ 0.40 & 0.60 & 0.70 \end{pmatrix}$$

# Neutrino MC Generators: A Theory/Experiment Interface

Model dependence encapsulated in comprehensive Neutrino MC Generators



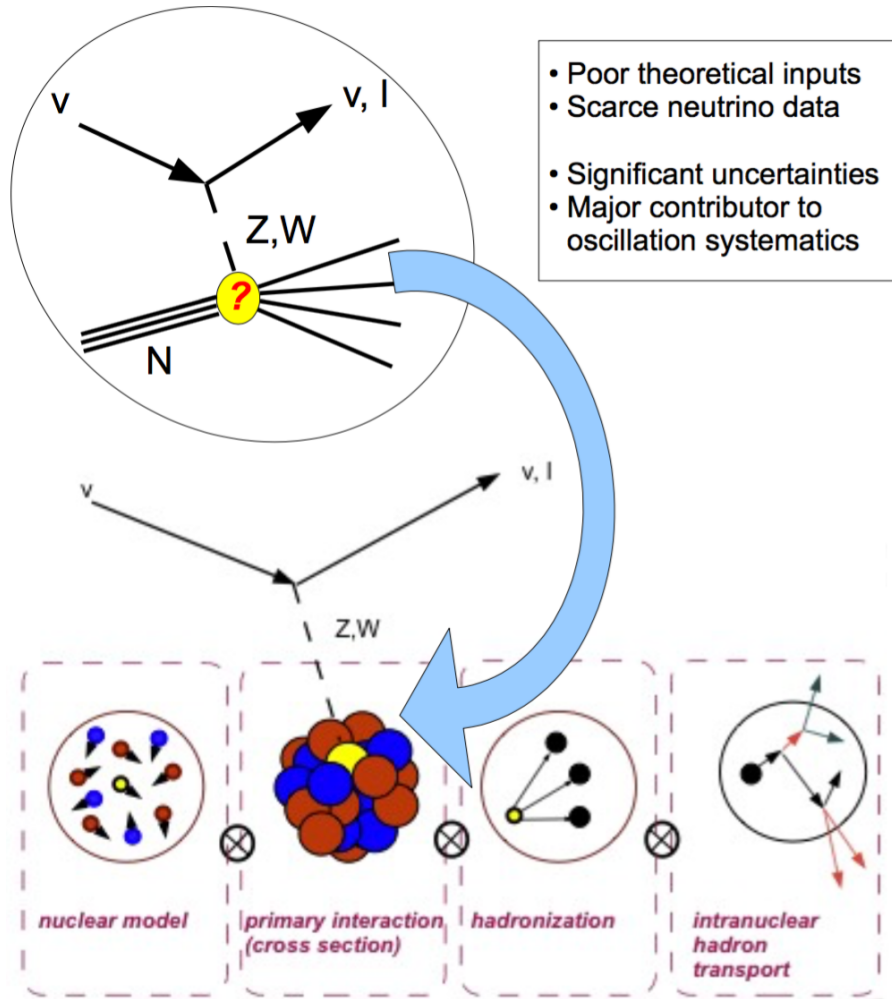
Neutrino MC Generators connect the true and observed event topologies and kinematics.

Every observable a convolution of flux, interaction physics and detector effects. Neutrino MC Generators allow experimentalists to access, improve, validate, assess the uncertainty of and tune the *physics* models that drive the result of that convolution.

Several such MC Generators in use: **GENIE**, **NuWro**, **NEUT**

# Neutrino MC Generator factorization

Cross-section calculation at the **neutrino - nucleon level** a starting point.



The nucleon is not a simple object!

Process dynamics described by the invariant amplitude  $|M|^2 = L_{\mu\nu} W^{\mu\nu}$   
where:

$$W_{\mu\nu} = W_1 \delta_{\mu\nu} + W_2 p_\mu p_\nu + W_3 \epsilon_{\mu\nu\alpha\beta} p^\alpha p^\beta + \\ + W_4 q_\mu q_\nu + W_5 (p_\mu q_\nu + p_\nu q_\mu) + W_6 (p_\mu q_\nu - p_\nu q_\mu)$$

Issue: Knowledge of  $W_1, W_2, \dots$  in a kinematical regime that bridges the non-perturbative and perturbative pictures of the nucleon.

Neutrino-nucleus simulations by adding effects:

- the initial nuclear state dynamics
- hadronization
- intranuclear hadron transport

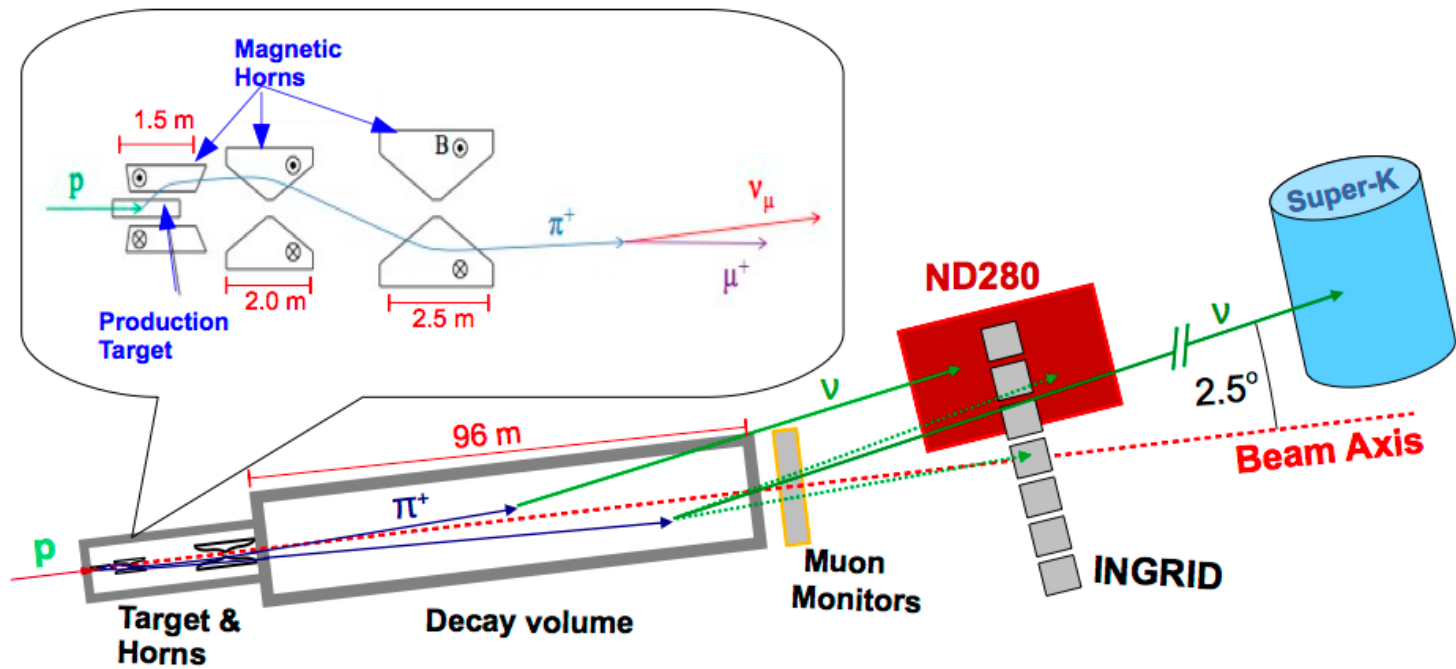
# Making the T2K neutrino beam

**Primary proton beam from the 30-GeV J-PARC proton accelerator.**



- Fast extraction
- 8 bunches/spill
- 581 nsec bunch interval
- 58 nsec bunch width
- Rep. rate (May '16): 2.48 sec
- p/spill (May '16):  $2.2 \times 10^{14}$
- p/spill (design):  $3.3 \times 10^{14}$
- Power (May '16): 420 kW
- Power (design): 750 kW

# Making the T2K neutrino beam



**Target:** A 2.6 cm wide, 91.4 cm (1.9 interaction lengths) long graphite rod

**Focussing:** 3 magnetic horns pulsed with 250 (max 320) kA currents generating  $\sim 2$  T field:  $\sim 16\times$  increase in  $\nu$  flux w.r.t unfocussed beam.

**Decay volume:** A 96 m long steel decay tunnel

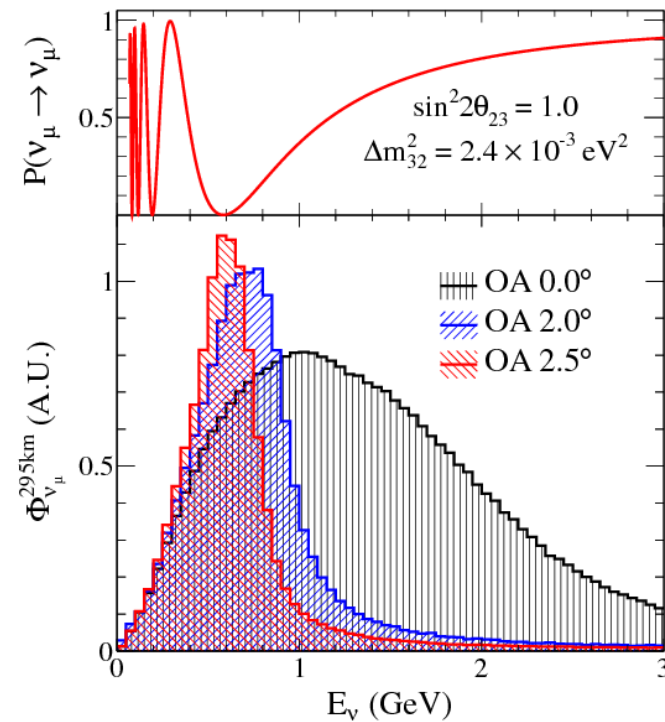
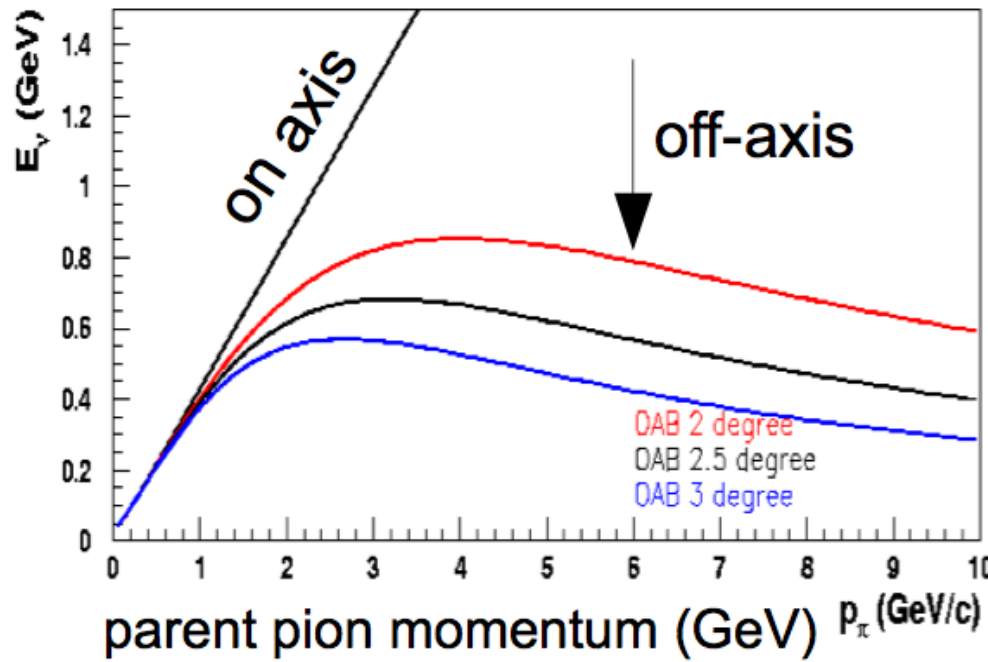
Where do our  $\nu$ 's come from?

- $\pi^+ \rightarrow \nu_\mu + \mu^+$
- $\pi^- \rightarrow \bar{\nu}_\mu + \mu^-$
- $\mu^+ \rightarrow \bar{\nu}_\mu + \nu_e + e^+$
- $\mu^- \rightarrow \bar{\nu}_e + \nu_\mu + e^-$
- $K^+ \rightarrow \nu_\mu + \mu^+$
- $K^+ \rightarrow \nu_e + \pi^0 + e^+$
- $K^+ \rightarrow \nu_\mu + \pi^0 + \mu^+$
- $K^- \rightarrow \bar{\nu}_\mu + \mu^-$
- $K^- \rightarrow \bar{\nu}_e + \pi^0 + e^-$
- $K^- \rightarrow \bar{\nu}_\mu + \pi^0 + \mu^-$
- $K_L^0 \rightarrow \bar{\nu}_\mu + \pi^+ + \mu^-$
- $K_L^0 \rightarrow \nu_\mu + \pi^- + \mu^+$
- $K_L^0 \rightarrow \bar{\nu}_e + \pi^+ + e^-$
- $K_L^0 \rightarrow \nu_e + \pi^- + e^+$

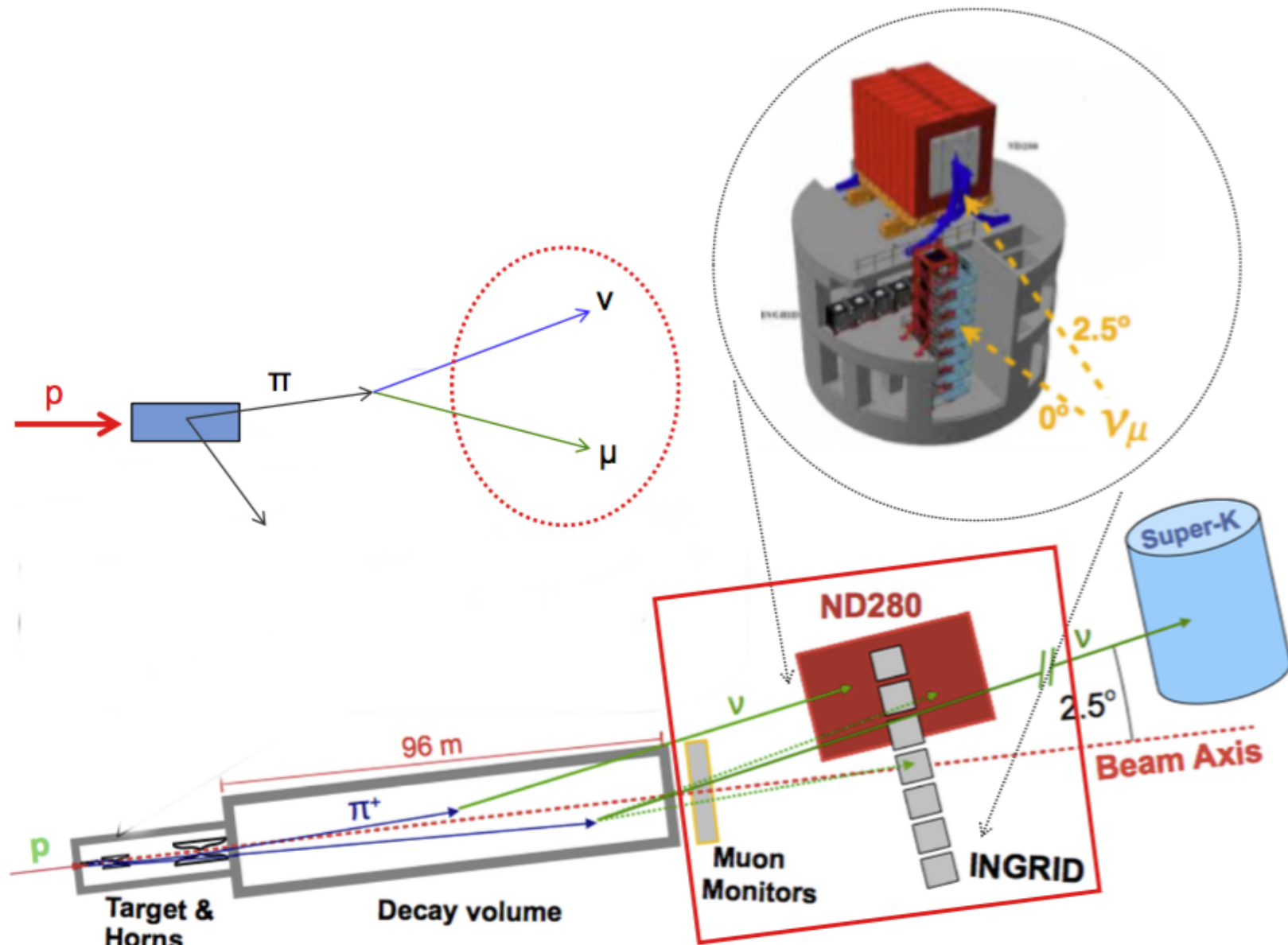
# Making the T2K neutrino beam

**T2K was the first accelerator experiment going off-axis.**

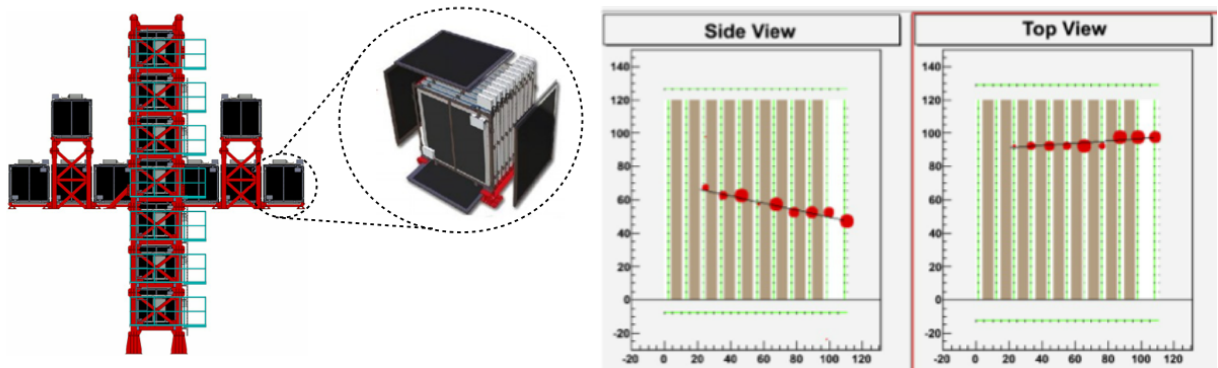
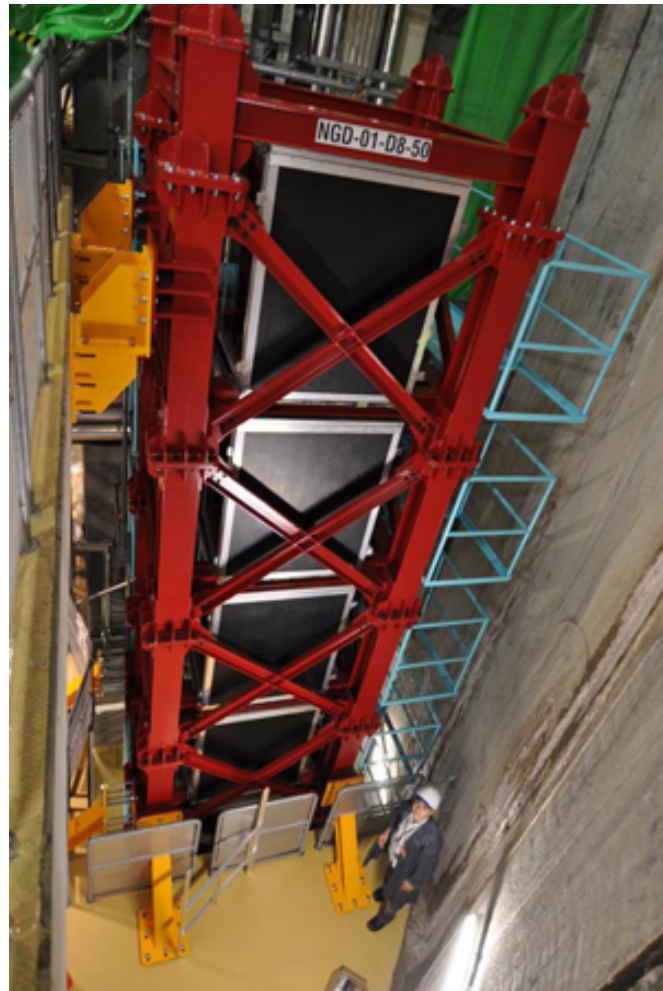
Exploits kinematical properties of pion decay to create a narrow-band neutrino beam peaked at an energy chosen so as to maximize the oscillation probability at the SuperK location.



# T2K near detector complex

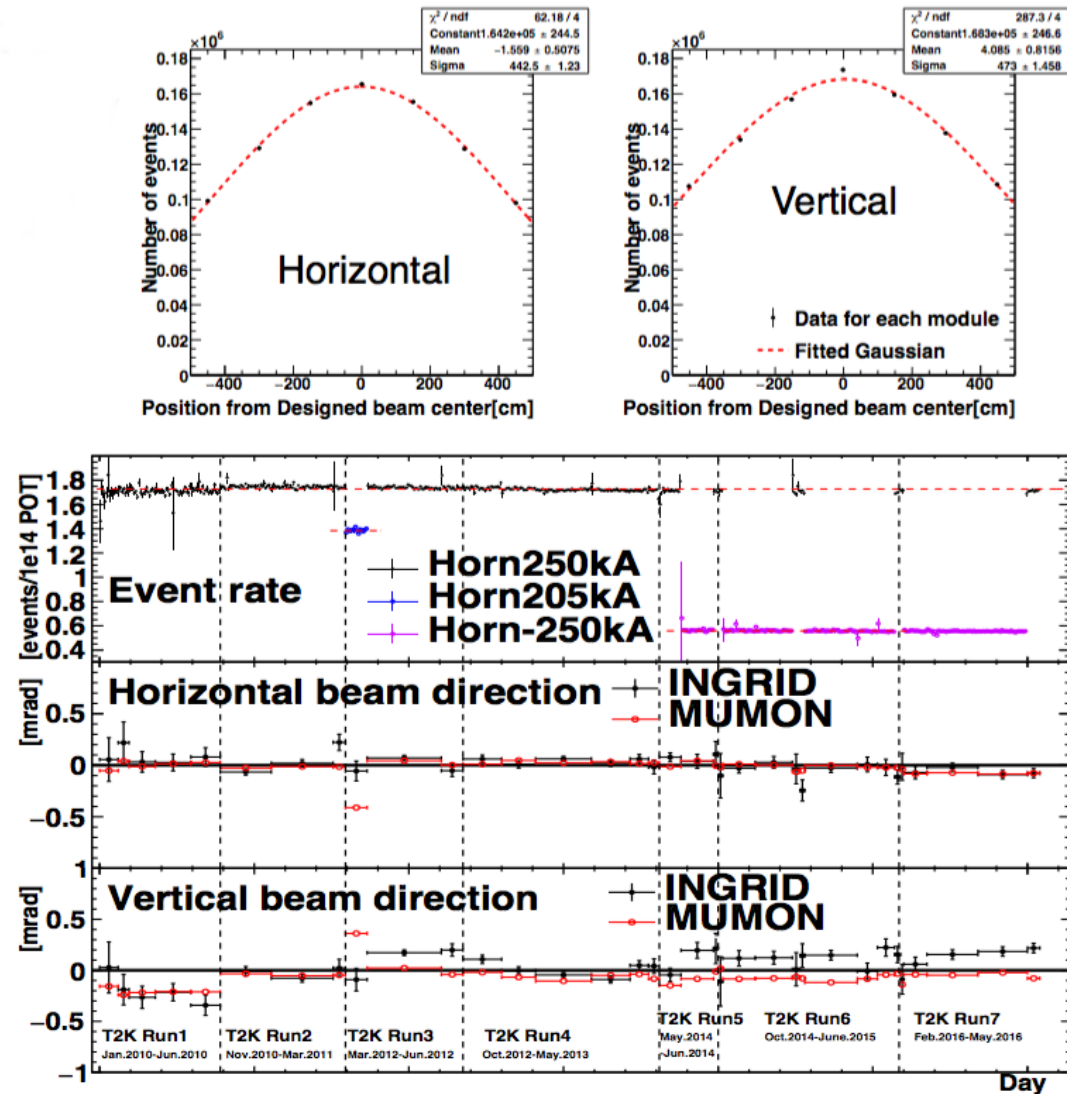


# T2K neutrino beam monitoring



- 16 modules (14 in cross configuration).
- Each module: 7 tons, alternating scintillator / iron planes.
- $10\text{ m} \times 10\text{ m}$  beam area coverage
- 1 event per  $\sim 6 \times 10^{13}$  protons on target.
- Monitors neutrino beam rate and profile.

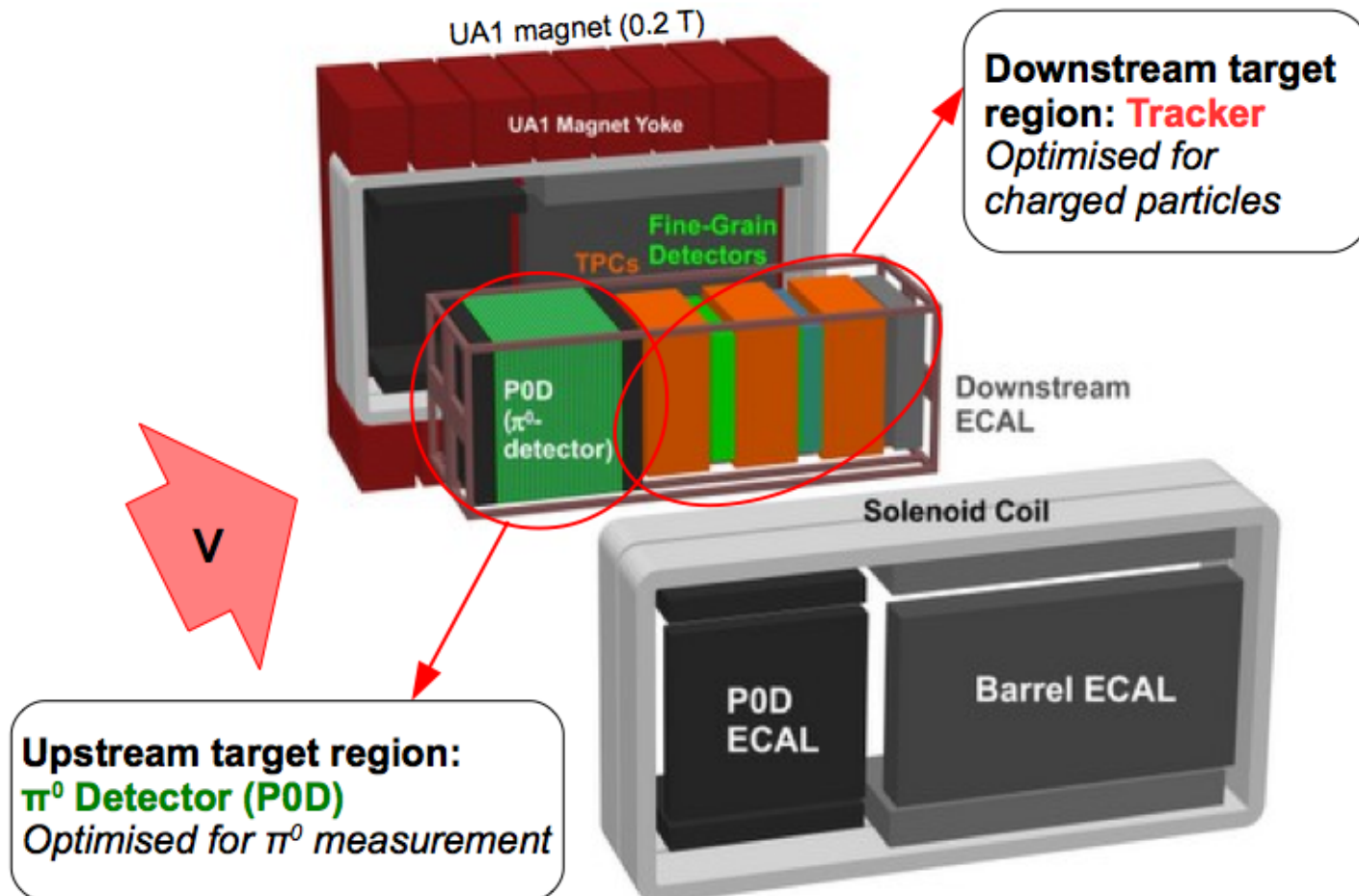
# T2K neutrino beam monitoring



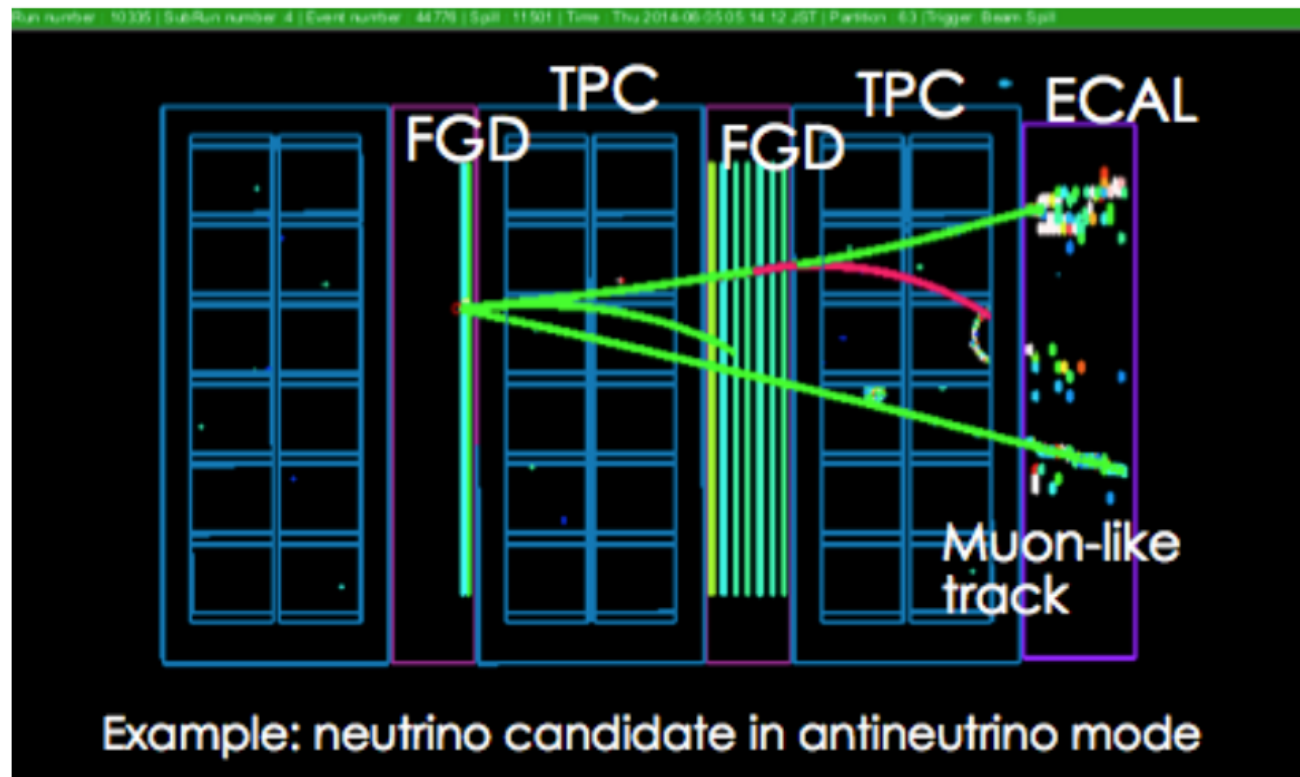
- Beam direction stable within 1 mrad (corresponding to less than  $\sim 2\%$  peak energy shift at SuperK)
- POT (Protons On Target) normalised event rate stable to better than 1%

# Off-axis near detector at 280 m

# Tracking Calorimeters and Time Projection Chambers in a 0.2 T B field. Polystyrene and water targets.

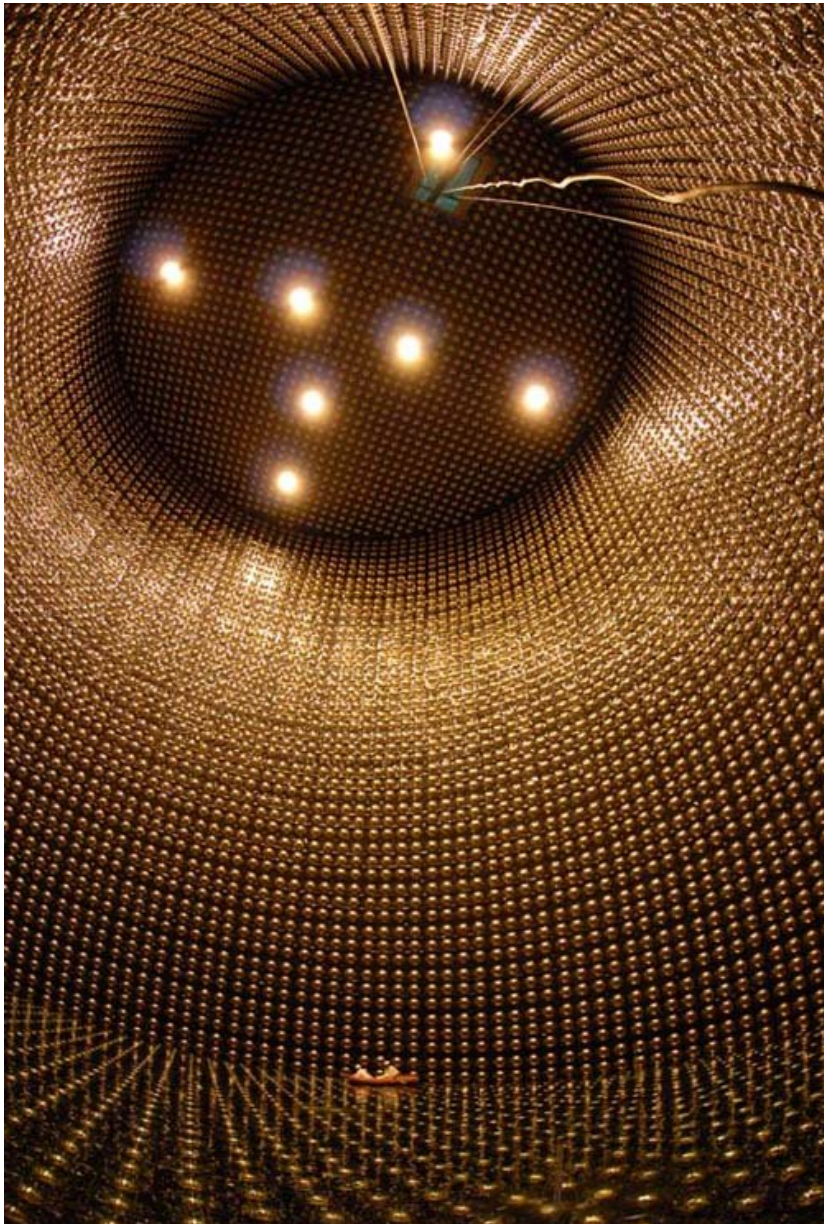


# Tracker system @ Off-axis Near Detector at 280 m



- 2 fine-grained scintillator detectors (FGDs) + 3 time projection chambers (TPCs).
- FGDs provide the target mass (FGD1: 1 ton scintillator, FGD2: 0.5 ton scintillator + 0.5 ton water).
- Momentum measurement of charged particles, PID via  $dE/dx$ .
- Better than 10%  $dE/dx$  resolution, and 10% momentum resolution at 1 GeV.

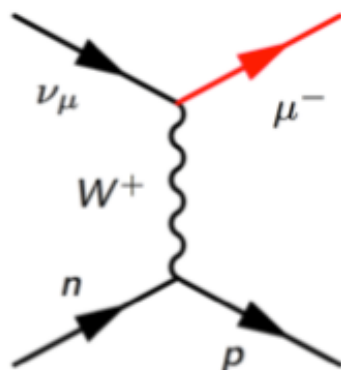
# The Far Detector (Super-Kamiokande IV)



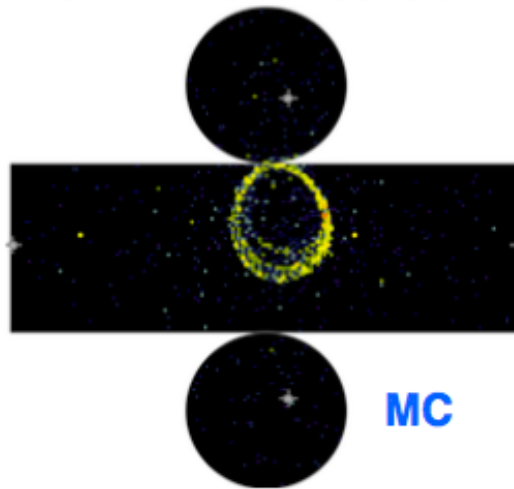
- 50 kt Water Cherenkov detector (22.5 kton fiducial)
- Overburden (shielding): 2700 mwe
- Inner Detector (ID): 11,129 20" PMTs (40% photo-cathode coverage)
- Outer Detector (OD): 1,885 8" PMTs
- DAQ: No dead-time
- Energy threshold:  $\sim 4.5$  MeV

# Water Cherenkov Imaging: Identifying $\nu_e$ and $\nu_\mu$

$\nu_\mu$  CCQE

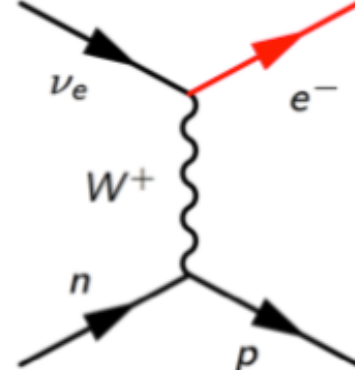


- Low scattering
- Ring with sharp edge
- Protons below Cherenkov threshold

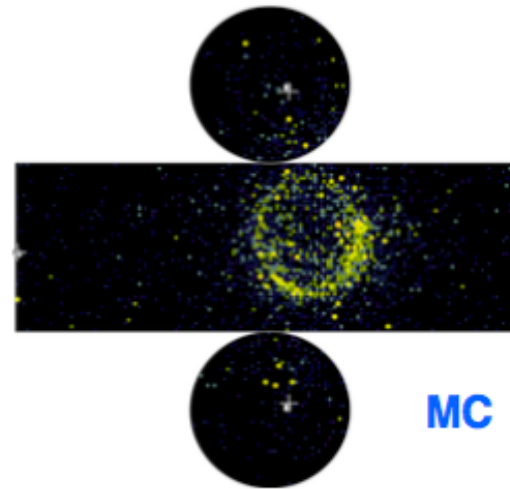


MC

$\nu_e$  CCQE

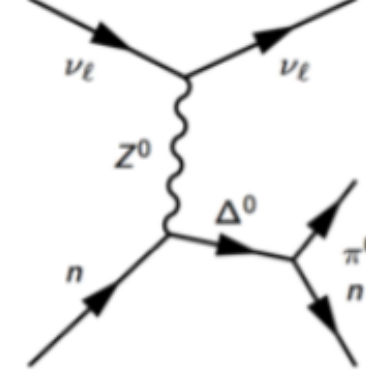


- Multiple scattering
- EM shower
- Ring with “fuzzy” edge

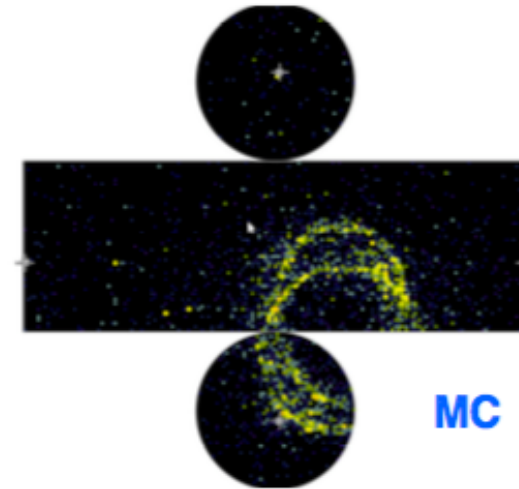


MC

Background



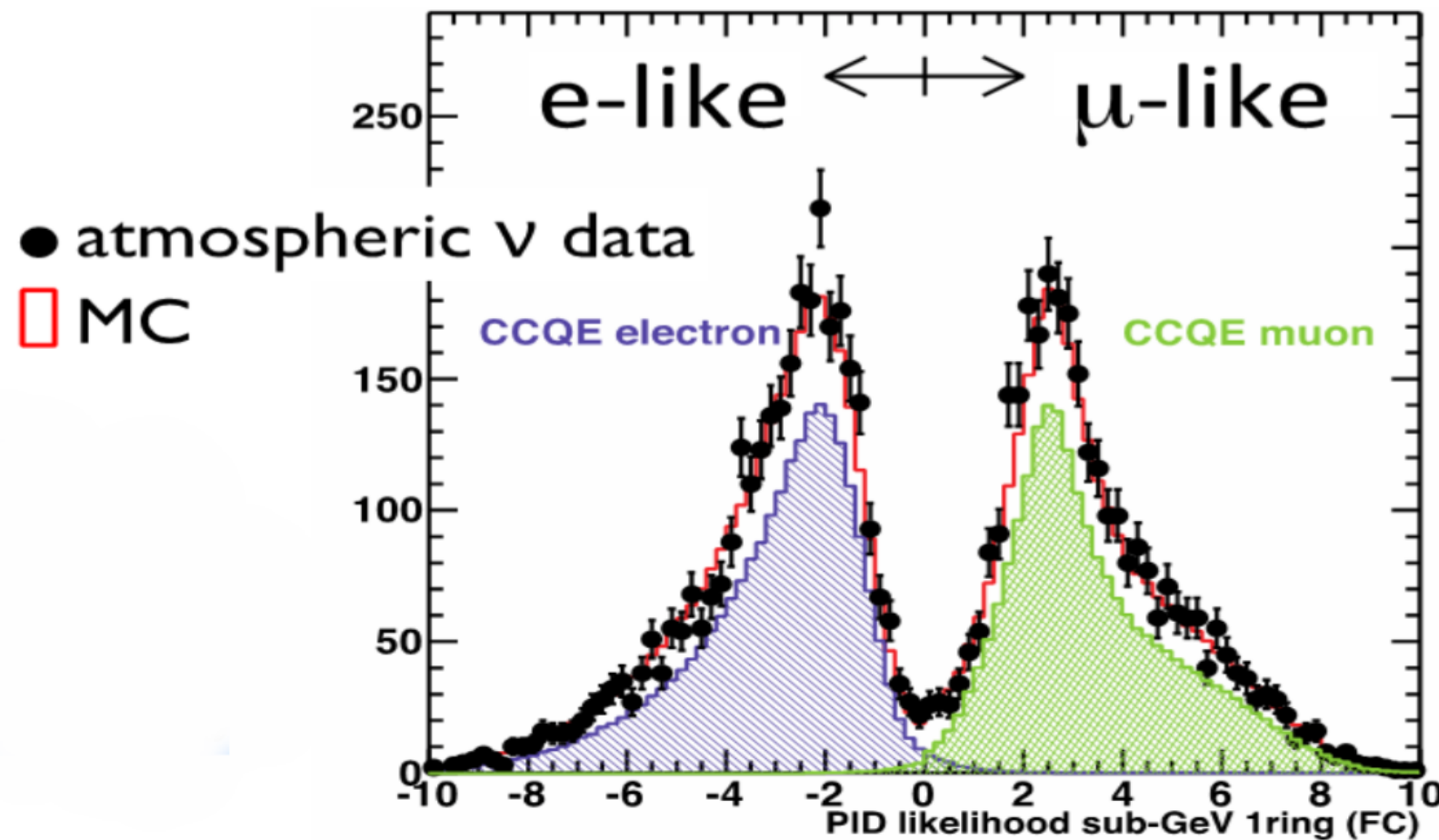
- EM shower from  $\pi^0 \rightarrow \gamma\gamma$
- Can be misidentified as an electron



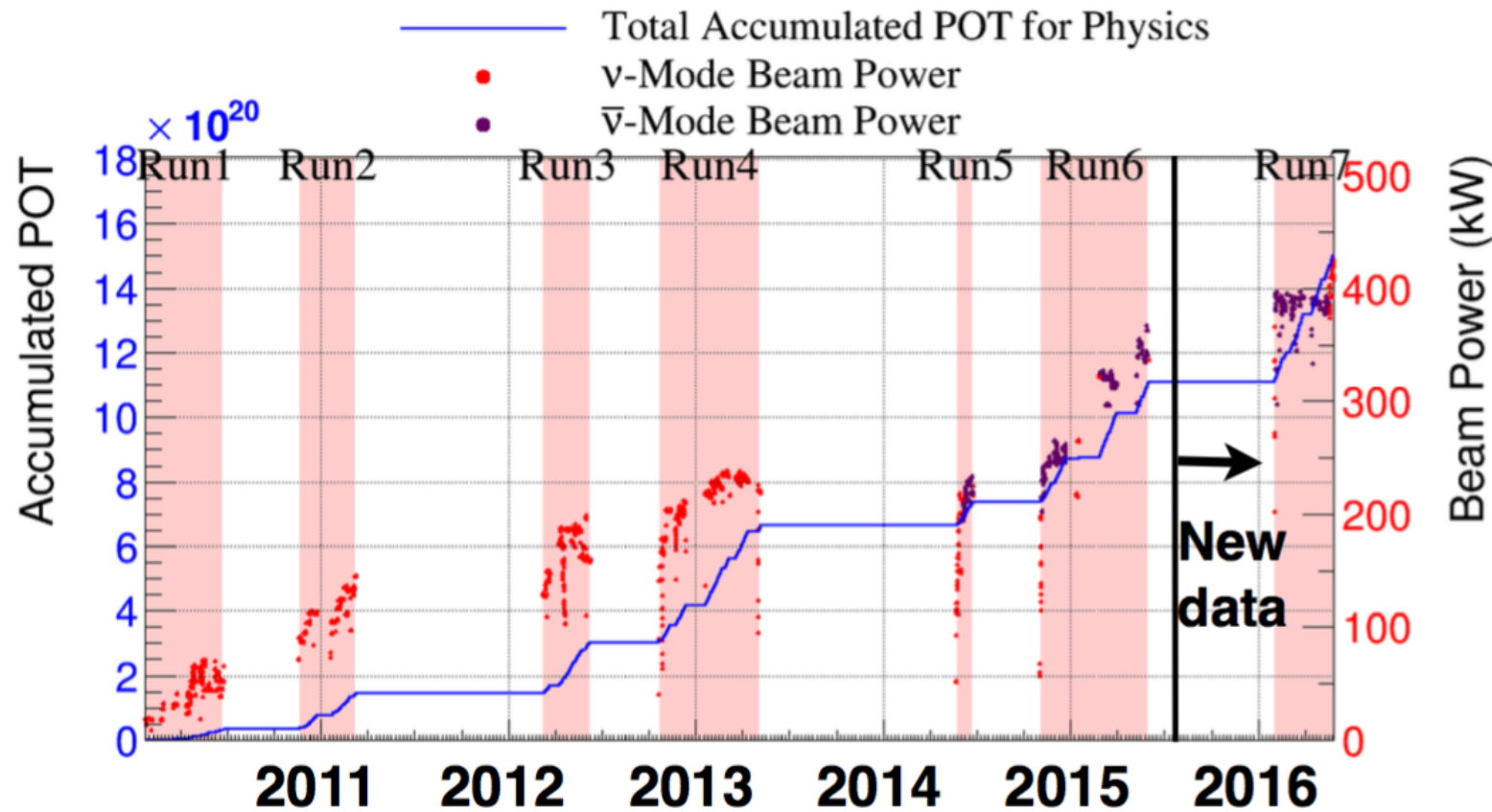
MC

# Water Cherenkov Imaging: Identifying $\nu_e$ and $\nu_\mu$

- Excellent e/ $\mu$  separation.
- Probability to misidentify a muon as an electron is smaller than 1%.



# T2K Datasets



Mode	Exposure in protons on target (POT)
Neutrino	$7.57 \times 10^{20}$
Antineutrino	$7.53 \times 10^{20}$
Combined	$1.510 \times 10^{21}$

- Steady improvement of beam power (increased up to 420 kW).
- Double antineutrino exposure in 2016.

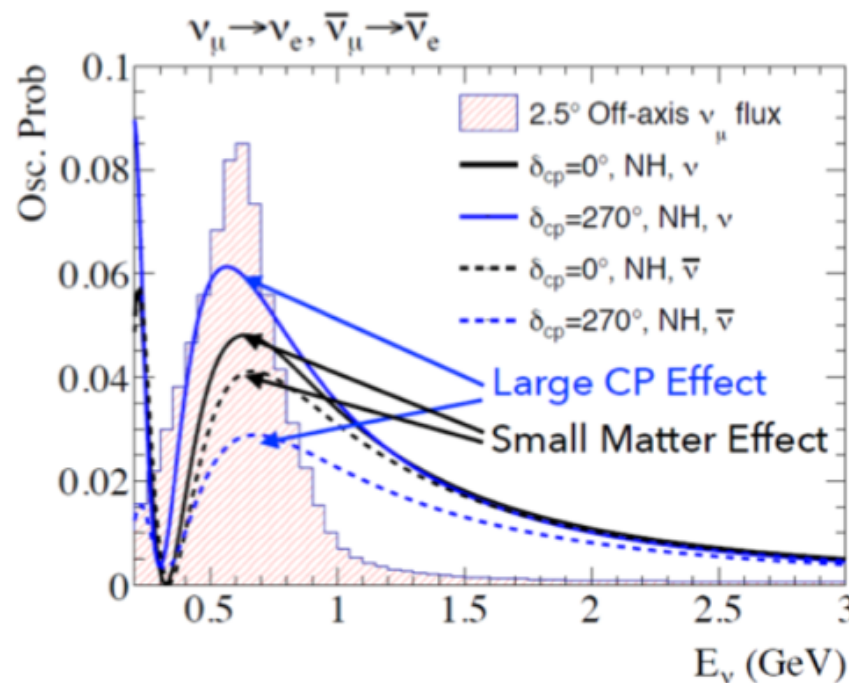
# Measuring neutrino oscillations at T2K

$$P(\nu_\mu \rightarrow \nu_e) \simeq \boxed{\sin^2 2\theta_{13} \times \sin^2 \theta_{23} \times \frac{\sin^2[(1-x)\Delta]}{(1-x)^2}}$$

*Phys. Rev. D64 (2001) 053003*  
**Leading term**

CP violating  $\textcolor{orange}{-\alpha \sin \delta_{CP}}$   $\times \sin^2 2\theta_{12} \sin 2\theta_{13} \sin 2\theta_{23} \times \sin \Delta \frac{\sin[x\Delta]}{x} \frac{\sin[(1-x)\Delta]}{(1-x)}$   
 “+” for antineutrino

$$\text{CP conserving} \quad \alpha \cos \delta_{CP} \times \sin 2\theta_{12} \sin 2\theta_{13} \sin 2\theta_{23} \times \cos \Delta \frac{\sin[x\Delta]}{x} \frac{\sin[(1-x)\Delta]}{(1-x)} + O(\alpha^2) \quad x = \frac{2\sqrt(2)G_F N_e E}{\Delta m_{31}^2} \quad \alpha = |\frac{\Delta m_{21}^2}{\Delta m_{31}^2}| \sim \frac{1}{30} \quad \Delta = \frac{\Delta m_{31}^2 L}{4E}$$



- $\delta_{CP}$  has asymmetric effect on  $P(\nu_\mu \rightarrow \nu_e)$  and  $P(\bar{\nu}_\mu \rightarrow \bar{\nu}_e)$ 
    - $\delta_{CP} = -\pi/2$ : Maximizes  $P(\nu_\mu \rightarrow \nu_e)$ , minimizes  $P(\bar{\nu}_\mu \rightarrow \bar{\nu}_e)$
    - $\delta_{CP} = +\pi/2$ : vice versa...
  - $\delta_{CP}$  effect is  $\pm 20\text{-}30\%$
  - Matter effect is  $\pm 10\%$

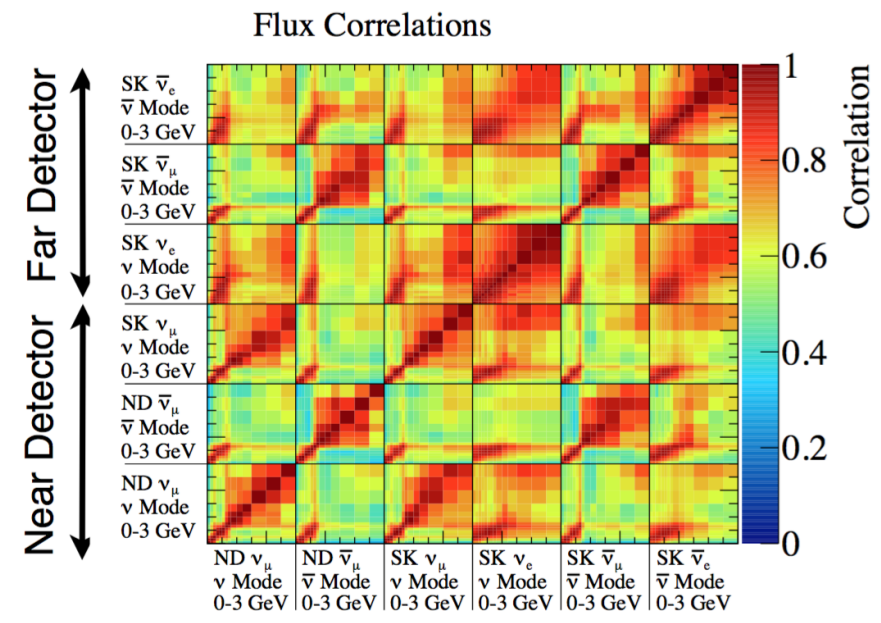
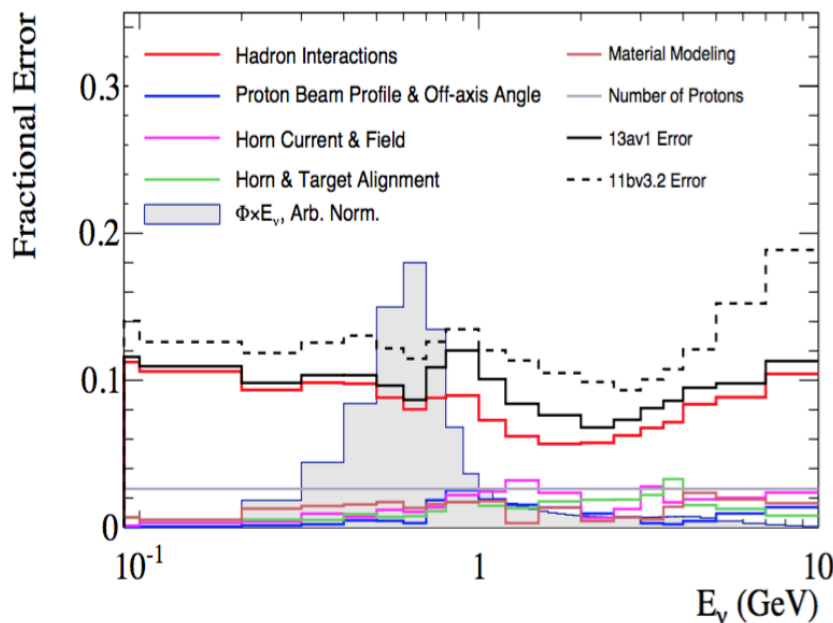
# Prior systematic error constraints

Neutrino flux tuned using hadro-production data from **NA61/SHINE**: Pion, proton and kaon production with a 31 GeV/c proton beam on

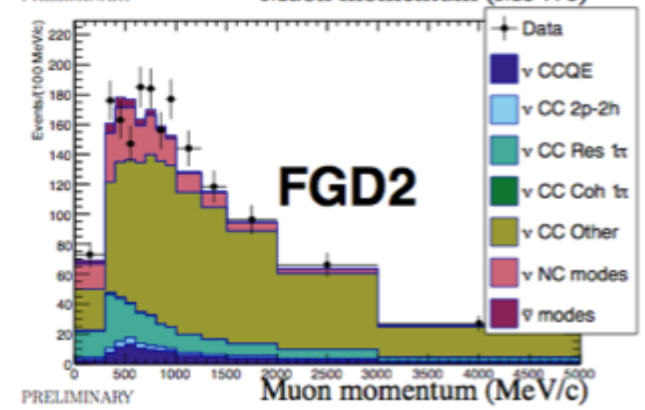
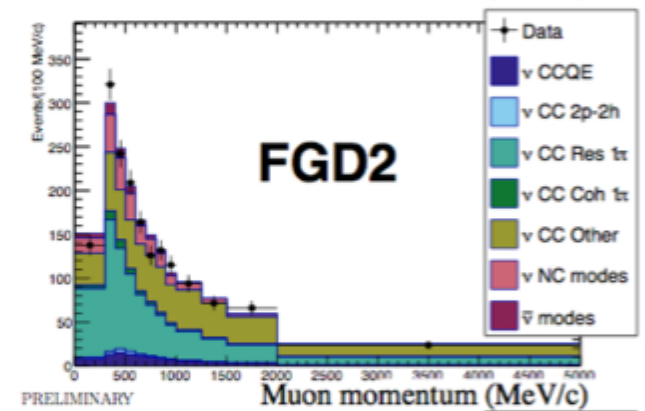
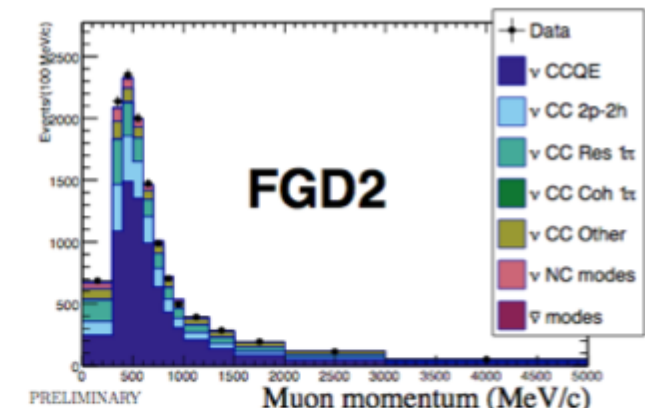
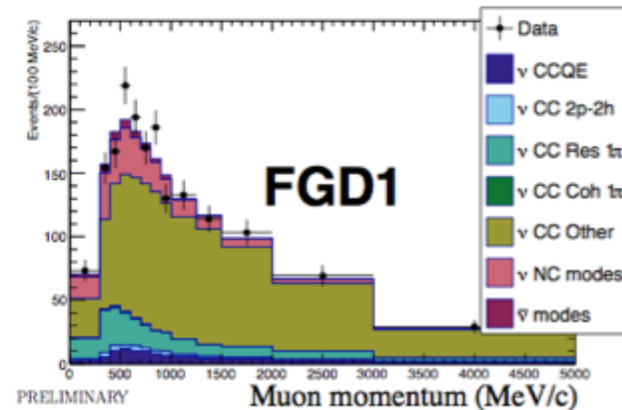
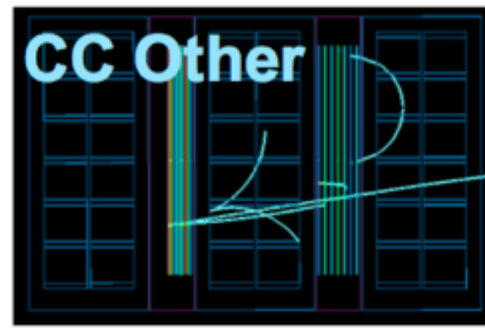
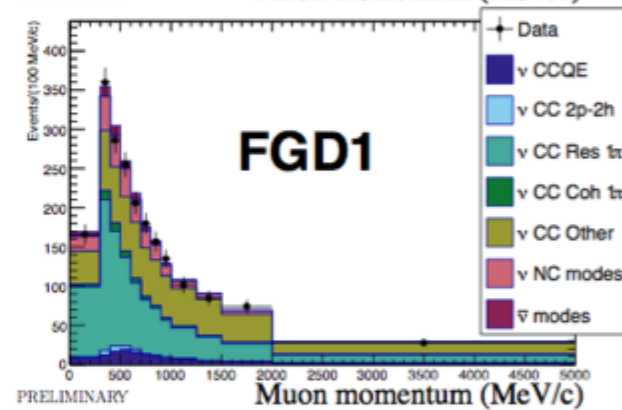
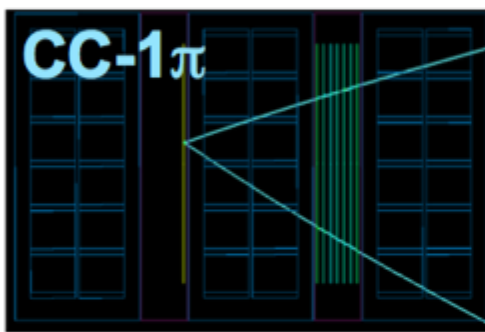
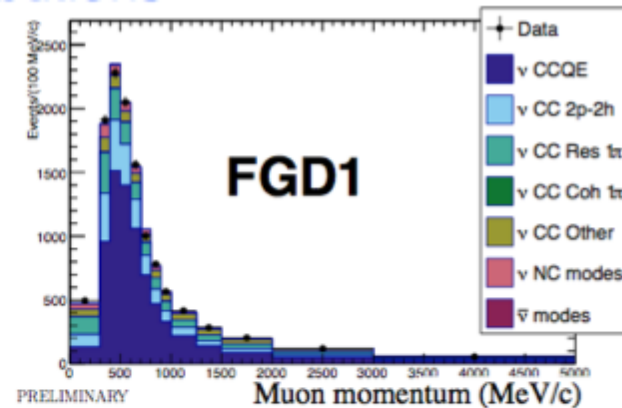
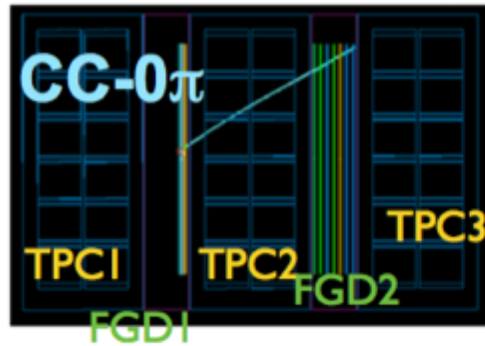
- a thin carbon target (4% of an interaction length) [EPJ C76, 84 (2016)]
- a T2K replica target [EPJ C76, 617 (2016)]

Data cover almost the full T2K kinematic space.

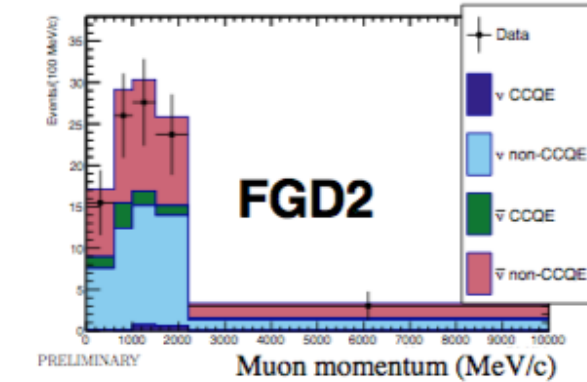
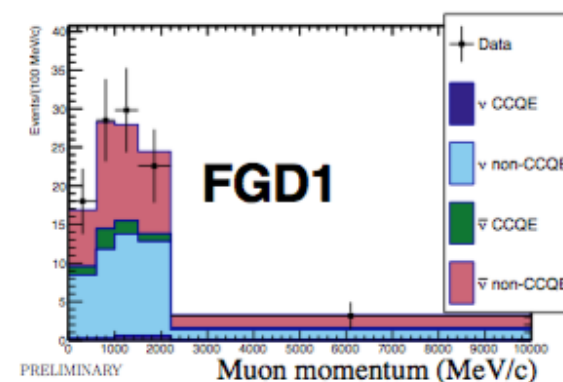
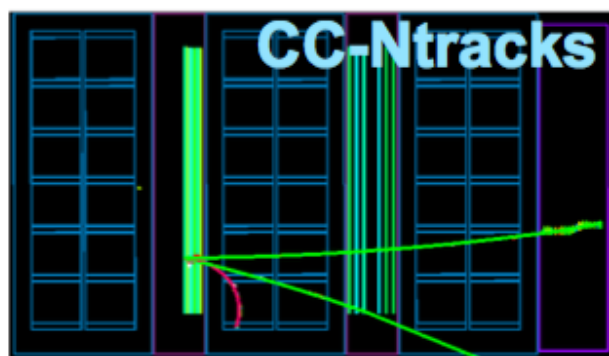
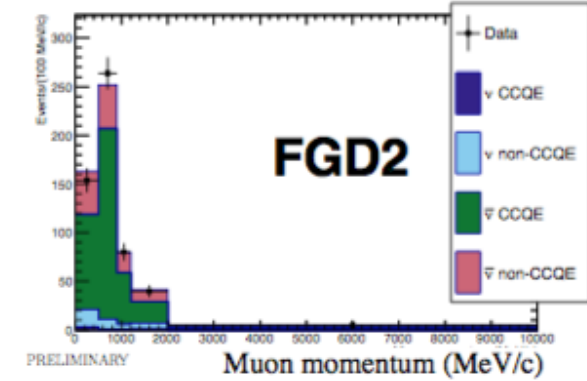
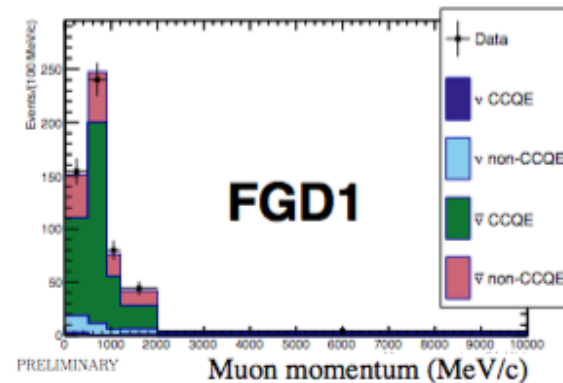
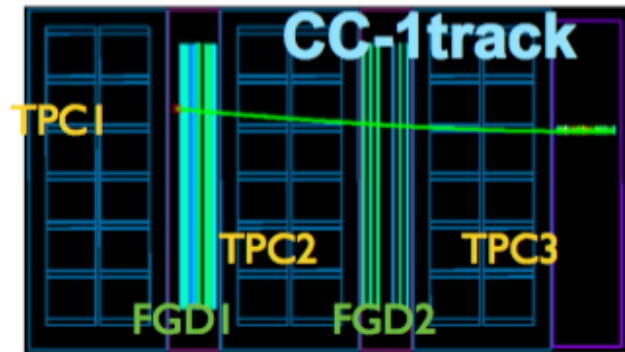
Flux systematic uncertainty reduced from  $\sim 30\%$  to  $\sim 10\%$ .



# Systematics constraint from the Near Detector



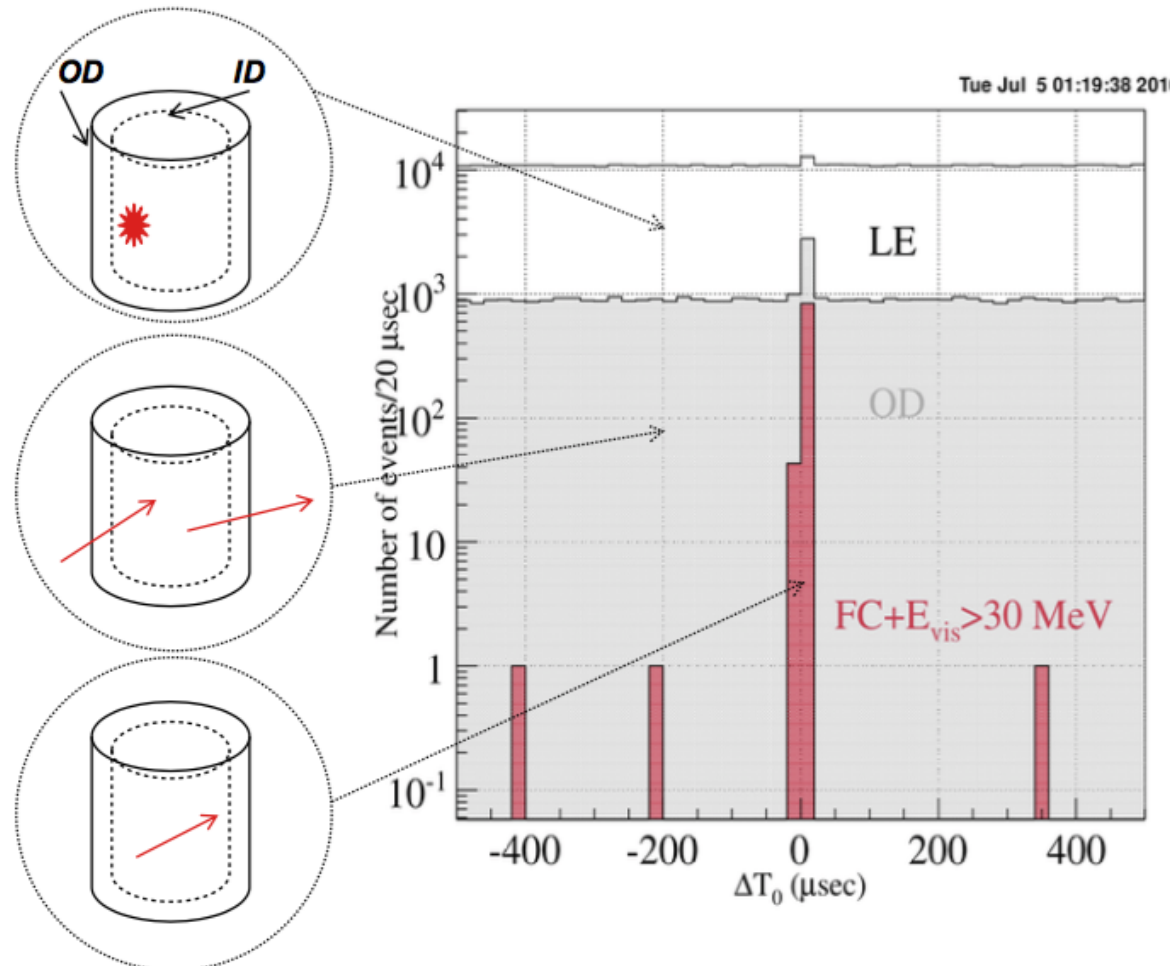
# Systematics constraint from the Near Detector



# SuperK event reduction

12.8M ‘good spills’ → 917 ‘on-time’ FC (Fully Contained) events.

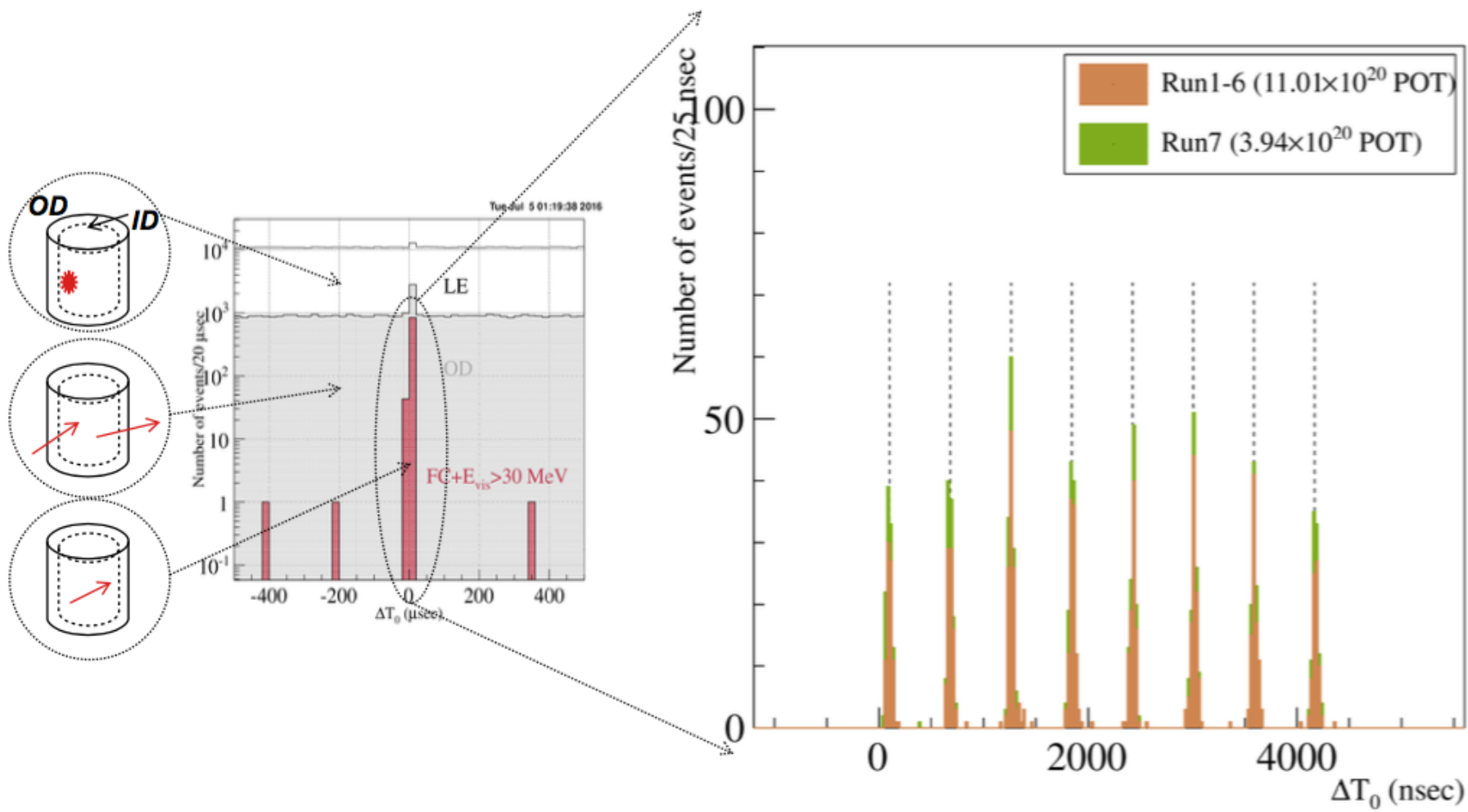
(‘on time’: within  $-2 \mu\text{sec}$  to  $+10 \mu\text{sec}$  from the arrival time of the leading edge of the spill)



Left:  $\Delta T_0$  distribution  
of events at 1 msec  
window around the  
beam arrival time.

# SuperK event reduction

Below:  $\Delta T_0$  distribution of all FC events zoomed into the spill on-timing window. The 8 bunch structure (581 nsec interval between bunches) of the J-PARC proton beam can be seen with neutrinos.



# SuperK event reduction

Out of the **917 FC events** (654 in  $\nu$  mode + 263 in  $\bar{\nu}$  mode):

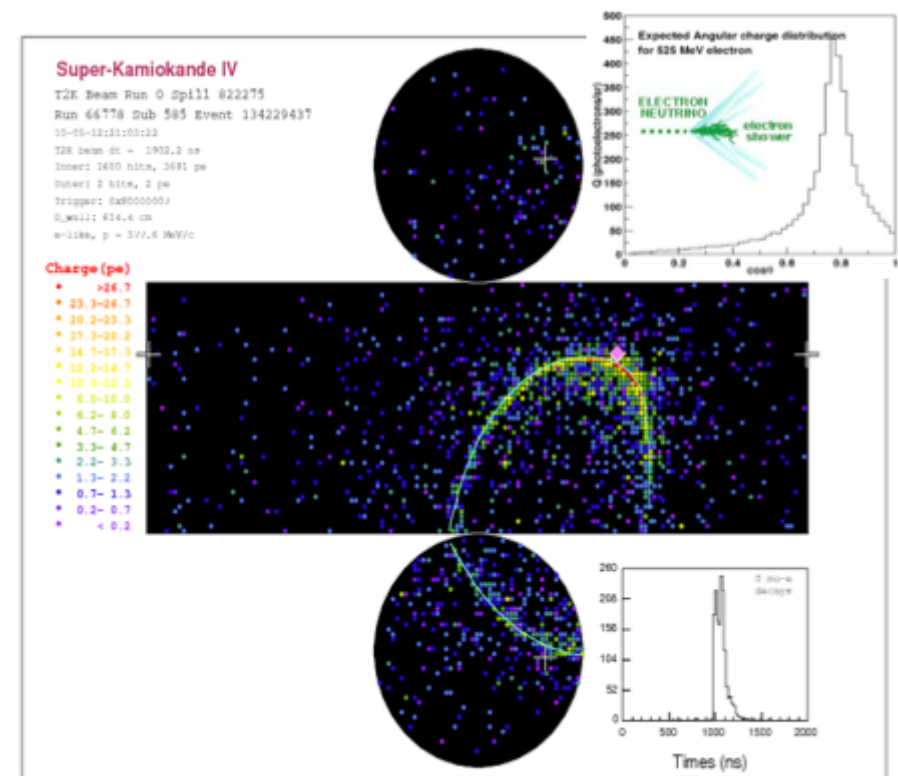
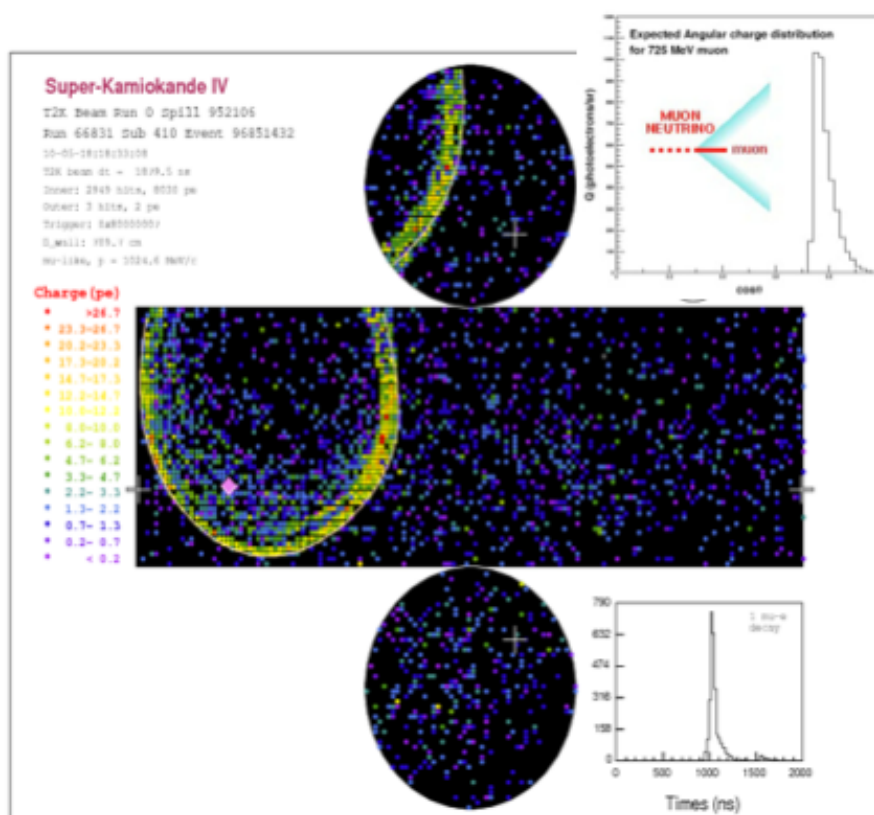
- **603 events** (433 in  $\nu$  mode + 170 in  $\bar{\nu}$  mode) events belong to the **FCFV subset**:
  - They have visible energy above 30 MeV, and
  - a vertex in the fiducial volume (2m away from a tank wall).
- The FCFV events are subdivided further based on the ring topology.

Sample	Data	Runs 1-7 (neutrino)			Runs 5-7 (antineutrino)			
		MC $\sin^2\theta_{13}=0.02$	MC $\sin^2\theta_{13}=0$	MC Unosc.	Data	MC $\sin^2\theta_{13}=0.02$	MC $\sin^2\theta_{13}=0$	MC Unosc.
FC	654	614.8	569.1	1289.2	263	255.9	248.1	472.3
FCFV	433	427.8	396.0	877.8	170	180.6	175.2	329.7
Single Ring	217	221.4	193.7	616.6	94	96.2	91.5	228.1
1R $\mu$ -like	147	155.1	156.5	565.6	78	74.5	75.1	209.0
$p_\mu > 200 \text{ MeV}/c$	147	154.8	156.2	564.5	78	74.4	75.0	208.8
1R $e$ -like	70	66.3	37.2	51.0	16	21.7	16.3	19.1
$p_e > 100 \text{ MeV}/c$	66	61.2	32.6	38.7	14	20.2	14.9	16.6
Multi-ring	216	206.4	202.3	261.2	76	84.4	83.7	101.6
MR $\mu$ -like	108	101.4	100.9	140.3	33	41.7	41.7	54.6
MR $e$ -like	108	104.9	101.4	120.9	43	42.7	42.0	47.0
2R $\pi^0$	26	25.0	24.5	25.5	9	11.0	10.9	10.9
non- $\pi^0$ w/ decay- $e$	53	51.9	51.0	67.1	19	20.2	20.1	24.5
non- $\pi^0$ no decay- $e$	29	28.0	25.9	28.2	15	11.6	11.0	11.5
FC non-FV	186	156.2	142.6	340.9	81	65.2	62.9	126.1

# SuperK oscillation analysis samples

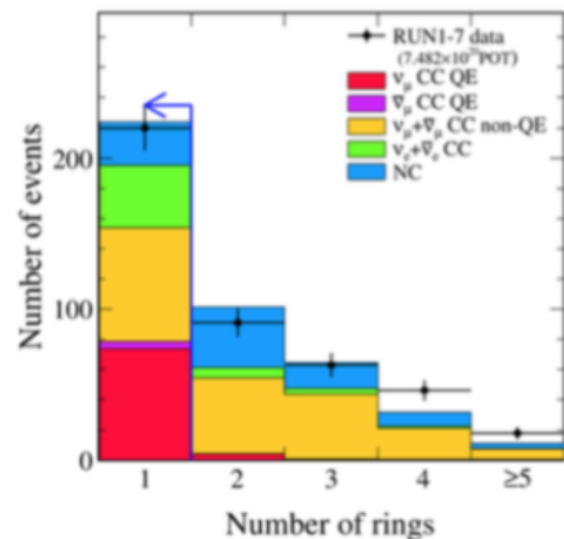
Current oscillation analysis is based only on events with

- a **single**  $\mu$ -like ring ( $\nu_\mu$ CC-like events), or
- a **single** e-like ring ( $\nu_e$ CC-like events)

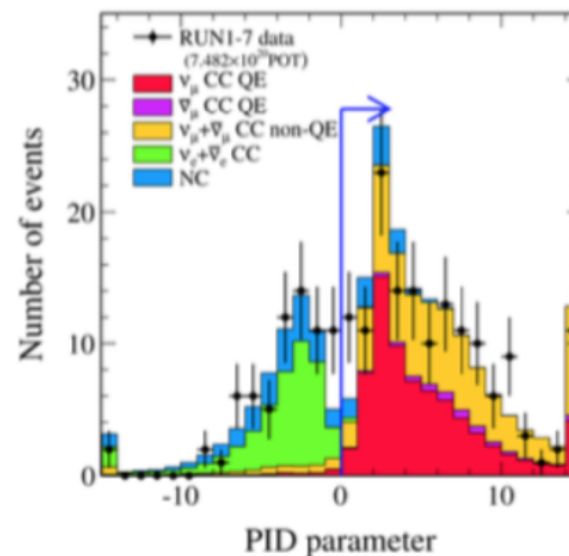


# $\nu_\mu/\bar{\nu}_\mu$ selections at SuperK

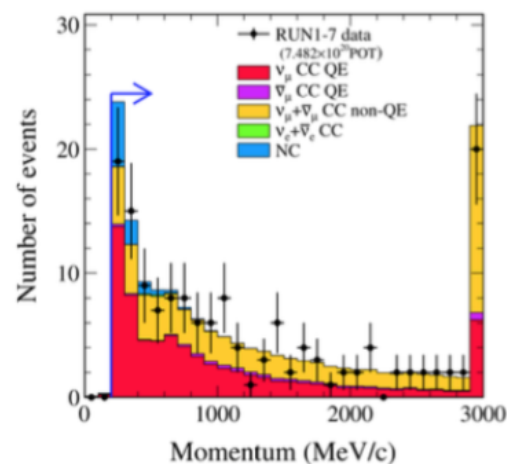
Single ring event



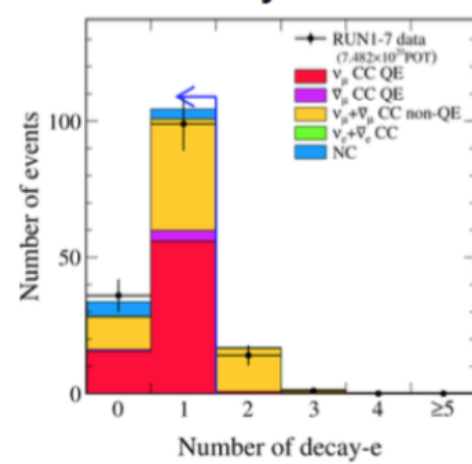
$\mu$ -like PID



Momentum > 200 MeV



# decay electron  $\leq 1$



- RUN1-7 data ( $7.482 \times 10^{20}$  POT)
- $\nu_\mu$  CC QE
- $\bar{\nu}_\mu$  CC QE
- $\nu_\mu + \bar{\nu}_\mu$  CC non-QE
- $\nu_e + \bar{\nu}_e$  CC
- NC

# $\nu_\mu/\bar{\nu}_\mu$ selections at SuperK

**Neutrino mode:**

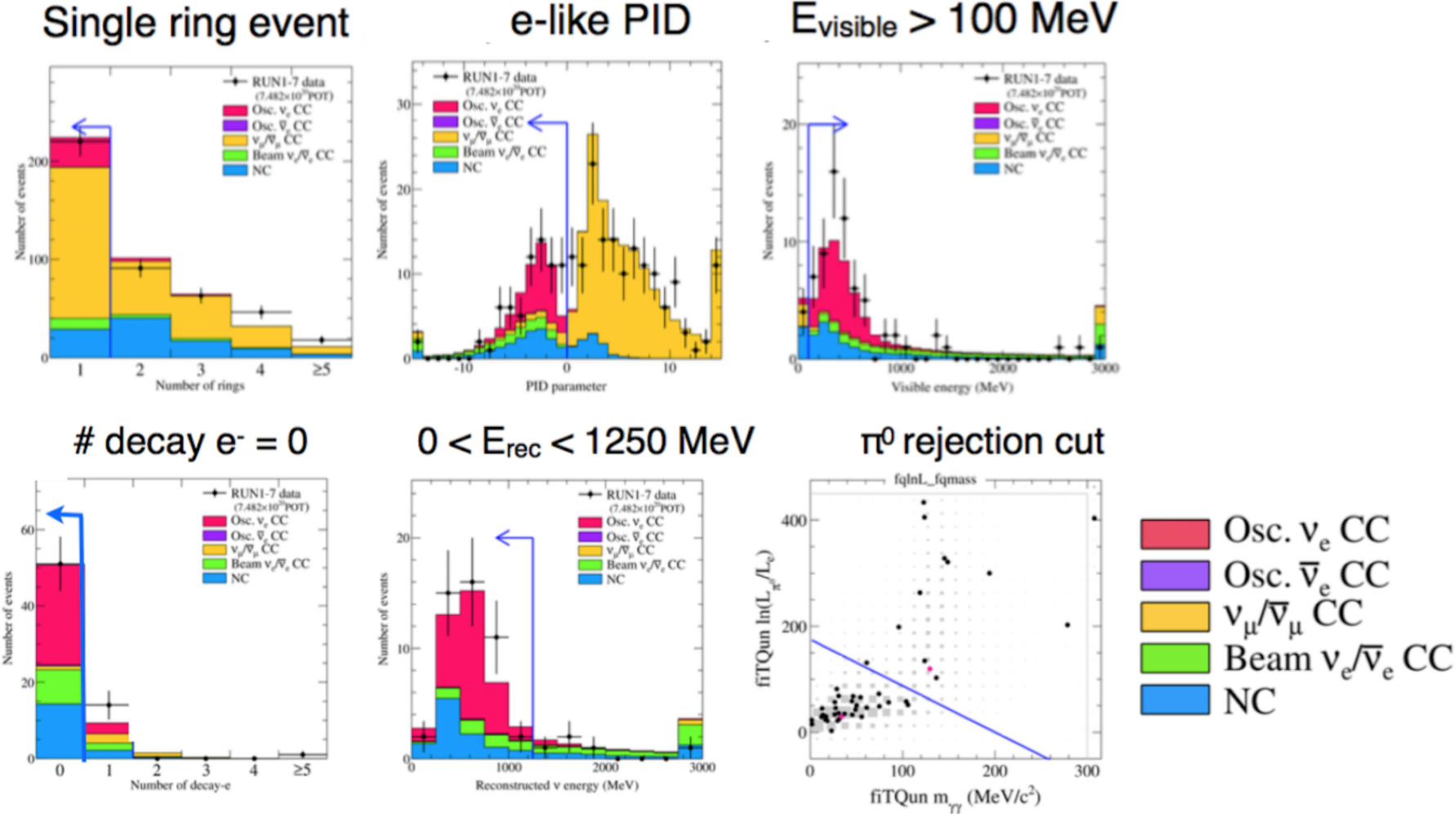
	Runs 1-7	Data	Expected					
			MC Total	$\nu_\mu$ CCQE	$\bar{\nu}_\mu$ CCQE	$\nu_\mu + \bar{\nu}_\mu$ CC non-QE	$\nu_e + \bar{\nu}_e$ CC	NC
Interactions in FV	654	744.8921	100.1736	6.4485	257.7017	54.4102	326.1581	
FCFV	438	431.8500	78.7501	4.8507	196.2819	53.2462	98.7212	
Single ring	220	223.4921	73.4936	4.6957	75.2087	41.4106	28.6836	
Muon-like PID	150	156.5553	72.2189	4.6532	70.0611	0.4657	9.1563	
$p_\mu > 200$ MeV/c	150	156.2370	72.0336	4.6504	70.0029	0.4657	9.0844	
$N_{decay-e} \leq 1$	135	137.7559	71.2831	4.6272	52.6050	0.4645	8.7760	
Efficiency from Interactions [%]	-	18.5	71.2	71.8	20.4	0.8	2.7	
Efficiency from FCFV [%]	-	31.9	90.5	95.4	26.8	0.9	8.9	

**Antineutrino mode:**

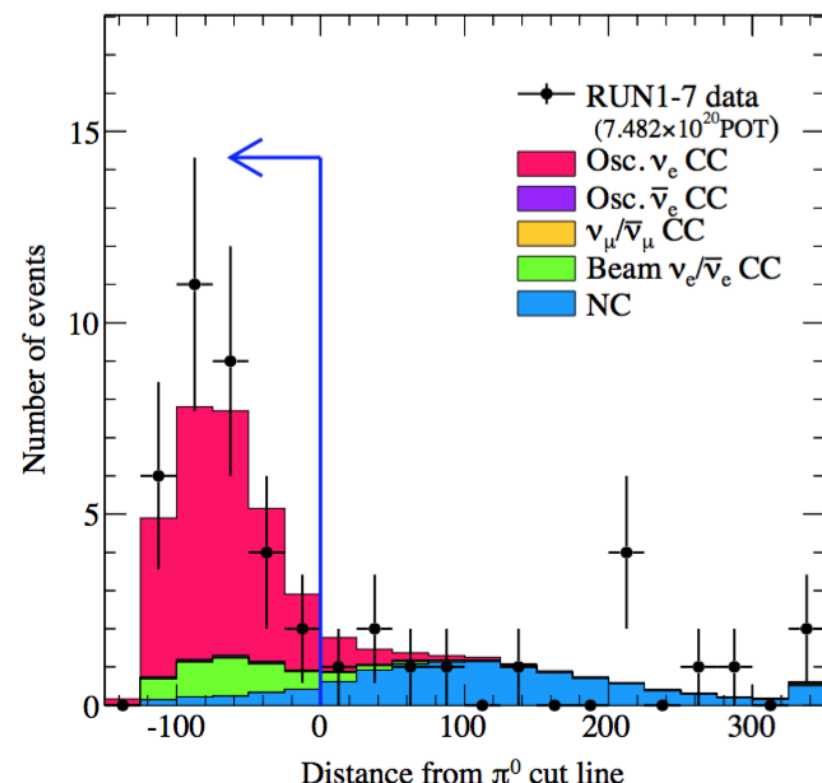
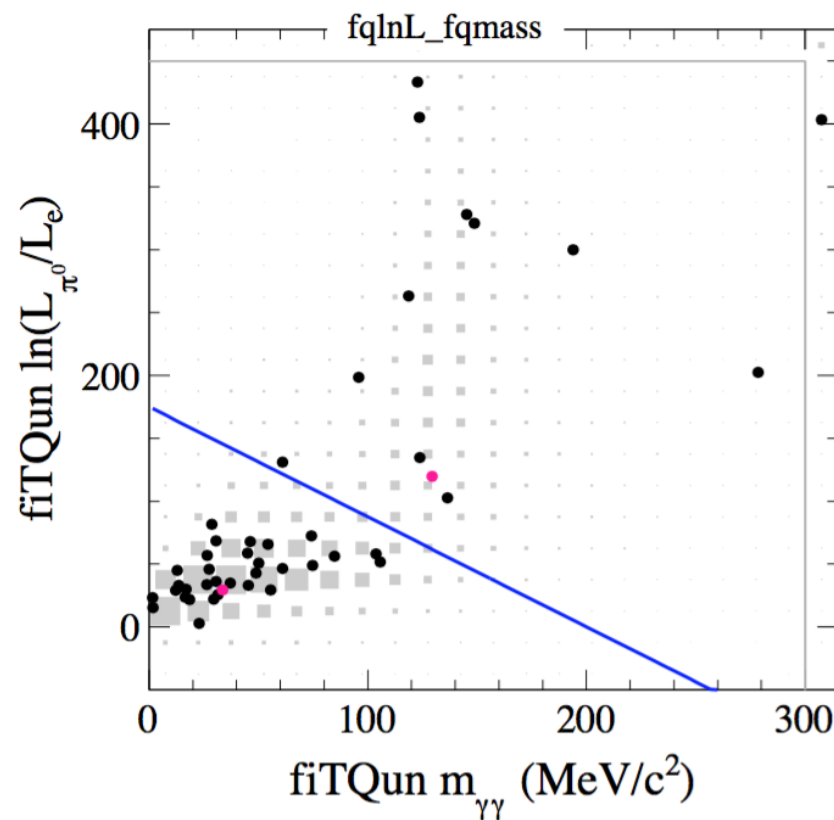
	Runs 5-7	Data	Expected					
			MC Total	$\nu_\mu$ CCQE	$\bar{\nu}_\mu$ CCQE	$\nu_\mu + \bar{\nu}_\mu$ CC non-QE	$\nu_e + \bar{\nu}_e$ CC	NC
Interactions in FV	263	312.3842	20.0413	30.7730	113.2287	15.5890	132.7521	
FCFV	170	180.4835	15.0375	24.9456	83.2607	15.1875	42.0523	
Single ring	94	96.0647	13.5195	24.2846	35.4103	10.9755	11.8747	
Muon-like PID	78	74.5169	13.3959	23.9567	33.5551	0.0922	3.5170	
$p_\mu > 200$ MeV/c	78	74.4175	13.3862	23.9221	33.5368	0.0922	3.4802	
$N_{decay-e} \leq 1$	66	68.2621	13.1816	23.8472	27.7887	0.0917	3.3528	
Efficiency from Interactions [%]	-	21.9	65.8	77.5	24.5	0.6	2.5	
Efficiency from FCFV [%]	-	37.8	87.7	95.6	33.4	0.6	8.0	

Parameters used:  $\sin^2 \theta_{12} = 0.304$ ,  $\sin^2 \theta_{13} = 0.0217$ ,  $\sin^2 \theta_{23} = 0.528$ ,  $\delta_{CP} = -1.601$ ,  
 $\Delta m_{21}^2 = 7.53 \times 10^{-5}$  eV $^2$ ,  $\Delta m_{32}^2 = 2.509 \times 10^{-3}$  eV $^2$ , MH: normal, L = 295 km, Earth density = 2.6 gr/cm $^3$

## $\nu_e/\bar{\nu}_e$ selections at SuperK



# $\nu_e/\bar{\nu}_e$ selections at SuperK



# $\nu_e/\bar{\nu}_e$ selections at SuperK

**Neutrino mode:**

	Runs 1-7	Expected				Data
		$\nu_\mu + \bar{\nu}_\mu$ CC	$\nu_e + \bar{\nu}_e$ CC	NC	$\bar{\nu}_\mu \rightarrow \bar{\nu}_e$	
Interactions in FV	364.3239	18.5526	326.1581	0.3909	709.4254	35.4668 654
FCFV	279.8826	18.0883	98.7212	0.3815	397.0736	34.7765 438
Single ring	153.3979	11.1480	28.6836	0.3153	193.5449	29.9473 220
Electron-like PID	6.4647	11.0647	19.5273	0.3130	37.3697	29.5672 70
Evis >100 MeV	4.5915	11.0085	16.8090	0.3114	32.7205	29.0584 66
No Decay-e	0.9690	8.9694	14.2433	0.3062	24.4879	26.1140 51
$E_\nu^{rec}$	0.2526	4.2586	10.8493	0.2163	15.5767	25.1362 46
fTQun $\pi^0$ cut	0.0890	3.6754	1.3494	0.1807	5.2945	23.2523 32
Efficiency from Interactions [%]	0.0	19.8	0.4	46.2	0.7	65.6 -
Efficiency from FCFV [%]	0.0	20.3	1.4	47.4	1.3	66.9 -

**Antineutrino mode:**

	Runs 5-7	Expected				Data
		$\nu_\mu + \bar{\nu}_\mu$ CC	$\nu_e + \bar{\nu}_e$ CC	NC	$\bar{\nu}_\mu \rightarrow \bar{\nu}_e$	
Interactions in FV	164.0430	9.0049	132.7521	2.2885	308.0886	4.2956 263
FCFV	123.2438	8.7503	42.0523	2.2411	176.2875	4.1961 170
Single ring	73.2145	5.5119	11.8747	1.7265	92.3276	3.7371 94
Electron-like PID	2.3068	5.4784	8.3577	1.7060	17.8489	3.6989 16
Evis >100 MeV	1.8266	5.4625	7.3923	1.6866	16.3680	3.6791 14
No Decay e	0.3284	4.7127	6.2416	1.4595	12.7421	3.6571 12
$E_\nu^{rec}$	0.0828	1.8870	4.8261	1.1858	7.9816	3.4192 9
fTQun $\pi^0$ cut	0.0190	1.5754	0.5968	1.0456	3.2368	3.0432 4
Efficiency from Interactions [%]	0.0	17.5	0.4	45.7	1.1	70.8 -
Efficiency from FCFV [%]	0.0	18.0	1.4	46.7	1.8	72.5 -

Parameters used:  $\sin^2 \theta_{12} = 0.304$ ,  $\sin^2 \theta_{13} = 0.0217$ ,  $\sin^2 \theta_{23} = 0.528$ ,  $\delta_{CP} = -1.601$ ,

$\Delta m_{21}^2 = 7.53 \times 10^{-5} \text{ eV}^2$ ,  $\Delta m_{32}^2 = 2.509 \times 10^{-3} \text{ eV}^2$ , MH: normal, L = 295 km, Earth density = 2.6 gr/cm<sup>3</sup>



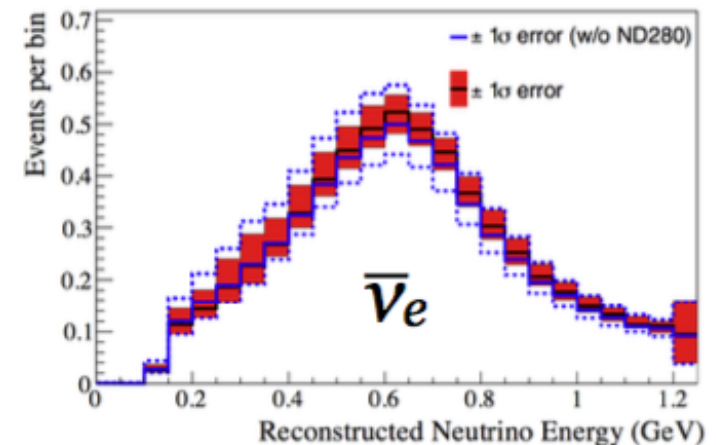
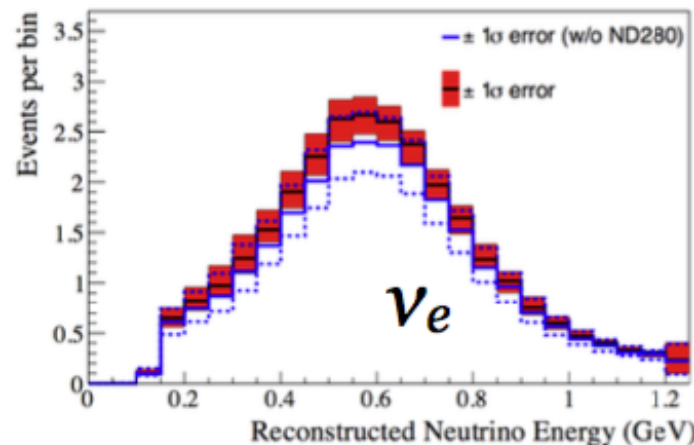
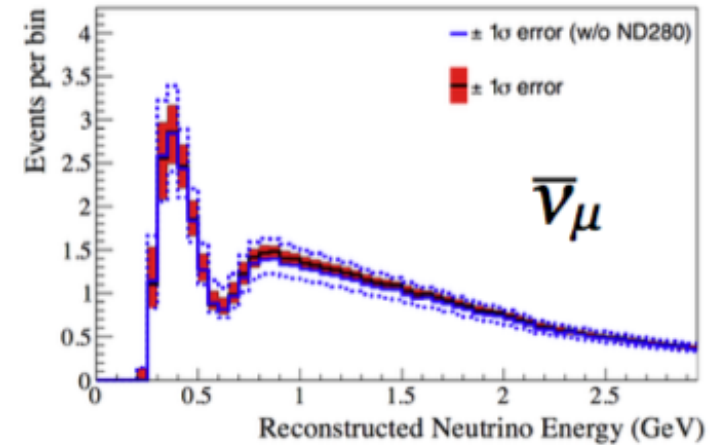
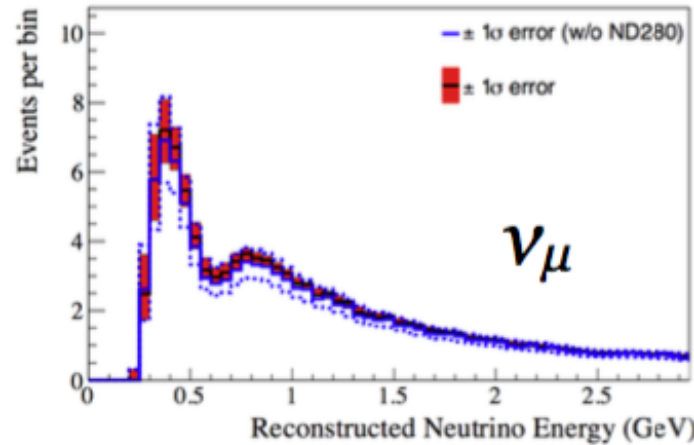
# Impact of systematic uncertainties

Substantial systematic error reduction with ND280 data:

	$\nu_\mu$ sample 1R $_\mu$ FHC	$\nu_e$ sample 1R $_\nu$ FHC	$\bar{\nu}_\mu$ sample 1R $_\mu$ RHC	$\bar{\nu}_e$ sample 1R $_\nu$ RHC
$\nu$ flux w/o ND280	7,6%	8,9%	7,1%	8,0%
$\nu$ flux with ND280	3,6%	3,6%	3,8%	3,8%
$\nu$ cross-section w/o ND280	7,7%	7,2%	9,3%	10,1%
$\nu$ cross-section with ND280	4,1%	5,1%	4,2%	5,5%
$\nu$ flux+cross-section	2,9%	4,2%	3,4%	4,6%
Final or secondary hadron int.	1,5%	2,5%	2,1%	2,5%
Super-K detector	3,9%	2,4%	3,3%	3,1%
Total w/o ND280	12,0%	11,9%	12,5%	13,7%
<b>Total with ND280</b>	<b>5,0%</b>	<b>5,4%</b>	<b>5,2%</b>	<b>6,2%</b>

Total $\delta N_{SK}/N_{SK}$			
Beam mode	sample	w/o ND280	ND280
neutrino	$\mu$ -like	12.0%	5.0%
neutrino	$e$ -like	11.9%	5.4%
antineutrino	$\mu$ -like	12.5%	5.2%
antineutrino	$e$ -like	13.7%	6.2%

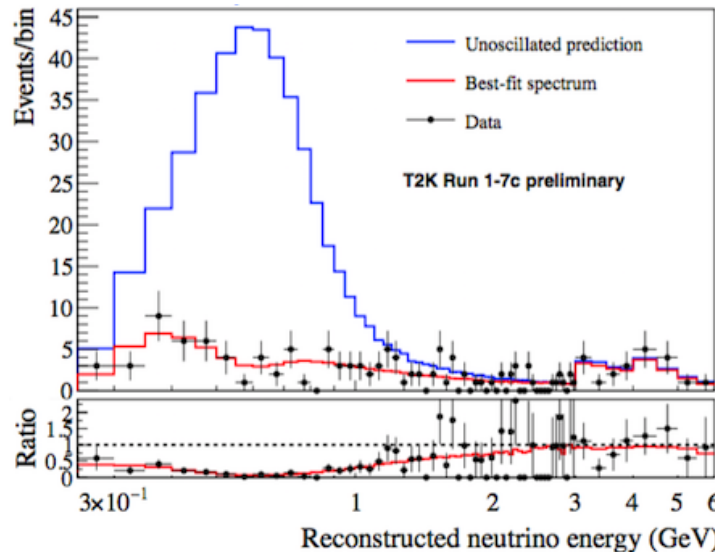
# Impact of systematic uncertainties



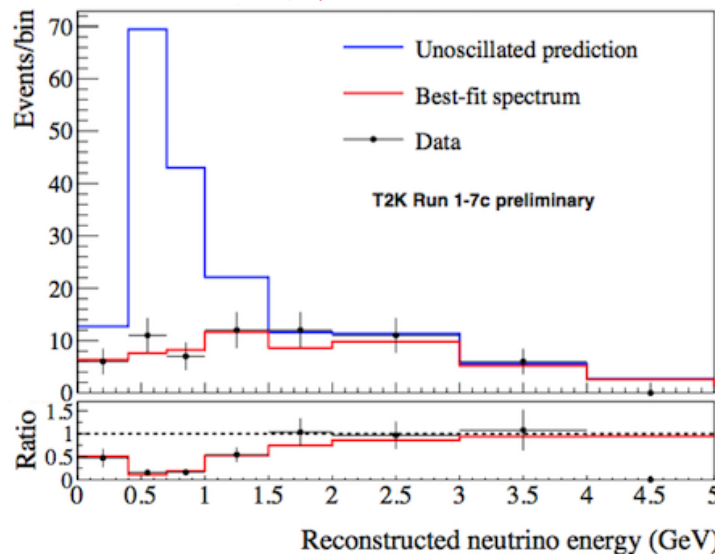
Low energy uncertainties mainly due to NC.

# T2K $\nu_\mu$ and $\bar{\nu}_\mu$ disappearance

$\nu$ -mode, 1-ring  $\mu$ -like candidates:



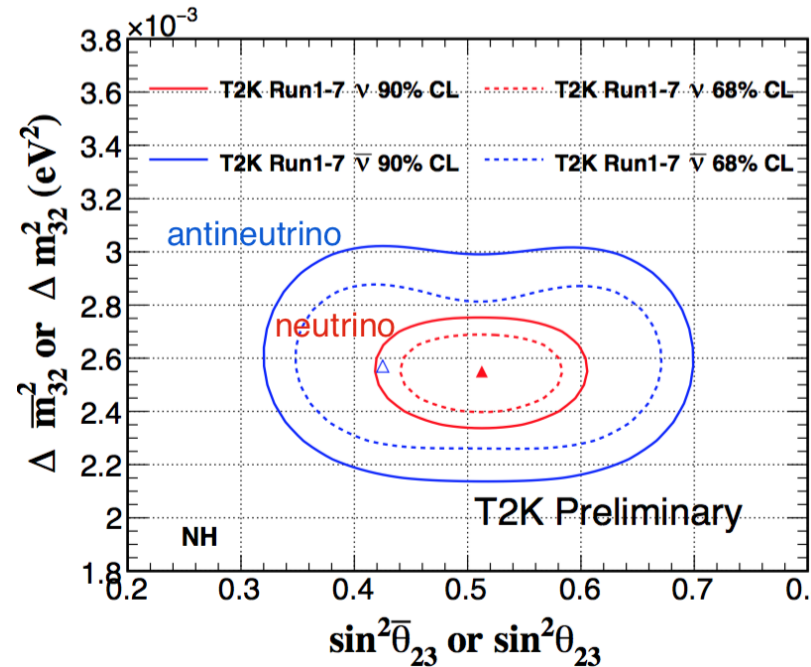
$\bar{\nu}$ -mode, 1-ring  $\mu$ -like candidates:



Mode	Expected (no osc.)	Observed
Neutrino	521.8	135
Antineutrino	184.8	66

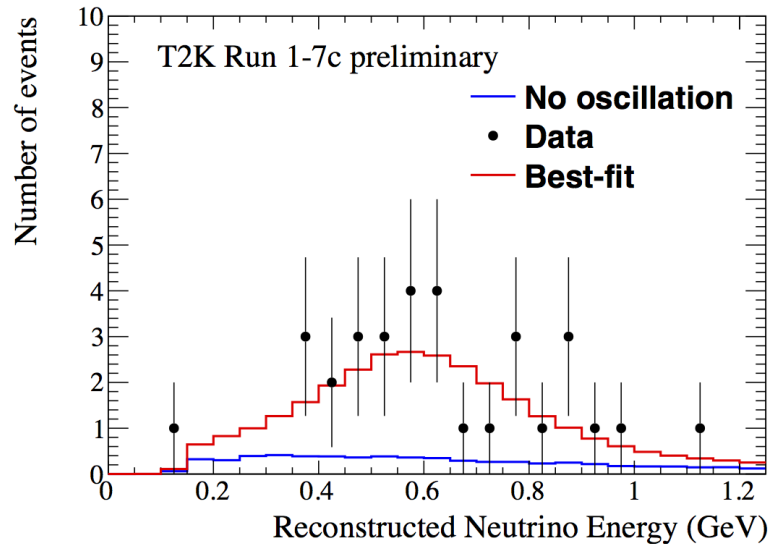
Dramatic energy-dependent deficit allows stringent constraints on  $\nu_\mu$  and  $\bar{\nu}_\mu$  disappearance parameters.

$$P(\nu_\mu \rightarrow \nu_\mu) \approx 1 - \cos^4 \theta_{13} \cdot \sin^2 2\theta_{23} \cdot \sin^2 \left( \frac{\Delta m_{31}^2 L}{4E} \right)$$

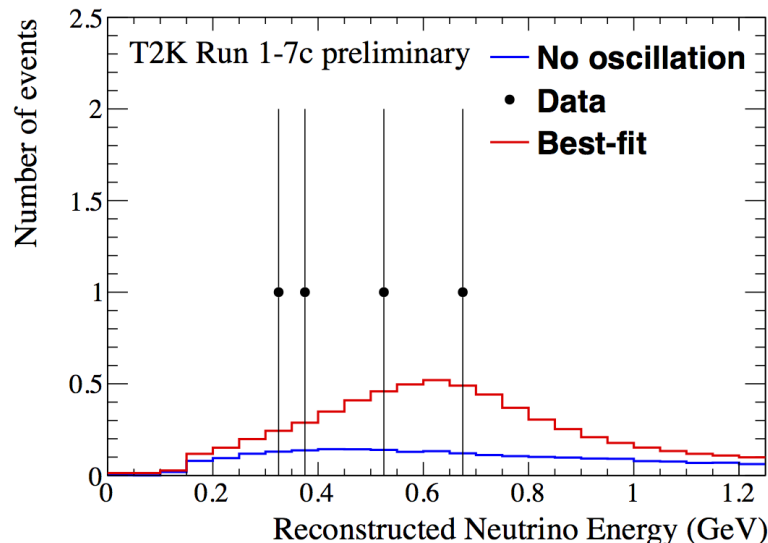


# T2K $\nu_e$ and $\bar{\nu}_e$ appearance

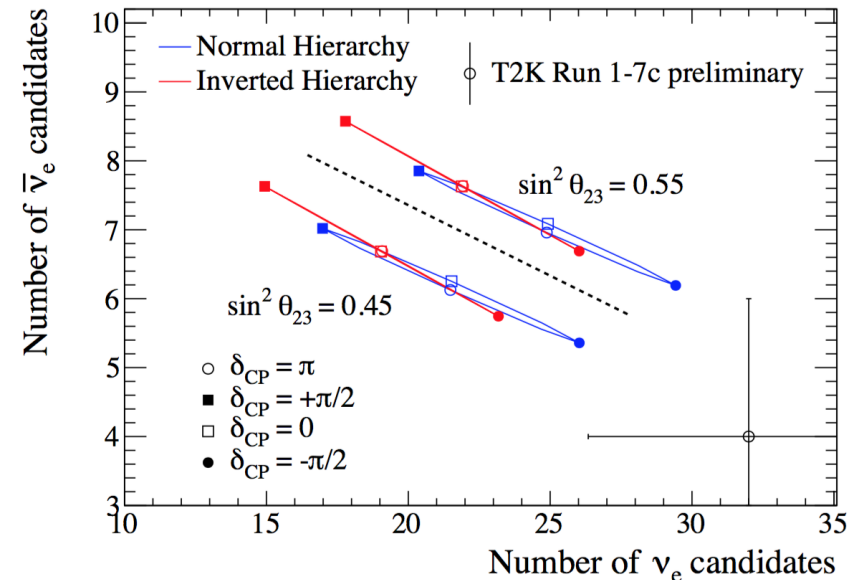
$\nu$ -mode, 1-ring e-like candidates:



$\bar{\nu}$ -mode, 1-ring e-like candidates:



- more  $\nu_e$ -like event appearance than expected in neutrino mode, and
- less  $\nu_e$ -like event appearance than expected in anti-neutrino mode

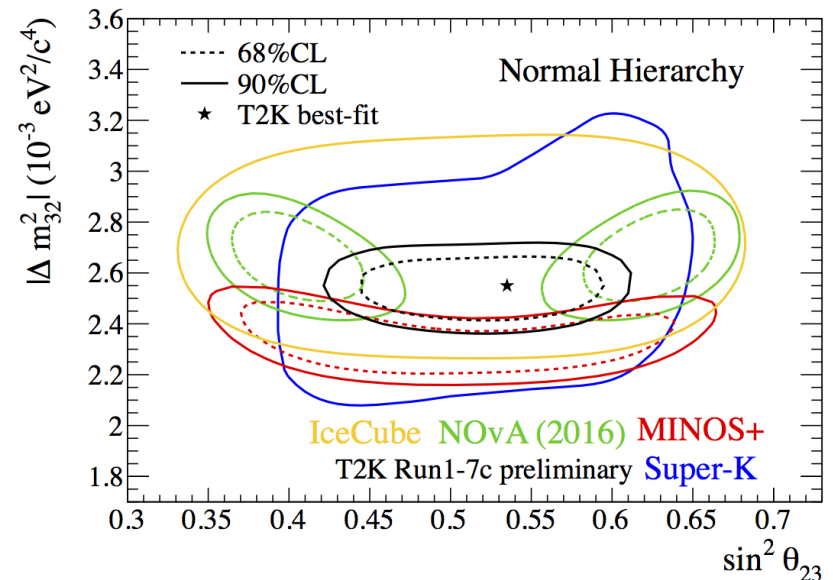
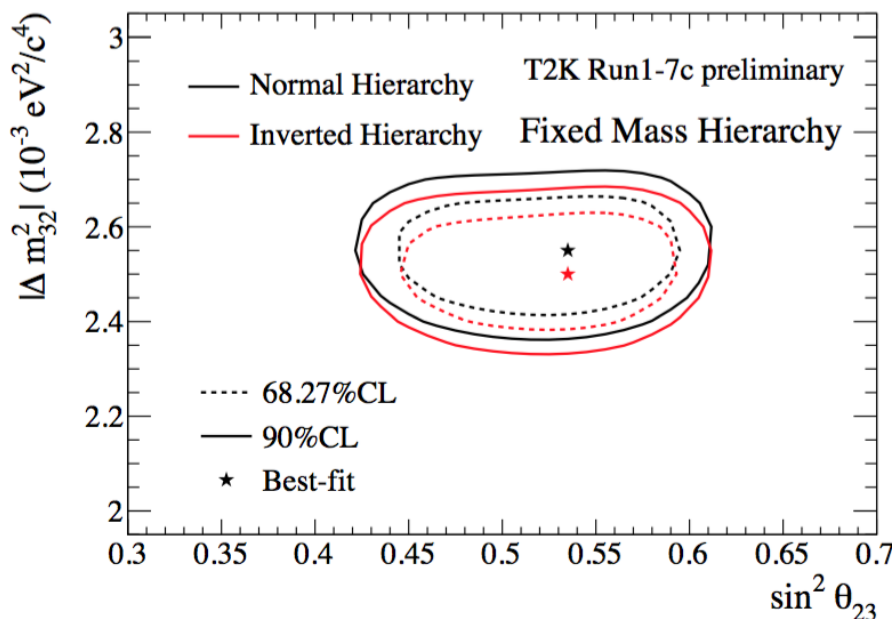


Mode	$\delta_{CP}$ , Normal hierarchy				Obs.
	$-\pi/2$	0	$\pi$	$\pi/2$	
$\nu$	28.7	24.1	24.2	19.6	32
$\bar{\nu}$	6.0	6.9	6.8	7.7	4

# T2K joint 3-flavour analysis: $\sin^2\theta_{23}$ and $|\Delta m_{32}^2|$

Joint measurement of  $\sin^2\theta_{23}$  and  $|\Delta m_{32}^2|$

- The  $\nu_\mu, \bar{\nu}_\mu$  disappearance constrain  $\sin^2 2\theta_{23}$  and  $|\Delta m_{32}^2|$ .
- The  $\nu_e, \bar{\nu}_e$  appearance samples help lift the  $\theta_{23}$  octant degeneracy.



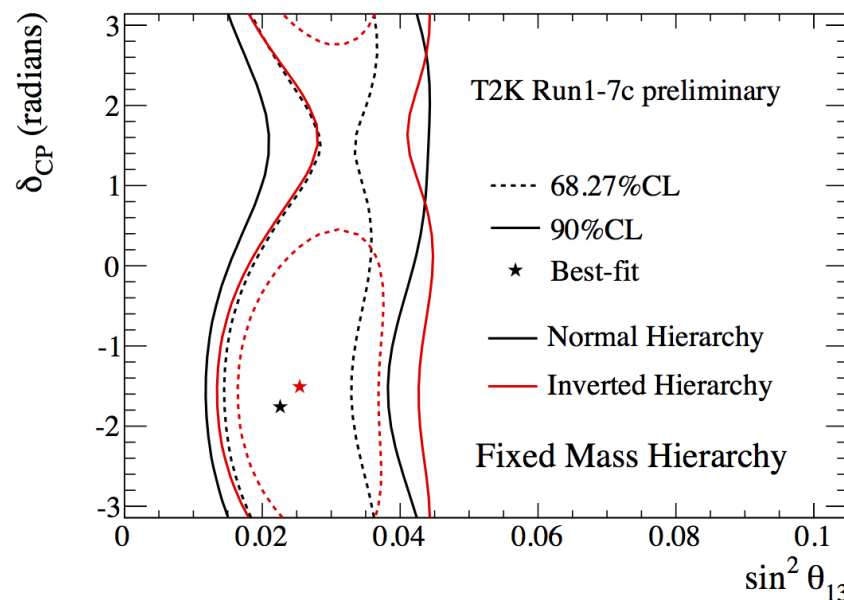
- Consistent with **maximal mixing**.
- Some tension with NOvA results.

Best-fit parameter	NH	IH
$\sin^2\theta_{23}$	0.532	0.534
$ \Delta m_{32}^2  (\times 10^{-3} \text{ eV}^2)$	2.545	2.510

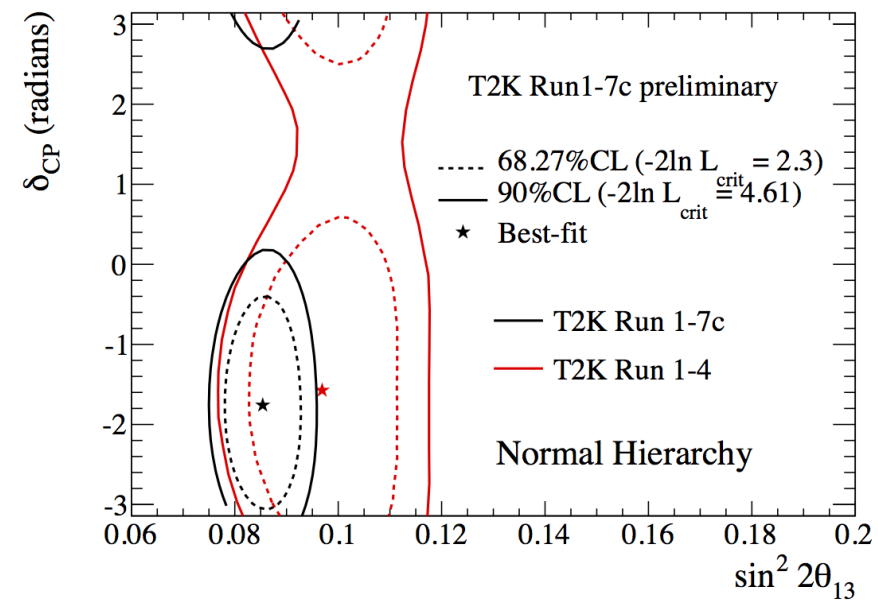
# T2K joint 3-flavour analysis: $\theta_{13}$ and $\delta_{CP}$

- Confidence intervals are slightly tighter than expected ones.

**T2K sensitivity,  $\delta_{CP} = \pi/2$**



**T2K-only data fit**

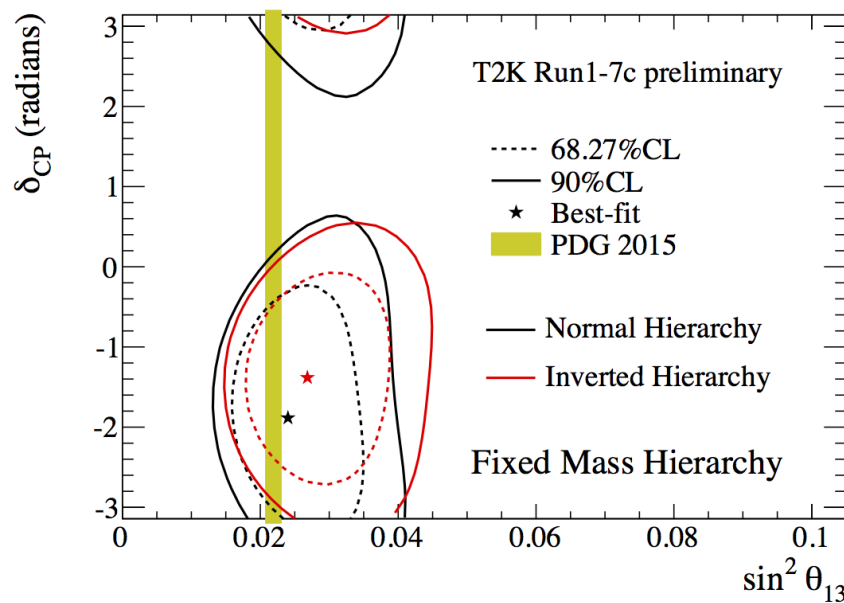


Mass hierarchy is fixed to either normal or inverted. Contours with constant  $\Delta\chi^2$  method (gaussian approximation)

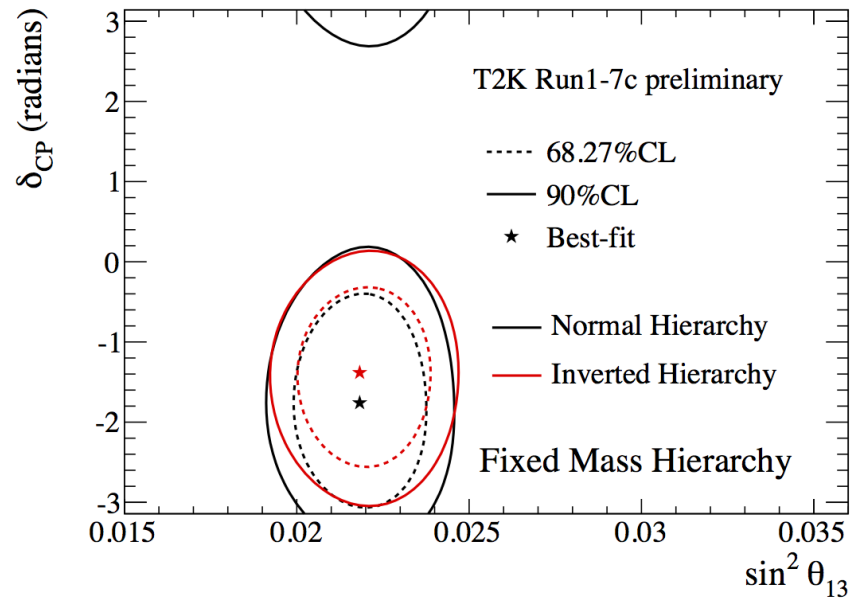
# T2K joint 3-flavour analysis: $\theta_{13}$ and $\delta_{CP}$

- Good agreement with the reactor measurement of  $\theta_{13}$ 
  - $\sin^2 2\theta_{13} = 0.085 \pm 0.005$  [PDG2015]
- T2K-only data **disfavor the region of  $\delta_{CP}$  around  $\pi/2$ .**
- T2K **prefers  $-\pi/2$**  for both NH and IH.

**T2K-only data fit**



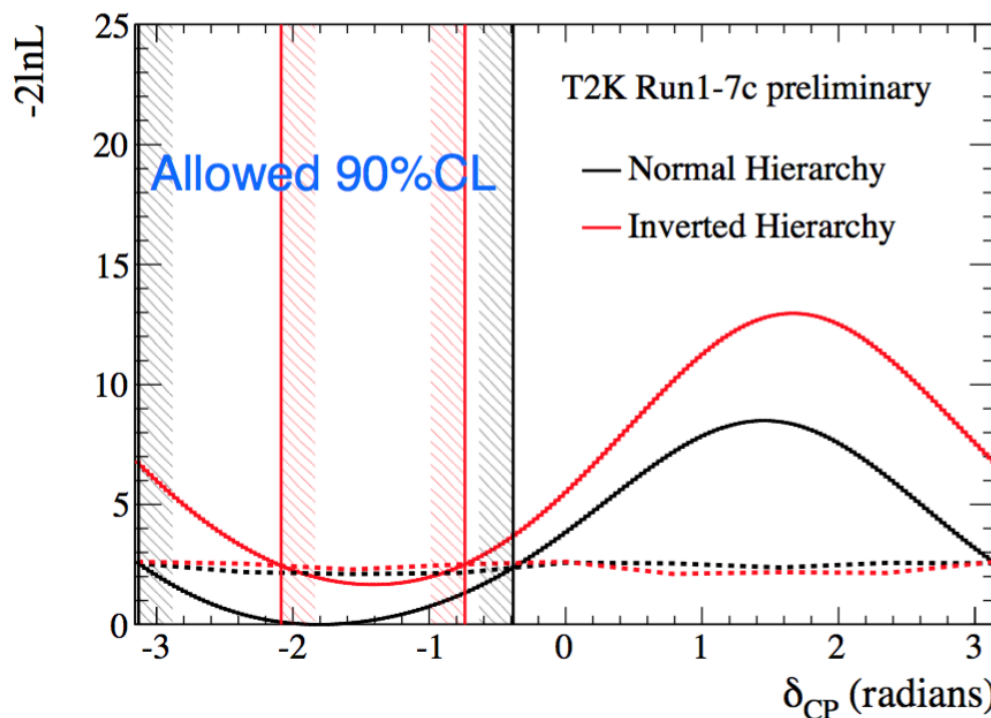
**T2K data fit with reactor constraint**



Mass hierarchy is fixed to either normal or inverted. Contours with constant  $\Delta\chi^2$  method (gaussian approximation)

# T2K joint 3-flavour analysis: $\delta_{CP}$

- Best-fit:  $\delta_{CP} = -1.885$ , NH
- $\delta_{CP} = 0$  is excluded at  $2\sigma$  C.L., while  $\delta_{CP} = \pi$  is excluded at 90% C.L.
- Allowed 90% C.L. regions:  $[-3.13, 0.39]$  (NH),  $[-2.09, -0.74]$  (IH)



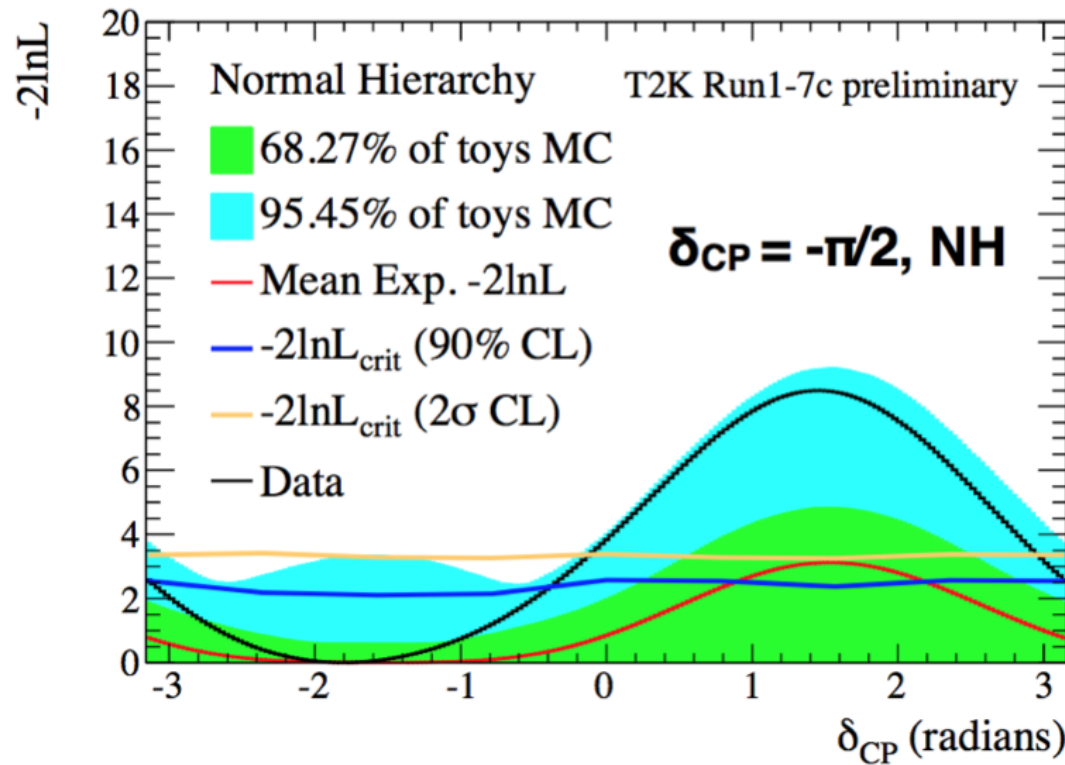
**“Conserved CP’ hypothesis excluded at 90% C.L.**

$$\sin^2 2\theta_{13} = 0.085 \pm 0.005 \text{ [PDG2015]}$$

Confidence intervals computed with Feldman-Cousins method to guarantee frequentist coverage.

# T2K joint 3-flavour analysis: $\delta_{CP}$

With the current exposure, there is about 5% chance to exclude the conserved CP hypothesis at 90% C.L., even if CP is actually conserved.



For NH and  $\delta_{CP} = \pi/2$ :

- Probability to exclude  $\delta_{CP} = 0$  at  $2\sigma$ : 9.2%
- Probability to exclude  $\delta_{CP} = \pi$  at 90% C.L.: 17.3%

# Effect of systematics on SuperK predictions

$\bar{\nu}$ -mode, 1-ring  $\mu$ -like candidates

Source of uncertainty	$\delta N_{SK}/N_{SK}$
SKDet+FSI+SI	3.90%
SKDet only	3.31 %
FSI+SI only	2.06 %
Flux	3.77%
Flux (pre-fit)	7.10%
2p-2h (corr)	2.96%
2p-2h bar (corr)	1.81%
NC other (uncorr)	0.75%
NC 1gamma (uncorr)	0.00%
XSec nue/numu (uncorr)	0.00%
XSec Tot (corr)	4.13%
XSec Tot	4.19%
XSec Tot (pre-fit)	9.32%
Flux+XSec (ND280 constrained)	3.26%
Flux+XSec (All)	3.35%
Flux+XSec+SKDet+FSI+SI	5.22%
Flux+XSec+SKDet+FSI+SI (pre-fit)	12.5%

$\bar{\nu}$ -mode, 1-ring e-like candidates

Source of uncertainty	$\delta N_{SK}/N_{SK}$
SKDet+FSI+SI	3.95%
SKDet only	3.09%
FSI+SI only	2.46%
Flux	3.77%
Flux (pre-fit)	8.03%
2p-2h (corr)	2.97%
2p-2h bar (corr)	2.36%
NC other (uncorr)	0.33%
NC 1gamma (uncorr)	2.95%
XSec nue/numu (uncorr)	1.50%
XSec Tot (corr)	4.32%
XSec Tot	5.45%
XSec Tot (pre-fit)	10.12%
Flux+XSec (ND280 constrained)	3.22%
Flux+XSec	4.63%
Flux+XSec+SKDet+FSI+SI	6.19%
Flux+XSec+SKDet+FSI+SI (pre-fit)	13.7%

Effect of  $1\sigma$  variations on the total number of events 1-ring  $\mu$ -like and e-like events for neutrino mode given by all the systematic uncertainties, obtained by performing 10k toys MC.

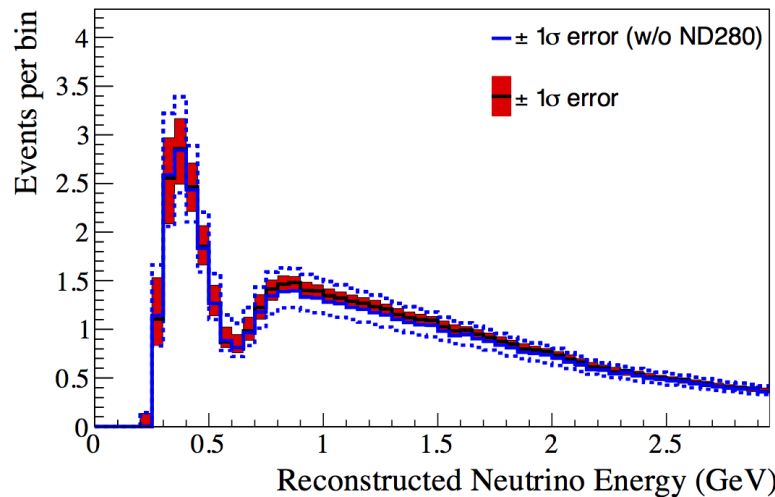
The RMS of the distribution is assumed to be the  $1\sigma$  uncertainty.

Using:  $\delta_{CP} = -1.601$ ,  $\theta_{23} = 0.528$  and  $\Delta m_{32}^2$  ( $\Delta m_{13}^2$ ) =  $2.509 \times 10^{-3} \text{ eV}^2/c^4$ .

The global values from PDG 2016 are used as uncertainties on  $\sin^2 \theta_{13}$ ,  $\sin^2 \theta_{12}$  and  $\Delta m_{21}^2$ .

# Effect of systematics on SuperK predictions

$\bar{\nu}$ -mode, 1-ring  $\mu$ -like candidates



$\bar{\nu}$ -mode, 1-ring e-like candidates

